NATIONAL NUCLEAR ENERGY SERIES
Manhattan Project Technical Section

Division II—Volume 16

ENGINEERING DEVELOPMENTS

IN THE GASEOUS DIFFUSION PROCESS

LIST OF CONTRIBUTING AUTHORS*

THE KELLEX CORPORATION

T. A. Abbott, Standard Oil Co. (Indiana), Chicago

A. Hustrulid, Department of Physics, University of Minnesota, Minneapolis

R. B. Jacobs, Standard Oil Co. (Indiana), Chicago

R. Landau, Scientific Design Co., Inc., New York

A. O. Nier, Department of Physics, University of Minnesota, Minneapolis

J. K. Pickard, Division of Engineering, U. S. Atomic Energy Commission, Washington, D. C.

S. C. Schuman, Hydrocarbon Research, Inc., New York

E. Simons, Department of Chemistry, Rutgers University, New Brunswick, N. J.

C. M. Stevens, Distillation Products, Inc., Rochester, N. Y.

W. I. Thompson, H. K. Ferguson Company, Inc., New York

T. P. Wilson, Carbide and Carbon Chemicals Corporation, South Charleston, W. Va.

H. F. Zuhr, Hydrocarbon Research, Inc., New York

PRINCETON UNIVERSITY

C. E. Birchenall, Carnegie Institute of Technology, Pittsburgh, Pa.

J. C. Elgin, Department of Chemical Engineering, Princeton University, Princeton, N. J.

G. G. Joris, Allied Chemical and Dye Central Research Laboratory, Morristown, N. J.

S.A.M. LABORATORIES (Columbia University and Carbide and Carbon Chemicals Corporation)

J. E. Binns, Brookhaven National Laboratory, Upton, N. Y.

F. S. Stein, Department of Physics, University of Buffalo, Buffalo, N. Y.

* The contributors are listed under that installation where their work for the Manhattan Project was done.

ENGINEERING DEVELOPMENTS IN THE GASEOUS DIFFUSION PROCESS

Edited by

MANSON BENEDICT

Hydrocarbon Research, Inc.; formerly of The Kellex Corporation

and

CLARKE WILLIAMS

Brookhaven National Laboratory; formerly of S.A.M. Laboratories, Columbia University, and Carbide and Carbon Chemicals Corporation

First Edition

New York · Toronto · London

McGRAW-HILL BOOK COMPANY, INC.

1949

ENGINEERING DEVELOPMENTS

IN THE GASEOUS DIFFUSION PROCESS

Printed in the United States of America

Lithoprinted
by
Edwards Brothers, Incorporated
Ann Arbor, Michigan

FOREWORD

The United States program of development of atomic energy has been described by Major General L. R. Groves, who, as Commanding General of the War Department's Manhattan Project, directed the program from mid-1942 until December 31, 1946, as "a generation of scientific development compressed into three years." The tremendous scope of the Manhattan Project Technical Section of the National Nuclear Energy Series, which has been in preparation since 1944, is a tribute to the unprecedented accomplishments of science, industry, government, labor, and the Army and Navy working together as a team. These volumes can be a firm foundation for the United States atomic energy program which, in the words of the Atomic Energy Act of 1946, is " . . . directed toward improving the public welfare, increasing the standard of living, strengthening free competition in private enterprise, and promoting world peace."

David E. Lilienthal, Chairman
U. S. Atomic Energy Commission

ACKNOWLEDGMENT

The Manhattan Project Technical Section of the National Nuclear Energy Series embodies results of work done in the nation's wartime atomic energy program by numerous contractors, including Columbia University. The arrangements for publication of the series volumes were effected by Columbia University, under a contract with the United States Atomic Energy Commission. The Commission, for itself and for the other contractors who contributed to this series, wishes to record here its appreciation of this service of Columbia University in support of the national nuclear energy program.

PREFACE

This volume is one of a series which has been prepared as a record of the research work done under the Manhattan Project and the Atomic Energy Commission. The name Manhattan Project was assigned by the Corps of Engineers, War Department, to the far-flung scientific and engineering activities which had as their objective the utilization of atomic energy for military purposes. In the attainment of this objective, there were many developments in scientific and technical fields which are of general interest. The National Nuclear Energy Series (Manhattan Project Technical Section) is a record of these scientific and technical contributions, as well as of the developments in these fields which are being sponsored by the Atomic Energy Commission.

The declassified portion of the National Nuclear Energy Series, when completed, is expected to consist of some 60 volumes. These will be grouped into eight divisions, as follows:

Division I — Electromagnetic Separation Project
Division II — Gaseous Diffusion Project
Division III — Special Separations Project
Division IV — Plutonium Project
Division V — Los Alamos Project
Division VI — University of Rochester Project
Division VII — Materials Procurement Project
Division VIII — Manhattan Project

Soon after the close of the war the Manhattan Project was able to give its attention to the preparation of a complete record of the research work accomplished under Project contracts. Writing programs were authorized at all laboratories, with the object of obtaining complete coverage of Project results. Each major installation was requested to designate one or more representatives to make up a committee, which was first called the Manhattan Project Editorial Advisory Board, and later, after the sponsorship of the Series was assumed by the Atomic Energy Commission, the Project Editorial Advisory Board. This group made plans to coordinate the writing programs at all the installations, and acted as an advisory group in all matters affecting the Project-wide writing program. Its last meeting was held on Feb. 9, 1948, when it recommended the publisher for the Series.

The names of the Board members and of the installations which they represented are given below.

Atomic Energy Commission Public and Technical Information Service	Alberto F. Thompson
Technical Information Branch, Oak Ridge Extension	Brewer F. Boardman
Office of New York Operations	Charles Slesser, J. H. Hayner, W. M. Hearon *
Brookhaven National Laboratory	Richard W. Dodson
Carbide & Carbon Chemicals Corporation (K-25)	R. B. Korsmeyer, W. L. Harwell, D. E. Hull, Ezra Staple
Carbide & Carbon Chemicals Corporation (Y-12) †	Russell Baldock
Clinton Laboratories ‖	J. R. Coe
General Electric Company, Hanford	T. W. Hauff
General Electric Company, Knolls Atomic Power Laboratory	John P. Howe
Kellex Corporation	John F. Hogerton, Jerome Simson, M. Benedict
Los Alamos	R. R. Davis, Ralph Carlisle Smith
National Bureau of Standards	C. J. Rodden
Plutonium Project Argonne National Laboratory	R. S. Mulliken, H. D. Young
Iowa State College	F. H. Spedding
Medical Group	R. E. Zirkle
SAM Laboratories §	G. M. Murphy
Stone & Webster Engineering Corporation	B. W. Whitehurst
University of California	R. K. Wakerling, A. Guthrie
University of Rochester	D. R. Charles, M. J. Wantman

* Represented Madison Square Area of the Manhattan District.

† The Y-12 plant at Oak Ridge was operated by Tennessee Eastman Corporation until May 4, 1947, at which time operations were taken over by Carbide & Carbon Chemicals Corporation.

‖ Clinton Laboratories was the former name of the Oak Ridge National Laboratory.

§ SAM (Substitute Alloy Materials) was the code name for the laboratories operated by Columbia University in New York under the direction of Dr. H. C. Urey, where much of the experimental work on isotope separation was done. On Feb. 1, 1945, the administration of these laboratories became the responsibility of Carbide & Carbon Chemicals Corporation. Research in progress there was transferred to the K-25 plant at Oak Ridge in June, 1946, and the New York laboratories were then closed.

Many difficulties were encountered in preparing a unified account of Atomic Energy Project work. For example, the Project Editorial Advisory Board was the first committee ever organized with representatives from every major installation of the Atomic Energy Project. Compartmentation for security was so rigorous during the war that it had been considered necessary to allow a certain amount of duplication of effort rather than to permit unrestricted circulation of research information between certain installations. As a result, the writing programs of different installations inevitably overlap markedly in many scientific fields. The Editorial Advisory Board has exerted itself to reduce duplication in so far as possible and to eliminate discrepancies in factual data included in the volumes of the NNES. In particular, unified Project-wide volumes have been prepared on Uranium Chemistry and on the Analysis of Project Materials. Nevertheless, the reader will find many instances of differences in results or conclusions on similar subject matter prepared by different authors. This has not seemed wholly undesirable for several reasons. First of all, such divergencies are not unnatural and stimulate investigation. Second, promptness of publication has seemed more important than the removal of all discrepancies. Finally, many Project scientists completed their contributions some time ago and have become engrossed in other activities so that their time has not been available for a detailed review of their work in relation to similar work done at other installations.

The completion of the various individual volumes of the Series has also been beset with difficulties. Many of the key authors and editors have had important responsibilities in planning the future of atomic energy research. Under these circumstances, the completion of this technical series has been delayed longer than its editors wished. The volumes are being released in their present form in the interest of presenting the material as promptly as possible to those who can make use of it.

The Editorial Advisory Board

The Manhattan Project Technical Section of the National Nuclear Energy Series is intended to be a comprehensive account of the scientific and technical achievements of the United States program for the development of atomic energy. It is not intended to be a detailed documentary record of the making of any inventions that happen to be mentioned in it. Therefore, the dates used in the Series should be regarded as a general temporal frame of reference, rather than as establishing dates of conception of inventions, of their reduction to practice, or of occasions of first use. While a reasonable effort has been made to assign credit fairly in the NNES volumes, this may, in many cases, be given to a group identified by the name of its leader rather than to an individual who was an actual inventor.

DIVISION EDITOR'S PREFACE

Research on the gas diffusion method for separating the uranium isotopes began at Columbia University in 1940 with the work of E. T. Booth, A. V. Grosse, and J. R. Dunning. Their results were encouraging enough to warrant continued effort with increased personnel and funds. Until May 1943 Dunning directed such research at Columbia under the auspices of the Office of Scientific Research and Development. At that time other aspects of uranium research there were combined under the Manhattan District with H. C. Urey as Director, and the organization was named the S.A.M. Laboratories, from the code words "Substitute Alloy Materials." Columbia University continued as the contracting party with the War Department until February 1, 1945, when responsibility for gas diffusion research at S.A.M. was assumed by Carbide and Carbon Chemicals Corporation with R. H. Crist as Director of Research. With the end of the war, it was thought desirable to transfer further activities to the site of the diffusion plant at Oak Ridge, Tenn., and the S.A.M. Laboratories were closed on July 1, 1946.

Concurrently with the early research and development at Columbia, plans were being made for the design and construction of a large-scale diffusion plant. To this end, early in 1942 the M. W. Kellogg Company was brought in by the Office of Scientific Research and Development to study the engineering feasibility of the project. Later in the same year, when the newly formed Manhattan District authorized detailed design and engineering of a production plant, Kellogg set up a special subsidiary, The Kellex Corporation, to handle the work. The Kellex Corporation's assignment included research, process development, design, engineering, equipment development and procurement, and supervision of construction. Over a period of months a nucleus staff of Kellogg personnel was expanded by recruiting men from leading universities and industrial firms. P. C. Keith was Technical Vice President until the summer of 1945. The Project Manager was A. L. Baker, who as Chief Engineer of the M. W. Kellogg Company organized The Kellex Corporation. In the later stages of the work, A. L. Baker was Vice President in charge. S. B. Smith as Assistant Project Manager, J. H. Arnold as Director of Research, Manson Benedict as Chief Process Engineer, and Allen J. Fruit as Chief Project Engineer all made material contributions.

Construction contractors were the J. A. Jones Construction Company, Inc. (for the main plant) and Ford, Bacon & Davis, Inc. (for one of the large auxiliary plants). The operating responsibility was assigned to Carbide and Carbon Chemicals Corporation, with G. T. Felbeck in charge.

While the major part of research and development of the separation process was carried on by S.A.M. and Kellex, many other laboratories contributed either in some specialized fields or in connection with production of components that were to be used in the large-scale diffusion plant. Among these were Princeton University, Bell Telephone Laboratories, Inc., the Bakelite Corporation, Houdaille-Hershey Corporation, Allis-Chalmers Manufacturing Company, Taylor Instrument Company, Crane Company, Chrysler Corporation, General Electric Company, and The Linde Air Products Company. Others are mentioned in the particular volumes of this series dealing with the work they accomplished.

Early in 1945 it became apparent that the imposing array of technical and scientific skill collected on the gaseous diffusion project would eventually become dispersed. The personnel on the project had come from numerous colleges, universities, research laboratories, and industries and had become experts on the peculiar problems involving isotope separation; their return to peacetime endeavors meant that their combined knowledge and experience would be dissipated. It was suggested by Dr. Crist, then Director of the S.A.M. Laboratories, that this pool of knowledge be recorded in a treatise that came to be known as the "Gas Diffusion Project Handbook." It was to deal with the research aspects of the subject only, paying little or no attention to production problems. Originally it was to be written entirely by S.A.M. personnel, but the results of other participating laboratories were to be included. The treatise was thus expected to be an authoritative and critical survey of the gas diffusion process that would serve not only as a record of its current status but also as a source of information and a foundation for any future research that might be done.

Work had begun on this undertaking when the broader writing program of the Manhattan Project was formulated. The S.A.M. program was then also expanded, but for various reasons not all the installations associated with the gas diffusion research were able to share in the writing, and the major part of it was undertaken by Kellex and S.A.M. Planning and general supervision of the writing were carried on by an Editorial Board composed of Clarence A. Johnson and Manson Benedict of The Kellex Corporation, Lyle I. Gilbertson and

Clarke Williams of the S.A.M. Laboratories, and the writer, also of S.A.M., as Editor-in-Chief. Helpful advice and criticism were secured from George Scatchard, E. T. Booth, R. H. Crist, W. F. Libby, Edward Mack, Jr., and H. S. Taylor. The completed manuscripts of the volumes have been reviewed further by R. B. Korsmeyer and the research staff at Oak Ridge, with many valuable comments as a result. Credits to others who aided in this work are given in the individual volumes.

The successful construction and operation of the gas diffusion plant at Oak Ridge is now well known to be an extraordinary achievement. It was possible only by the combined efforts of the many workers on the Manhattan Project. These volumes should form a permanent record of their contributions.

George M. Murphy
Division Editor

VOLUME EDITORS' PREFACE

As process development and design of the diffusion plant progressed, it was found that a number of novel auxiliary devices would be needed. This volume describes research and engineering developments undertaken in connection with these auxiliary devices, when they are of sufficient novelty or general interest to warrant inclusion in the National Nuclear Energy Series.

The volume is divided into four parts: Part 1, "Special Plant Instruments and Devices"; Part 2, "Vacuum Engineering"; Part 3, "Development of Heat-transfer Equipment"; Part 4, "Absorption of UF_6 and Fluorine."

Special Plant Instruments. The devices described in Part 1 and the first portion of Chap. 4 were developments of the Kellex Instrument Department, which was originally under the direction of G. W. Watts and J. B. McMahon, and later under the direction of G. W. Watts and T. A. Abbott. The Kellex Instrument Department laboratory was headed by A. O. Nier, who originated the mass spectrometer for process analysis described in Chap. 1, the recording ionization chamber for traces of UF_6 described in Chap. 2, and the mass spectrometer for leak detection described in the first part of Chap. 4.

Vacuum Engineering. Important contributions to vacuum engineering, described in Part 2, were made by the University of Minnesota, The Kellex Corporation, and the S.A.M. Laboratories. A preliminary model of the leak detector described in Chap. 4, constructed by Nier while at the University of Minnesota, was later perfected by Nier and Stevens at Kellex and put into mass production by the General Electric Company. It was used for virtually all the vacuum testing for the K-25 plant. The leak-detector mass spectrometer of a different type described in the last section of Chap. 4 was developed by J. E. Binns and F. S. Stein of the S.A.M. Laboratories toward the close of the project. Although it was not used extensively, it appears to have some advantages over the standard instrument.

The principal groups engaged in leak testing and vacuum engineering were those at The Kellex Corporation, Carbide and Carbon Chemicals Corporation, and the S.A.M. Laboratories. The Kellex group was part of the Cleaning and Testing Department headed by R. E. Powers. The vacuum-engineering work of this department was under the direction of R. B. Jacobs, assisted by H. F. Zuhr, J. R. Downing,

F. Raibel, A. Nerken, and many others. This group developed procedures and techniques, set vacuum-tightness specifications for all plant equipment, checked the mechanical design for acceptable vacuum construction, instructed equipment manufacturers in vacuum-testing their products, and coordinated vacuum testing of the K-25 plant proper. The work of this group is described in Chap. 5. Testing at the K-25 plant was originally performed by this group, but was later transferred to Carbide.

The Carbide vacuum-testing group was directed by F. C. Armistead and later by L. C. Anthony. After July 1944 this group tested the K-25 plant as construction was completed and certified as to its vacuum tightness.

The S.A.M. vacuum-testing group was under the general direction of E. T. Booth, and was originally supervised by C. G. Ellis; after December 1943 it was headed by J. E. Binns. It tested a variety of laboratory and pilot-plant equipment for tightness both at S.A.M. and a number of other Manhattan District contractors. Much of this work was done with vacuum-testing devices that it had developed. This group also conducted a vacuum-engineering school for training plant leak-testing personnel, thereby contributing greatly to the success of the vacuum-testing program of the gaseous diffusion project.

Development of Heat-transfer Equipment. The process design and development of heat-transfer equipment described in Part 3 was one of the functions of the Kellex Process Development Division headed by M. Benedict. W. I. Thompson developed the theory of condensation of this equipment, and G. T. Cooper carried out the detailed process design, assisted by J. J. Barker, J. Grossman, R. J. McGarry, I. Resnick, and R. L. Young. Experimental testing of heat-transfer equipment was conducted in the Kellex Jersey City laboratories by M. C. Chervenak, H. C. Anderson, and R. A. Matthews, under the general direction of S. C. Schuman.

Absorption of UF_6 and Fluorine. Laboratory studies of processes for the absorption of UF_6 and fluorine were conducted at the Jersey City laboratories of The Kellex Corporation under the direction of S. C. Schuman, at Princeton University under the direction of G. G. Joris and J. C. Elgin, and at The Johns Hopkins University under the direction of W. B. Burford III.

The engineering development of processes and equipment for this purpose was carried out by Ralph Landau of the Special Chemicals Division of The Kellex Corporation.

The process for UF_6 absorption described in Chap. 7 was tested at Princeton University by G. G. Joris, J. C. Elgin, and C. E. Birchenall. The process for fluorine absorption described in Chap. 8 was developed by Ralph Landau of Kellex; it was demonstrated on the laboratory scale at the Kellex Jersey City laboratory by S. C. Schuman, M. C. Chervenak, and R. H. Lafferty, and on a somewhat larger scale at The Johns Hopkins University by W. B. Burford III. Absorption of the gas F_2O is described in Chap. 9.

Manson Benedict
Clarke Williams

April, 1949
New York, N. Y.

CONTENTS

Part 1

SPECIAL PLANT INSTRUMENTS AND DEVICES

Chapter 1

RECORDING MASS SPECTROMETER FOR PROCESS ANALYSIS

By A. O. Nier, T. A. Abbott, and J. K. Pickard*

1. INTRODUCTION

The purpose of this chapter is to describe the use of the recording mass spectrometer in making continuous analyses of the process-gas stream. The recording mass spectrometer was selected to make the analyses because of the many advantages it has over other instruments considered. These advantages are:

1. Ability to measure each component of the process stream.
2. Negligible consumption of the extremely valuable material to be analyzed.
3. Rapid response to changes in the composition of the gas stream.
4. Continuous automatic recording of the principal components of the gas stream.

2. THE RECORDING MASS SPECTROMETER

A schematic diagram of a recording mass spectrometer is shown in Fig. 1.1. The sample gas enters the system from the incoming manifold; flows through the adjustable leak, the Pirani-gauge flowmeter, and the chemical trap; and enters the spectrometer tube. The emission regulator supplies the tube with controlled currents and voltages. Automatic switching equipment in the recorder and main control panel changes the value of the accelerating voltages through a prearranged sequence of values corresponding to the desired analyses

*The original design of the recording mass spectrometer was made by members of The Kellex Corporation, and, after modifications to improve the reliability and facilitate the manufacture, a large number of the instruments were built by the General Electric Co. The following Kellex laboratory personnel have made significant contributions to the design and development of these instruments: I. R. Brenholdt, D. L. Drukey, G. Goertzel, W. T. Leland, C. M. Stevens, T. I. Taylor and R. B. Thorness.

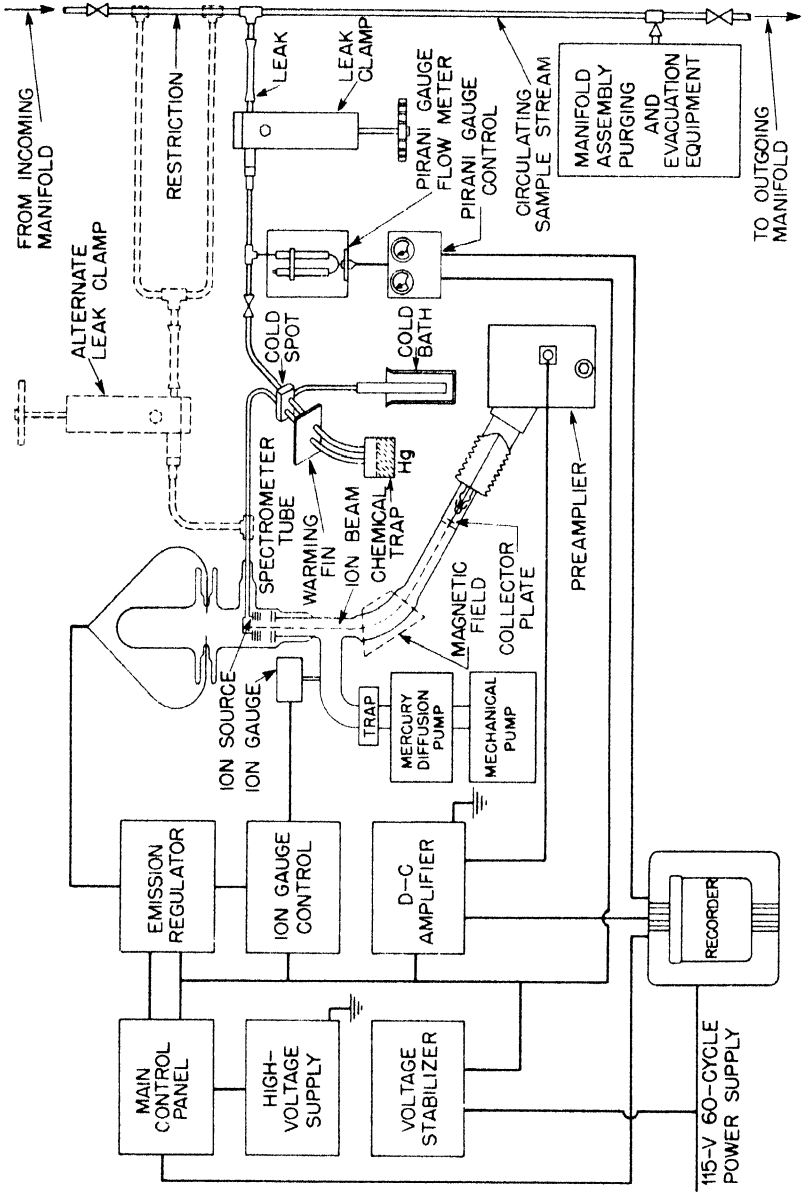

Fig. 1.1—Schematic diagram of the recording mass spectrometer, showing the two gas inlet systems and the interconnections of the component parts.

of the gas. The ion currents are amplified by the preamplifier and the amplifier and are recorded on the recorder.

2.1 Spectrometer Tube. A drawing of the spectrometer tube is shown in Fig. 1.2. The sample gas enters the ionization chamber through the inlet lead. Because of the construction of the tube T, the

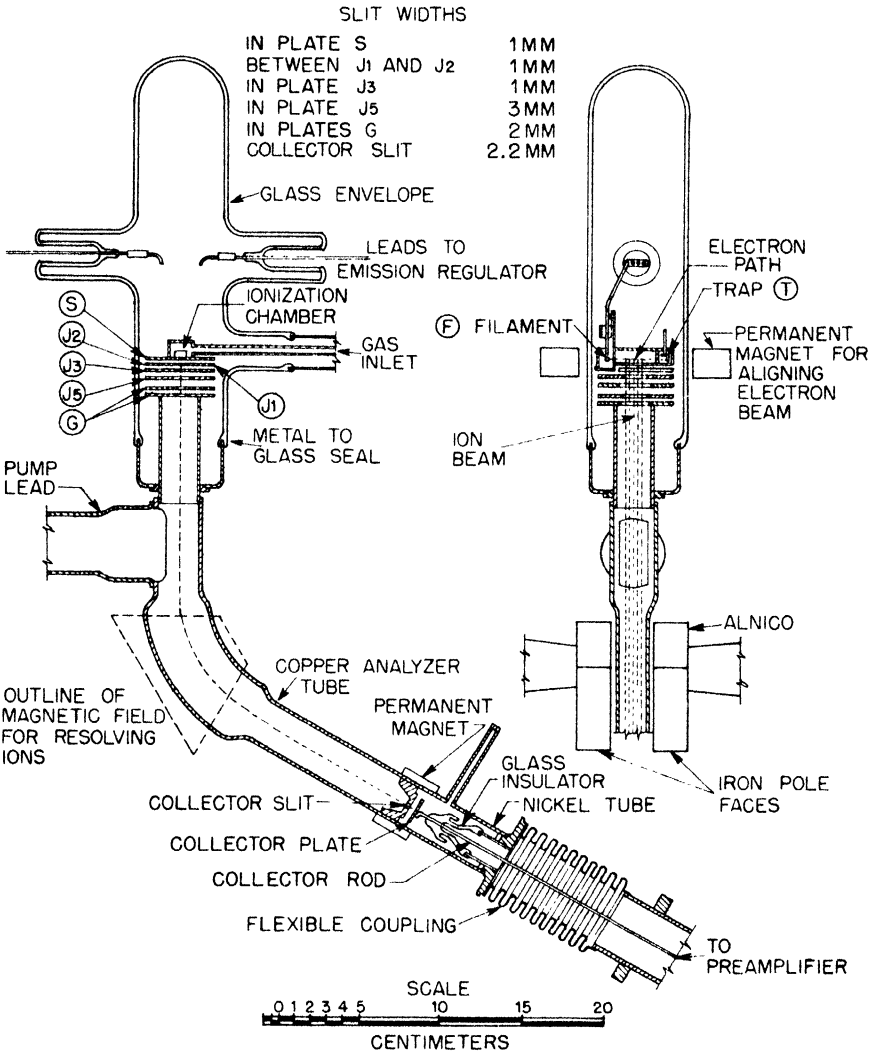

Fig. 1.2—Detail of recording-mass-spectrometer tube.

pressure in the ionization chamber is higher than in the rest of the tube. The sample gas is ionized by electrons emitted from the heated filament F. The ions are then aligned by a magnetic field and accelerated by a potential difference between the filament and the ionization chamber. Since the useful electron beam consists of a fine pencil of electrons which is directed into the trap, the trap current is an accurate indication of the electron current. Ions formed by collision of the electrons with the gas molecules are forced through the slit in the shield S and are accelerated through the plates J1, J2, J3, J5, and G by the voltages on them. The plates J1 and J2, which have independently adjustable voltages, serve to bend the ion beam to one side or the other to compensate for imperfections in construction as well as for the slight bending caused by the magnetic field used in aligning the electron beam. The plates marked G are fastened to the tube body, which is electrically grounded. The ion beam is resolved in passing through the transverse magnetic field created by the permanent magnets. The operating conditions for a typical recording mass spectrometer are as follows:

Potential between S and J1	Approximately 100 volts
Potential between S and J2	Approximately 100 volts
Potential between S and J3	120 volts
Potential between J5 and G	0.6 of the potential between S and G
Potential between S and T	90 volts
Potential between F and S	75 volts
Accelerating potential between S and G	Adjustable from 0 to 2,500 volts
Total electron emission	100 μa
Total trap current	100 μa
Electron-aligning magnet strength	250 gausses
Main magnet strength	3,250 gausses
Mass 28 accelerating voltage	1,050 volts

Although the ions impinging on the collector and nearby surfaces produce secondary electrons, these do not contribute to the collector current, inasmuch as a weak magnetic field is present. This field is produced by a small instrument magnet.

2.2 Electrical Components. The electrical components of the recording mass spectrometer consist of switching, regulating, and amplifying equipment. These components are separated on a functional basis and mounted on separate relay-rack panels. The interconnections are made with plug-in type cables (Fig. 1.2). All circuits — with the exception of the high-voltage supply, which is self-stabilized — are operated from stabilized 115-volt 60-cycle power.

The ionizing and accelerating voltages of the spectrometer ion source are produced by the emission regulator and the high-voltage supply and are controlled by the automatic switches in the recorder, which operate relays located on the main control panel. The emission regulator supplies (1) regulated current to the spectrometer filament, (2) stabilized voltage to the electron trap, and (3) stabilized voltages to the accelerating plates S, J1, J2, and J3. Potentiometers and meters are used in each of the circuits for adjusting the voltages. The ion-accelerating voltages for plates S and J5 are provided by the high-voltage supply. Two potential dividers — one for manual and one for automatic operation on the main control panel — permit the selection of the different accelerating voltages required to tune the spectrometer to the different mass numbers. It is possible to select any accelerating voltage between 0 and 2,500 volts. In automatic operation, however, several specific voltages, corresponding to various components of the process gas, may be used.

The ion currents to the collector plate are amplified by an inverse-feedback d-c amplifier. This amplifier has four stages, the first two of which, consisting of two 954 tubes and a 5×10^9 ohm input resistor, make up the preamplifier and are mounted in an aluminum box. This box is mounted on vibration insulators and connected to the spectrometer tube by a bellows assembly.

The amplified ion currents are measured by a self-balancing potentiometer-type recorder. A motor-driven switch in the recorder, synchronized with the switch used to change the accelerating voltage, automatically selects any one of seven sensitivity factors between 1 and 100. The recorder, which has 16 channels, records the amplifier zero and the Pirani-gauge readings as well as the eight mass measurements on a 24-sec-per-channel cycle. All 16 channels are used, and thus some measurements are recorded more frequently than others.

An ionization gauge is used to measure the pressure in the spectrometer tube. A special protective feature that has been added to the ion-gauge control prevents the filaments of the gauge and of the spectrometer tube from burning out by automatically cutting off their currents when the pressure exceeds a predetermined value.

2.3 Gas Inlet Systems. Two gas inlet systems are illustrated in Fig. 1.1; the first system is shown in continuous lines, the second in dotted lines. The system chosen depends on the relative quantities of UF_6 in the sample stream. If the samples contain high concentrations of UF_6, the first inlet system may be used. Since such samples cause the rapid formation of insulating coatings on those electrodes in the spectrometer tube that are bombarded by electrons, the gases are

not admitted directly to the tube but are first passed through a chemical trap, which removes the UF_6. In this system the pressure in the spectrometer is adjusted in such a way that the ion current of each constituent at the appropriate mass number is proportional to its concentration in the original mixture. This adjustment is made possible by building into the gas inlet system a set of resistances and a Pirani gauge. When the flow is adjusted so that the Pirani reading is held constant, the ion current of each constituent in the spectrometer is proportional to its concentration in the original mixture.

If the samples contain small amounts of UF_6, the second inlet system may be used. In this system the gases are admitted directly to the tube through the alternate leak without absorption of UF_6.

The adjustable leak with its capillary tube is an extremely low-flow nonfractionating valve. Its details are shown in Fig. 1.3. It has been designed so that a flow rate of 25 ml-μ/sec may be obtained when the absolute upstream pressure varies between 1 and 60 cm Hg with a downstream pressure of a few microns of mercury. The leak is adjusted by turning the handle, which forces the shoes to move in and out along the inclined planes in the clamp arms, thereby closing and opening the annular space between the leak tube and the leak plug. In meeting the range requirements, the jaws move approximately 0.003 in. for 35 turns of the handle. A force of approximately 5,000 lb is necessary to compress the leak tube. The performance of the leak depends on the accuracy with which the parts are made. The critical dimensions and their associated tolerances are given in Fig. 1.3.

The capillary tube used upstream of the adjustable leak ensures that a representative sample of the gas will flow to the leak and that the variable fractionating performance of the leak will not affect the composition of the gas going to the spectrometer tube. The length of the capillary has been chosen so that even at the lowest pressures the flow through it is viscous. Figure 1.4 shows the fractionation of the leak with and without the capillary.

The chemical trap is shown in Fig. 1.1. The mercury reservoir, which is kept at room temperature, produces mercury vapor, which diffuses to the cold spots, condenses, and falls back into the trap. When UF_6 is flowing into the system, it meets the mercury stream at the first cold spot, and a reaction takes place in which solid products are formed and accumulate on the walls of the tubing. The cold spots are held at approximately 0°C. The one in the lead to the spectrometer tube limits the mercury pressure in the tube, whereas the one in the lead to the leak confines the reaction region. To make certain that the mercury does not condense before reaching the cold spots, a warming fin is attached as shown in the diagram.

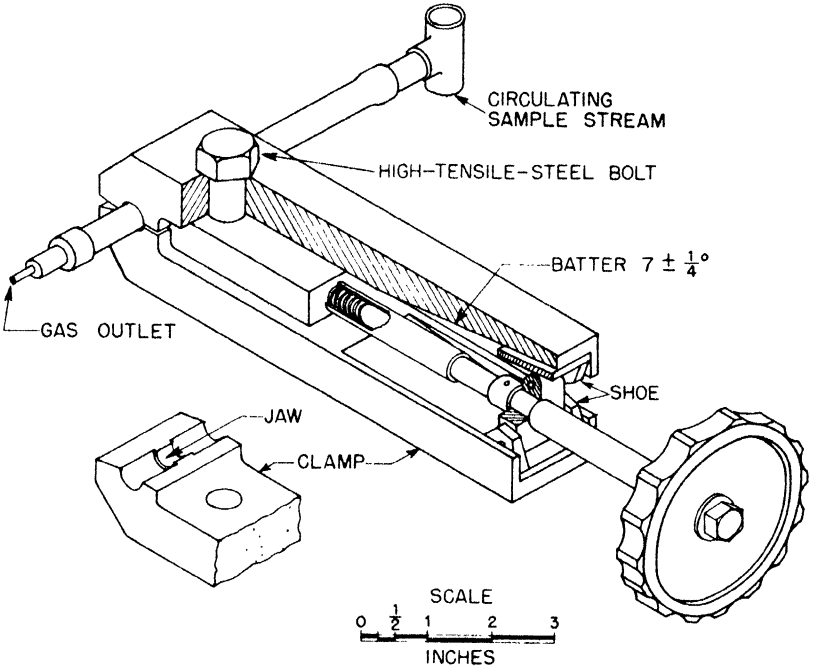

CRITICAL DIMENSIONS

O.D. OF LEAK TUBE AT JAW .3750"
I.D. OF JAW .3695 ± .0005"
I.D. OF LEAK TUBE AT JAW .3125"
O.D. OF LEAK TUBE AT JAW .3115 ± .0002"

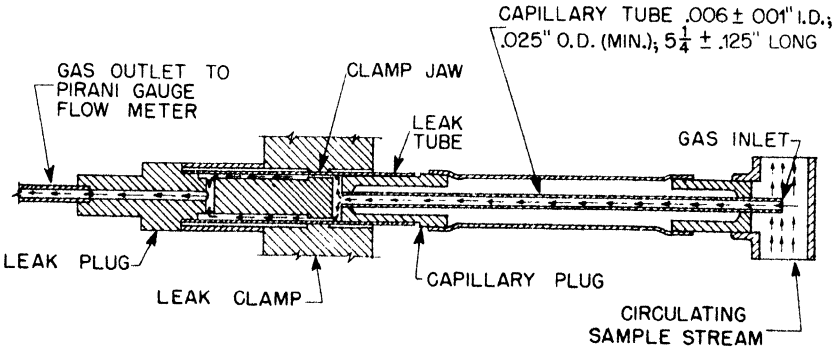

Fig. 1.3—Schematic and isometric drawing of the adjustable leak and capillary tube used on the recording mass spectrometer.

The reading of the Pirani gauge depends on the composition of the gas stream and on the pressure at the gauge. For a flow of pure UF_6 the pressure is determined by the flow resistance of that portion of the gas line between the Pirani gauge and the chemical trap. For a

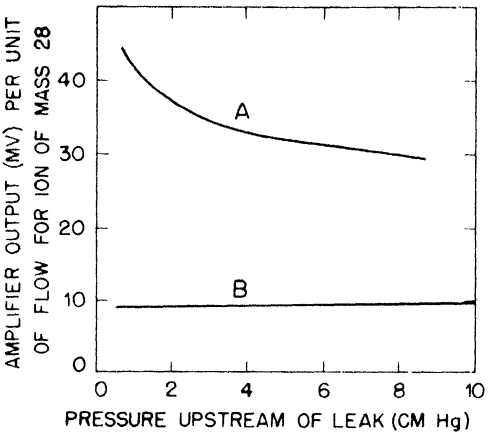

Fig. 1.4 — Effect of the capillary tube in compensating for the fractionating property of the adjustable leak. Measurements were made on sample gas mixtures of N_2 and UF_6. A, leak without capillary tube; B, leak with capillary tube.

flow of nitrogen or air the pressure is determined by the resistance of that portion of the line between the Pirani gauge and the diffusion pump. These resistances have been chosen so that, when the Pirani-gauge reading is held constant, the output of the amplifier corresponding to the nitrogen peak is approximately proportional to the concentration of nitrogen in the gas stream being analyzed. The instrument is calibrated with mixtures of nitrogen and UF_6 of known composition, and a correction curve is provided to relate amplifier output to nitrogen concentration.

The pressure-sensitive element of the Pirani gauge forms one arm of a bridge circuit. The unbalance of the bridge circuit is read on an indicating millivoltmeter as well as on the recorder. The pressure-sensitive element, consisting of a 0.003-in. nickel wire, is encased in a monel tube and has been found to be stable despite the corrosive nature of the sample gases. The normal operating pressure at the gauge is approximately 10μ Hg.

3. PERFORMANCE OF THE RECORDING MASS SPECTROMETER

Most of the recording mass spectrometers in the diffusion plant are used for automatic analysis of the process stream and are equipped with Pirani flowmeters and chemical traps for handling high UF_6 concentrations. A spectrometer chart is shown in Fig. 1.5. On the chart a nitrogen surge is observed at approximately 1:55 A.M. Concentrations of the gases for this test are indicated in the figure. The accuracy of their measurement is approximately 5 per cent of the reading, depending on the care taken in calibrating the instrument. The concentration of HF cannot be determined accurately with the standard instruments, since this gas is strongly adsorbed by the gas inlet system, and hence the response of the spectrometer is extremely sluggish.

The average consumption of UF_6 is less than 40 mg per instrument per day. Thirty seconds after the composition of the gas in the sample stream has changed, the spectrometer-tube ion current reflects this change. Most of this delay is caused by the time required for the gas to pass through the capillary tube at the adjustable leak. The appearance of this change on the recorder depends on the printing cycle. For nitrogen, which is printed every other point on the recorder, a change in concentration is recorded within a minute after it occurs in the sample stream.

Several of the recording mass spectrometers are provided with the alternate inlet system, as shown in Fig. 1.1. These are used to measure low concentrations of UF_6 and HF. Concentrations of UF_6 as low as 0.1 mole % and those of HF of 1 mole % may be measured with an accuracy of 10 per cent. The response time of these instruments is appreciably less than that of the others.

When it is desirable to obtain a complete analysis of all impurities in the sample stream, the multipoint recorder is replaced by a single-pen recorder and the ion-accelerating voltage is varied continuously with time so that the recorder draws a mass spectrum from mass 12 to mass 500. Figure 1.6 shows a portion of such a spectrum when dry air is introduced into the instrument. The spectrum includes several masses such as 20 (HF^+), 200 (Hg^+), and 100 (Hg^{++}), which are from residual gases in the system.

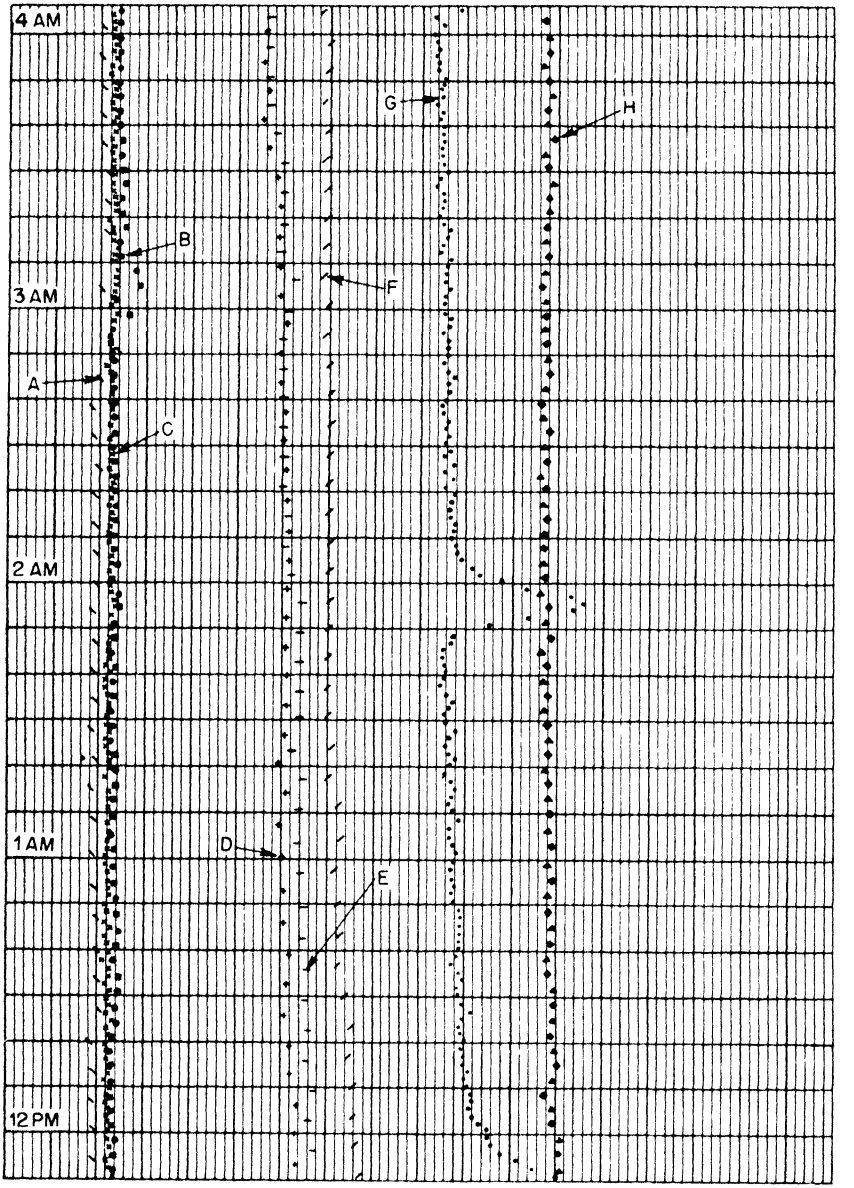

Fig. 1.5—A recording-mass-spectrometer chart showing concentrations of process-stream components. A, amplitude zero; B, O_2 mass 32, 0.2 per cent; C, N_2 mass 14, 6 per cent; D, HF mass 20, 2 per cent; E, CO_2 mass 44, 0.1 per cent; F, fluorocarbon mass 69, 0.2 per cent; G, N_2 mass 28, 6 per cent; H, total gas flow as measured by the Pirani gauge.

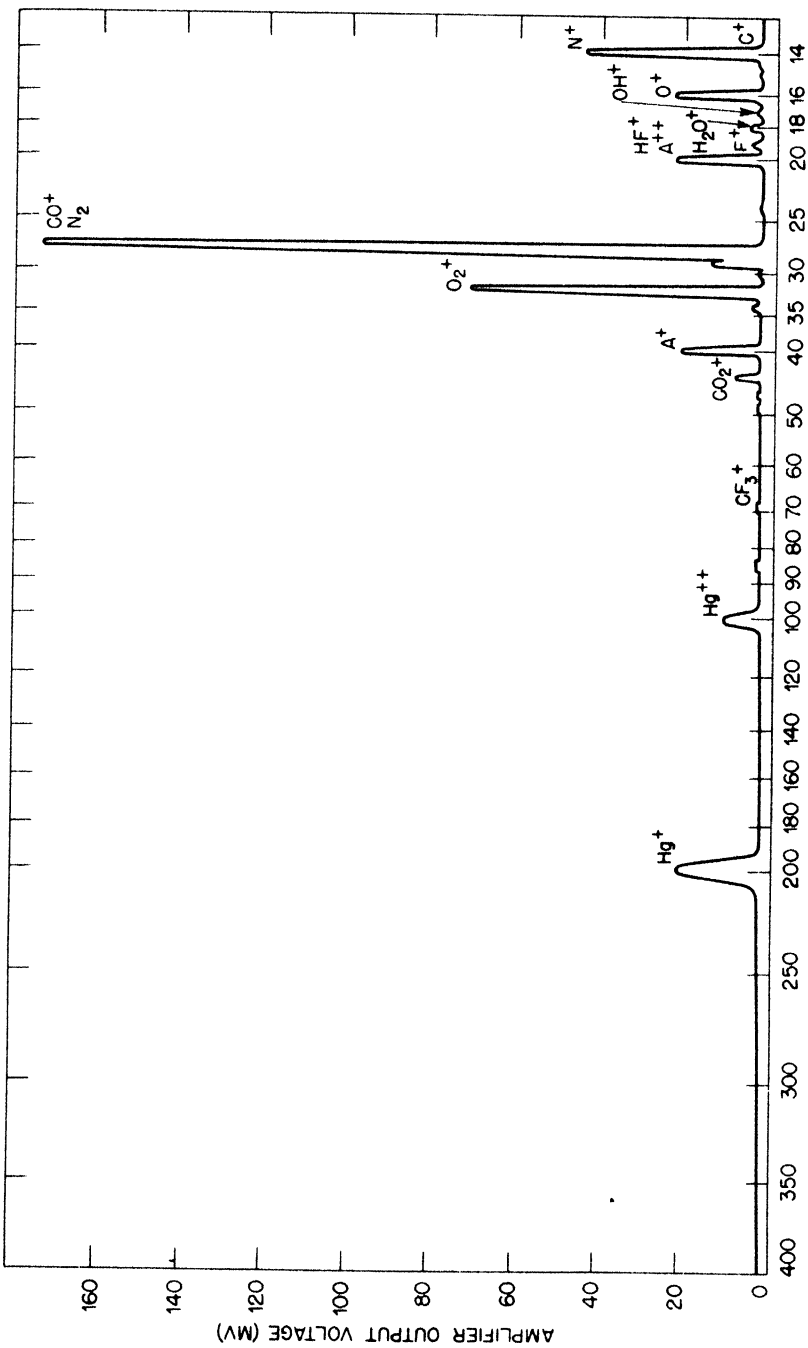

Fig. 1.6 — Typical automatic mass scan of air taken on recording mass spectrometer.

Chapter 2

RECORDING IONIZATION CHAMBER FOR TRACES OF RADIOACTIVE GASES

By A. O. Nier, C. M. Stevens, T. A. Abbott, and J. K. Pickard

1. INTRODUCTION

The recording ionization chamber described in this chapter is used to analyze continuously the UF_6 content of gas mixtures containing from 1×10^{-5} to 1 per cent of this substance in nitrogen. The recording mass spectrometer described in Chap. 1 is used for UF_6 concentrations between 0.1 and 100 per cent.

2. THE RECORDING IONIZATION CHAMBER

The recording ionization chamber measures the electrical conductivity of a fixed volume of sample gas. The conductivity of the gas, which results from the ionization caused by the radioactive disintegration of the uranium isotopes, is proportional to the quantity of uranium present. The range and accuracy of the instrument depend on the size and pressure of the sample, the background ionization, and the sensitivity of the conductivity measurement.

As used in the uranium plant, the ionization chamber is equipped for continuously analyzing and recording the UF_6 concentration. A typical installation of two instruments is shown in Fig. 2.1. The ionization chambers and their associated pumps, valves, and instruments are mounted in the steel housing shown at the right. One of the chambers can be seen through the open door; the other chamber is located inside the closed portion of the housing at the left.

A schematic diagram showing the interconnections of the component parts is given in Fig. 2.2. The sample gas is circulated through the chamber by special sylphon-sealed pumps. An automatically operated valve maintains constant pressure in the chamber.

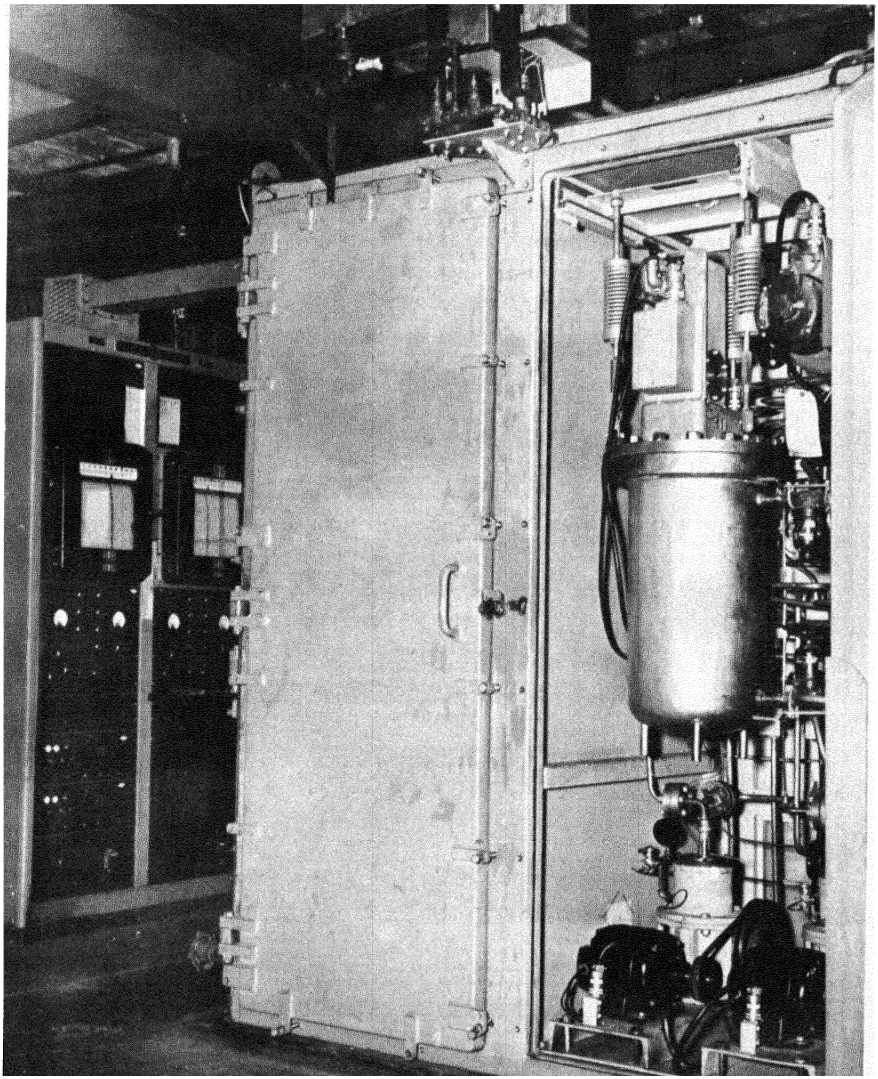

Fig. 2.1 — A typical installation of two recording ionization chambers as manufactured by the General Electric Company.

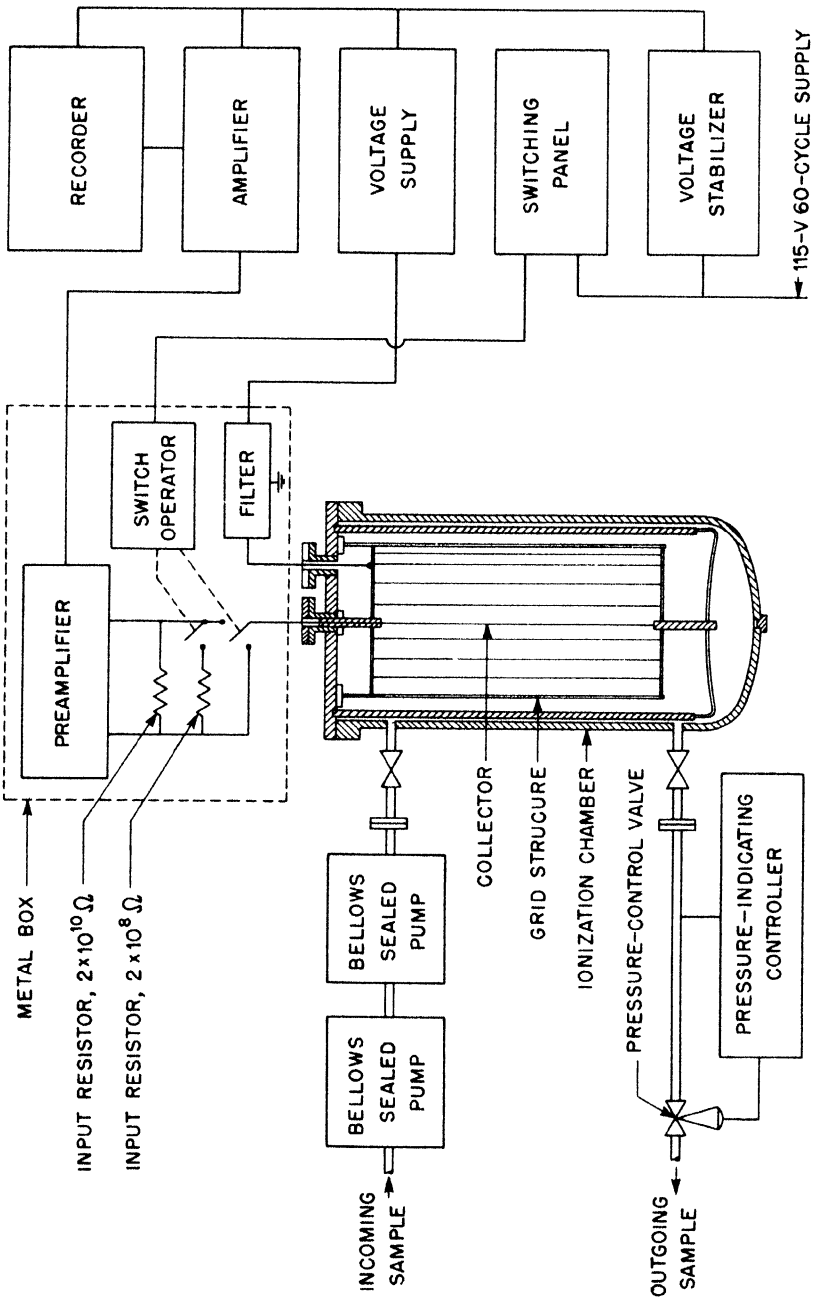

Fig. 2.2—Schematic diagram of the recording ionization chamber.

2.1 The Chamber. The radioactivity of UF_6 consists in the emission of high-energy alpha particles at a uniform rate. Since each of the uranium isotopes U^{234}, U^{235}, and U^{238} emits alpha particles at a different but definite rate, the combined rate depends on the relative isotopic constitution. The energy of the particles is approximately the same for the three different uranium isotopes. The particles lose their energy in the production of approximately 130,000 ion pairs. The range of the particles in gas at standard conditions is about 3 cm.

In order to detect low concentrations of UF_6 at a sample gas pressure of 10 psia, it is necessary to employ a chamber having an internal volume of approximately 1.5 cu ft. Although the sensitivity could be improved by using a gas pressure higher than 10 psia, it has not been found practicable with the available pumps. Because of the corrosive nature of UF_6, all surfaces in the chamber are made of nickel, with the exception of the insulators, which are made of a special noncorroding plastic.

The electrodes are mounted on the cover of the chamber as shown in Fig. 2.3. The collector, 0.025 in. in diameter, extends along the axis of the chamber and, after passing through a vacuum-tight plastic disk, connects to the preamplifier mounted outside the chamber. The disk has ten concentric grooves cut into its inner surface in order to increase the length of the electrical-leakage path. A grid structure consisting of a cage approximately 20 in. long and 8 in. in diameter is made of 0.0031-in. nickel wires, which are parallel with the collector and located around the cage at 1-in. intervals. These wires are mounted on a frame that consists of six insulated parts, a top and bottom ring structure for holding the grid wires, and diagonal bracing for increasing the rigidity. The entire structure is constructed of nickel, and every effort has been made to hold the surface area to a minimum.

The potential of the collector wire never rises more than a few millivolts above that of the chamber walls, which are held at ground potential. The grid structure is connected to a positive source of potential of several hundred volts. Thus, positive ions formed within the grid structure are collected by the collector wire. If the chamber is operated at a pressure of 10 psia or higher, none of the alpha particles originating from corrosion products on the inside wall of the chamber have sufficient range to penetrate the grid assembly. Hence the background ionization current in the device is due only to alpha particles originating on the grid structure and collector wire and to beta and gamma particles from decay products of uranium compounds on the inside surfaces of the chamber.

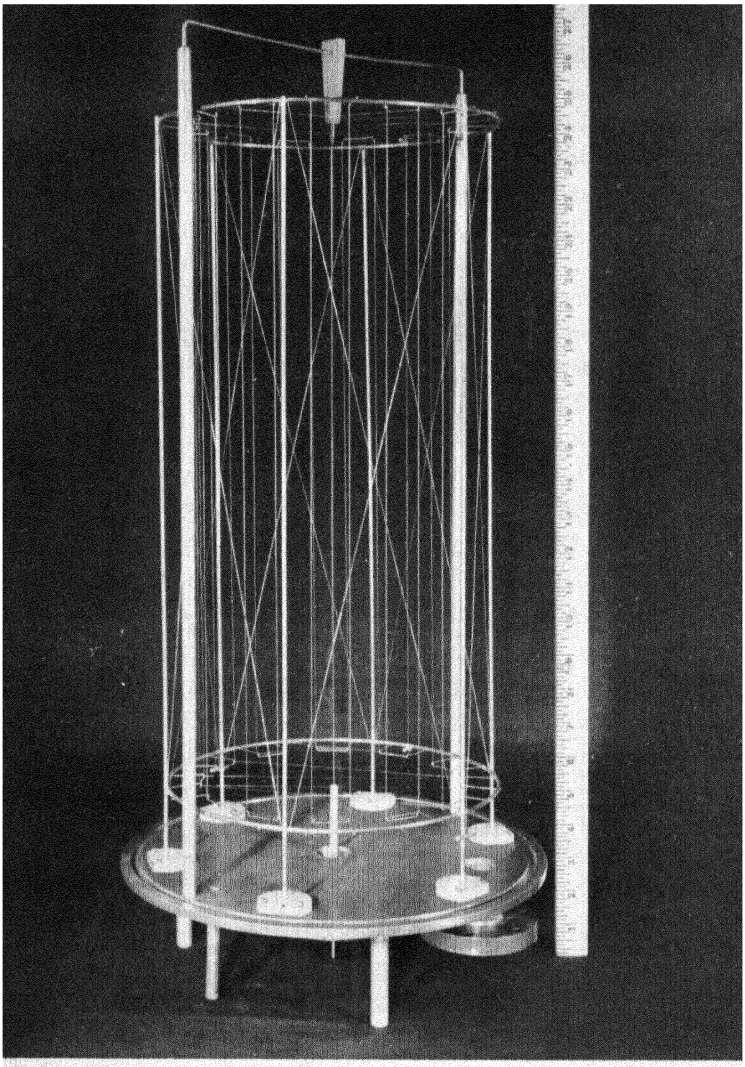

Fig. 2.3 — Electrode structures for the ionization chamber.

2.2 Voltage Supply. The voltage-supply circuits produce the constant regulated potential for the grid structure in the chamber. Positive potentials of either 300 or 750 volts are available. These voltages are carefully controlled and filtered, since any variation of the grid potential will induce charges on the collector wire and affect the stability of the current measurement.

2.3 Amplifier and Recorder. The small ion currents to the collector wire are amplified by an inverse-feedback d-c amplifier and measured on an indicating or recording instrument. The amplifier consists of four stages, the first two of which use 954 tubes and are mounted in a metal case attached to the cover of the ionization chamber.

Normally the ion current flows through the 2×10^{10} ohm amplifier input resistor. By a remotely operated switch, a 2×10^{8} ohm resistor may be connected in parallel with the normal grid resistor to change the range of the instrument by a factor of 100.

At 30-min intervals the collector lead is automatically switched from one end of the input resistor to the other to check the amplifier drift.

3. PERFORMANCE

The concentration of the UF_6 can be related to the ion current only when the relative concentrations of the uranium isotopes and their alpha activities are known. In those locations in the diffusion plant where the ionization chamber is used, the isotopic concentrations are measured by other instruments. For a pressure of 10 psia and a temperature of 50°C, the ionization current is 5×10^{-10} amp for each per cent UF_6, of normal isotopic composition, in air or nitrogen.

Only in the case of low concentrations of UF_6 in the chamber is the ion current proportional to the concentration. For high concentrations recombination of ions before collection takes place causes a deviation from linearity. For example, for an ion current of 5×10^{-10} amp with a grid voltage of 300 volts, an error of 10 per cent is introduced if linearity is assumed. This effect is smaller if a higher grid voltage is used. Figure 2.4 shows the percentage of ions collected as a function of the ion current. If the ion current exceeds 6×10^{-9} amp, the effect of recombination becomes so great that accurate measurement of UF_6 concentration is not practicable with a sample pressure of 10 psia. High concentrations can be measured by lowering the operating pressure of the chamber.

The residual ion current puts a lower limit on the concentration of UF_6 that can be measured in the ionization chamber. This current is due to a number of causes:

1. All materials contain traces of radioactive elements. Thus the materials of the chamber contribute to the residual current.

2. The passage through the chamber of gamma rays and cosmic rays produces a small residual ionization current. The combined effect of (1) and (2) produces a current of less than 10^{-13} amp.

3. The radioactive disintegration of uranium results in the formation of actinon and radon. The quantities of these gases are small, and their contribution to the residual current is entirely negligible.

4. The admission of UF_6 to the chamber results in the production of two additional sources of residual currents.

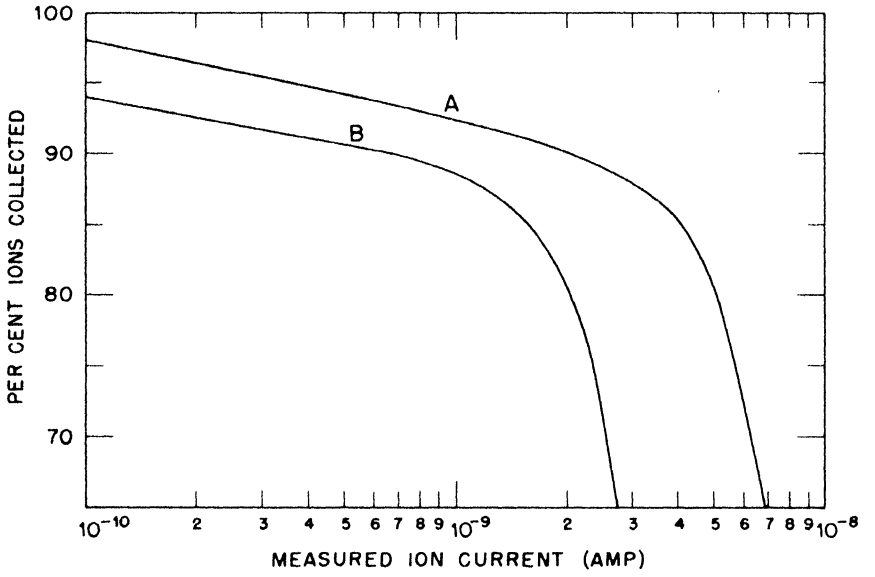

Fig. 2.4—Effect of recombination on the collected ion current. A, grid voltage, 750 volts; B, grid voltage, 250 volts.

a. The chemical reaction of UF_6 with the surfaces of the chamber or with any substances on the surfaces, such as water vapor, produces nonvolatile uranium compounds. The grid structure is located several centimeters from the walls of the chamber, so that alpha particles from the latter cannot reach the structure and hence do not contribute to the ion current. Despite the fact that the grid-structure surface has been reduced to a minimum, enough uranium compounds accumulate on it to emit an appreciable number of alpha particles into the collecting region.

b. The radioactive disintegration of the uranium in UF_6 results in the formation of nonvolatile beta and gamma emitters, which deposit on the walls of the chamber. Because of the great range of these particles the grid structure is ineffective in reducing the ionization current caused by them.

Figure 2.5 shows the manner in which the background depends on the exposure of the chamber to normal UF_6 under average plant conditions. Exposure is arbitrarily defined as the integration of concentration of UF_6 in mole per cent with respect to the number of hours of running. At the normal operating pressure of 10 psia, the residual

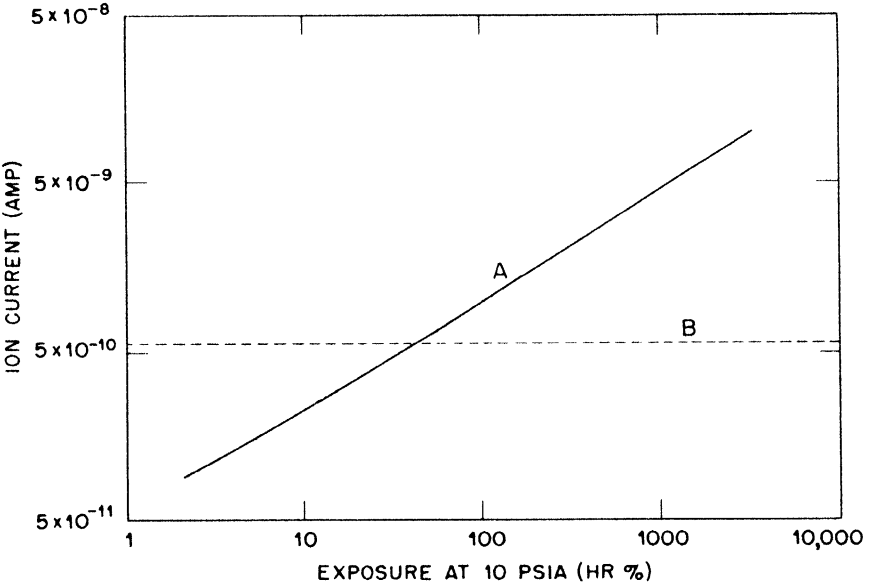

Fig. 2.5 — Effect of exposure on background ion current. A, ion current due to background at 10 psia; B, ion current for 10^{-3} mole % UF_6 of normal isotopic composition.

current continually rises as indicated in the figure. Extensive tests on the chamber at different operating pressures indicate that only a portion of this rise can be attributed to the formation of uranium compounds on the surfaces of the chamber. It is reasonable to assume that this rising residual current is due to beta particles, gamma rays, or both, coming from the radioactive disintegrations of the decay products of uranium, which accumulate in the chamber. The useful life of the chamber before cleaning is dependent on the degree of sensitivity of the measurements to be taken. Satisfactory measurements have been made after exposures of 100 hr %.

When the gas stream contains more than 5 per cent HF, the instrument is inoperable because of electrical leakage taking place across the insulators.

Chapter 3

MAGNETIC GEAR FOR TORQUE TRANSFER TO A CLOSED SYSTEM

By T. A. Abbott and J. K. Pickard*

1. INTRODUCTION

During the design of the uranium diffusion plant many methods of transferring motion to a totally enclosed system were considered. Certain special requirements such as the magnitude of the transmitted torque and displacement, the allowed diameters of outside and inside gears, and vacuum tightness of the inner parts complicated the problem. The magnetic arrangement about to be described could be used for transmitting both translational and rotational motions into closed systems.

2. MAGNETIC TRANSMISSION SYSTEMS

The design of magnetic transmission systems involves the disposition of magnetic poles in such a way that the relative motion of the driver and the driven member produces distortion in a magnetic field and thereby force between the members. Since it is desirable to obtain the maximum force with a given-size gear, a design employing several pole pieces, or teeth, was used.

The spacing and configuration of the gear teeth are the most important factors in the design of a magnetic gear, because they directly affect the flux density and distribution and consequently determine the maximum value of the transmitted force. In choosing the proper values of these factors, it is necessary to consider the effect which each of the tooth dimensions has on the force. Analysis of the problem is

*The authors wish to acknowledge the contributions made by L. T. Rader (now at the Illinois Institute of Technology, Chicago) and R. C. Goodwin of the General Electric Company; of J. B. McMahon (now at Republic Flow Meters Co., Chicago) of The Kellex Corporation; and of the Republic Flow Meters Company, which manufactured the gear and valve.

difficult because of the many variables, the complexity of the magnetic field, and the nonlinearity of the magnetic relationships. Many experimental data have been taken, and it is this rather than a rigorous analysis which has determined the design of the gear.

A schematic sketch of the equipment used in testing the teeth is shown in Fig. 3.1. Teeth were cut in steel blocks, which were bolted

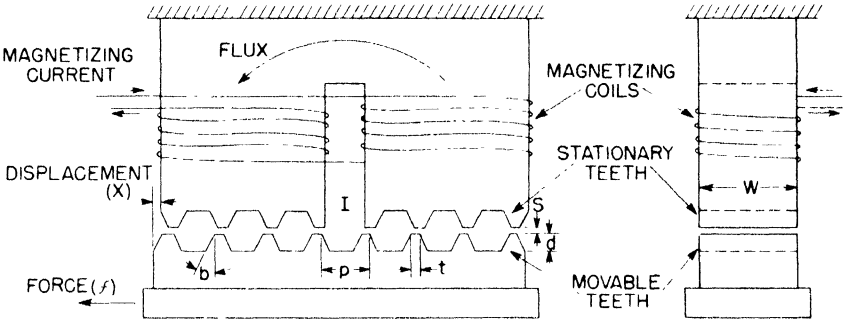

Fig. 3.1 — Schematic arrangement for testing different tooth shapes and spacings.

in a fixture the bottom part of which was mounted on steel balls and thus could move freely in a horizontal direction. The flux was set up by the current through the coils, and its value was determined on a flux meter. For a constant value of flux, the displacement, x , was determined for the force, f, between zero and its maximum value. Characteristic force-displacement curves are shown in Fig. 3.2.

More than 30 sets of teeth were tested by the arrangement shown in Fig. 3.1. The ranges of tooth dimensions and other variables that were tested are given in Table 3.1.

Table 3.1 — Values of Tooth Dimensions and Other Variables Tested

Tooth pitch (p)	0.375 to 0.8125 in. (8 values)
Tooth width (t)	0.109 to 0.2065 in. (8 values)
Tooth length (w)	1.00 in.
Tooth depth (d)	0.250 to 0.4375 in. (7 values)
Tooth angle (b)	0, 10, and 20 deg
Air gap (s)	0.045 to 0.065 in. (4 values)
Flux density at end of tooth	25 to 45 kilo-lines/sq in. (r values)

Tests were made on each set of teeth at three or more different values of zero displacement flux. For convenience in comparing the data taken under different conditions, the force has been expressed in pounds per square inch of total surface area.

The effect of the tooth angle, b, on the maximum force is pronounced and reasonably consistent over the range of values tested. The maximum force decreases as the angle increases. The force at 10 deg is approximately 70 per cent of that at 0 deg, and at 20 deg approximately 60 per cent of that at 0 deg. Representative values are shown by the curves in Fig. 3.2.

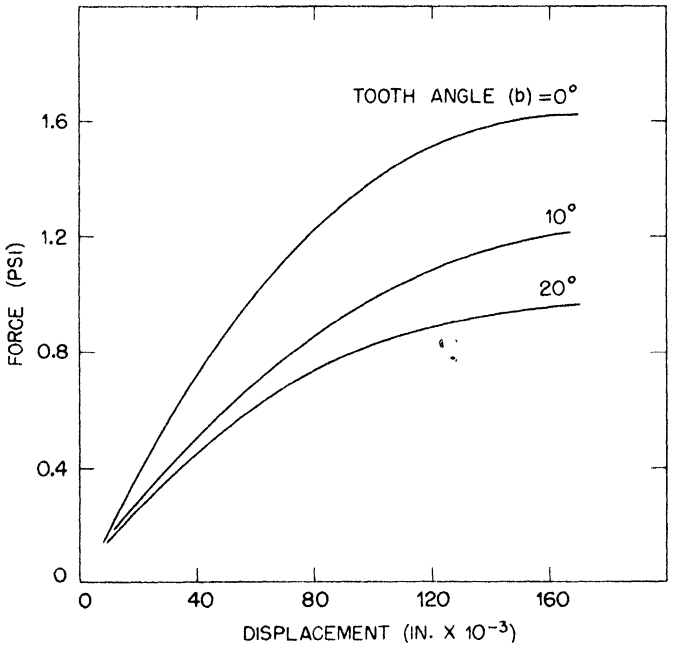

Fig. 3.2—Typical force-displacement curves for different tooth angles, where p = 0.6555 in., t = 0.1875 in., d = 0.375 in., w = 1.00 in., s = 0.055 in., and air-gap flux at tooth end = 35 kilo-lines/sq in.

For each value of tooth width, t, and depth, d, there is a value of tooth pitch which yields a maximum force. Figure 3.3 shows the nature of this relationship for values of t and d substantially the same as those used in the final design of the magnetic gear.

The available data indicate that the optimum value of tooth depth occurs when the depth equals approximately twice the tooth width (d = 2t).

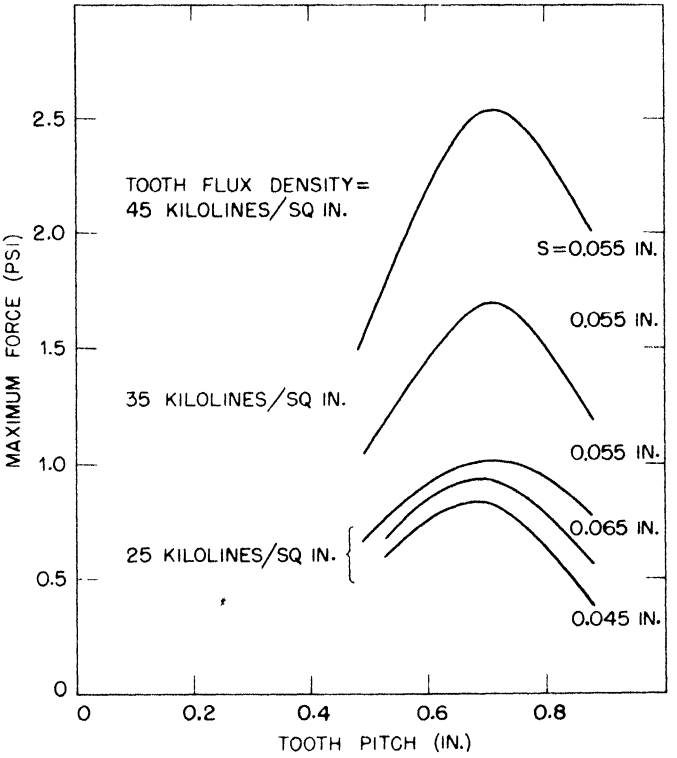

Fig. 3.3—Effect of tooth pitch on maximum force transmitted across air gap for different values of tooth flux density and air gap, s, where t = 0.1875 in., d = 0.375 in., w = 1.00 in., and b = 0 deg.

For a given flux density and given tooth dimensions, there is a value of gap, s, which produces a maximum force. This optimum value of s for the dimensions of teeth tested is approximately 0.06 in. The maximum force increases approximately as the square of the flux density.

3. MAGNET DESIGN

The magnetic circuit should be so designed that the teeth operate near the knee of the saturation curve and thus create a maximum

value of useful flux with a minimum value of leakage flux. If permanent magnets are used, the maximum output of the magnet as well as the saturation of the teeth must be considered. The most efficient design is that one which delivers the greatest transmitted force per square inch of surface area per ampere turn of magnetomotive force, or per pound of permanent magnetic material. This basis for the evaluation of a design differs from that discussed above by including the value of magnetomotive force required to set up the flux. The effect of tooth design proved to be substantially the same for this new basis as for the original one, where only the pull-out force per square inch of surface area was considered.

The maximum pull-out force depends to a considerable degree on the leakage flux in the region I of Fig. 3.1. If the upper and lower teeth are lined up, the leakage flux varies inversely as the tooth pitch, since the tooth pitch determines the distance between the magnets. A typical value of leakage is 6 to 10 kilo-lines/sq in. in the region I, with a tooth pitch of 0.4375 in., a gap of 0.050 in., and a flux density of 29 kilo-lines/sq in. at the end of the teeth. By separating the magnets and their pole pieces a distance of a two-tooth instead of a one-tooth pitch, the pull-out force per tooth for the condition just described was increased 35 per cent. However, the pull-out force per square inch of surface was decreased 20 per cent. Thus, in choosing the tooth pitch, consideration should be given to maintaining a favorable balance between the leakage and effective flux.

4. APPLICATION OF THE MAGNETIC GEAR

The design of a magnetic gear for use in the uranium plant had to meet certain rather exacting specifications. The casing and diaphragm surrounding the inner parts had to be vacuum-tight and able to withstand a pressure difference of 15 psi. The inner bearings had to operate dry. The maximum transmitted torque had to exceed 10 lb-ft and have a displacement associated with this torque of no more than 5 deg. The total travel of the vane had to be at least 70 deg. Space limitation in the plant indicated that the outside diameter of the gear should not exceed 14 in. The strength of the diaphragm limited the width of the internal face of the gear to 1.125 in.

The final design of the gear is shown in Fig. 3.4. Ten permanent magnets made of Alnico II are mounted on the inner side of a ring of soft iron. This assembly serves as the outer rotor. It is carried on an overhanging bearing and driven by a standard air-diaphragm motor. The sealing diaphragm, which has a thickness of 0.025 in., is spot-welded to the circular end walls. The total gap between the driving and driven teeth is 0.065 in.

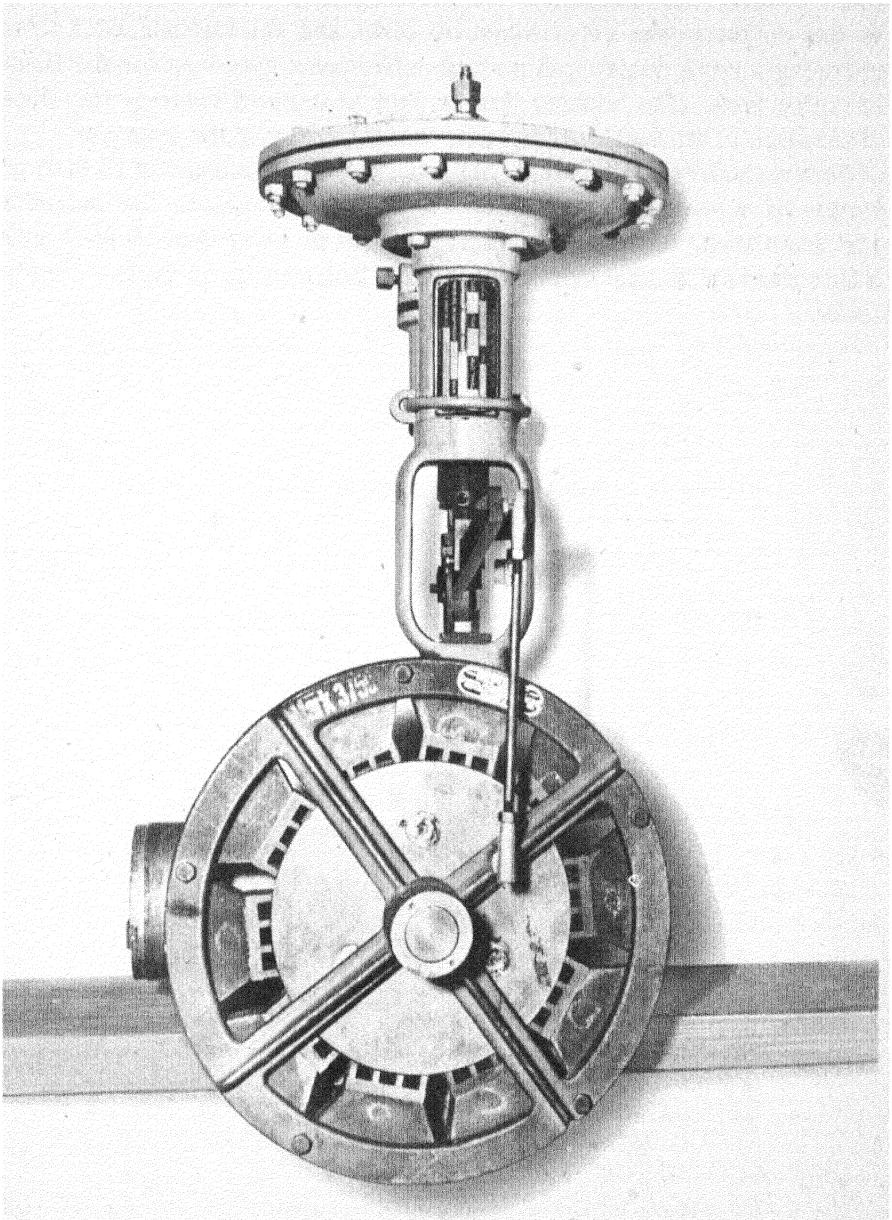

Fig. 3.4 — Magnetic gear as used with a standard air motor.

A total of 40 pairs of teeth having a p/t ratio of 3.5, a pitch of approximately 0.65 in., and an average depth of about 0.38 in. have been found to give the maximum transmitted torque. The optimum size of the magnets was determined by tests and calculations after first choosing a tooth design and making sufficient allowances for the flux-carrying iron. The leakage flux is kept at a small value by the wide separation of the teeth and the trapezoidal shape of the magnets.

Under plant conditions the gears develop approximately 13 lb-ft of torque at a maximum displacement of 2.5 deg. Before the magnets are stabilized, the gear develops a torque of more than 15 lb-ft with a flux density of approximately 36 kilo-lines/sq in. at the face of the teeth.

Part 2

VACUUM ENGINEERING

Chapter 4

MASS SPECTROMETERS FOR LEAK DETECTION

By A. O. Nier, C. M. Stevens, A. Hustrulid, T. A. Abbott, F. S. Stein, and J. E. Binns*

1. INTRODUCTION

The problem of finding small leaks in a high-vacuum system constructed of metal or of glass and metal has always been a difficult and tedious task. Many methods for facilitating the location of leaks have been studied and described.[1,2] Most of the methods depend upon looking for a change of pressure in the system when the part suspected of leaking is waxed or closed with some other substance; or upon looking for a change in the nature of the gas or vapor in the system when the part under test is painted with ether, carbon tetrachloride, or other liquids, or when a stream of gas, such as carbon dioxide, hydrogen, or helium, is directed on it. The device for indicating changes in pressure or in the nature of the vapor mixture must be very sensitive in order to find small leaks in systems having many leaks or in systems having surfaces which outgas and hence act as virtual leaks.

Of the various methods for hunting leaks, the scheme of directing a stream of relatively inert test gas at the suspected part of the apparatus and then looking for changes in the concentration or the presence of this particular gas in the system under test has many advantages. Some of these are:

1. The test gas will not contaminate the system or the pumps.
2. It will enter the system readily through small leaks.
3. There is no danger of closing a leak and having it open some time later.

*The authors wish to acknowledge the many contributions made by R. B. Thorness to the design and development of the leak-detecting spectrometer.

4. Once a leak is found, there is no time lost in continuing the hunt because the test gas entering the system is quickly pumped out.

The ideal "leak detector" is, then, an instrument that continually samples the gas in the system and instantly notes the presence or change in concentration of the test gas regardless of the presence of other gases or vapors.

A method that has been used with success in the construction of large vacuum equipment employs a new leak-detecting instrument and improved vacuum techniques. The outstanding contributions have been the development of a special mass spectrometer and a method of using it with a tracer gas in the location of minute leaks.[3]

A typical testing arrangement employing the tracer-gas method, and using a mass spectrometer as a detector, is shown in Fig. 4.1. The system that is thus being tested is evacuated by the continuous action of the vacuum pumps. An atmosphere of tracer gas may completely surround the system, or a small jet of it may be used to probe the suspected zones. Any tracer gas that leaks into the system is rapidly detected by the mass spectrometer, which continuously samples the gas being pumped from the system under test. Helium is one of the best tracer gases because it has a low molecular weight, does not occur to any extent in air or in other gases, is not adsorbed on the surfaces, can be readily pumped out of the test equipment, and is easily procured.

2. THE NIER-KELLEX-GENERAL ELECTRIC LEAK DETECTOR

It was decided that the problem of leak testing could best be met by the use of a mass spectrometer with helium as probe gas.

The first portable instrument of this kind was built at the University of Minnesota by Nier in the spring of 1943. It was a simplified form of the mass spectrometer with the 60-deg sector-shaped magnet which he had been using since 1940 for isotopic analysis.

Working in The Kellex Corporation laboratories, Nier and Stevens later improved this preliminary model by including an all-metal spectrometer tube and diffusion pump and a special electrode at the collector end of the tube for decreasing the background ion current.

The completed instrument is shown in Fig. 4.2, and the details of the all-metal spectrometer tube in Fig. 4.3.

The gas enters the tube at the top and is ionized by a stream of electrons, which are emitted from the heated filament and accelerated toward the trap. The number of ions produced depends on the electron emission and energy and on the gas pressure in the ionizing electron beam.

The ions are pulled out of the electron beam and accelerated by an electric field between the shield and the plate containing the source slit. The emission regulator contains the necessary electronic rectifying and regulating circuits for maintaining the desired potentials on the accelerating and focusing plates as well as for holding the electron emission constant at any desired value.

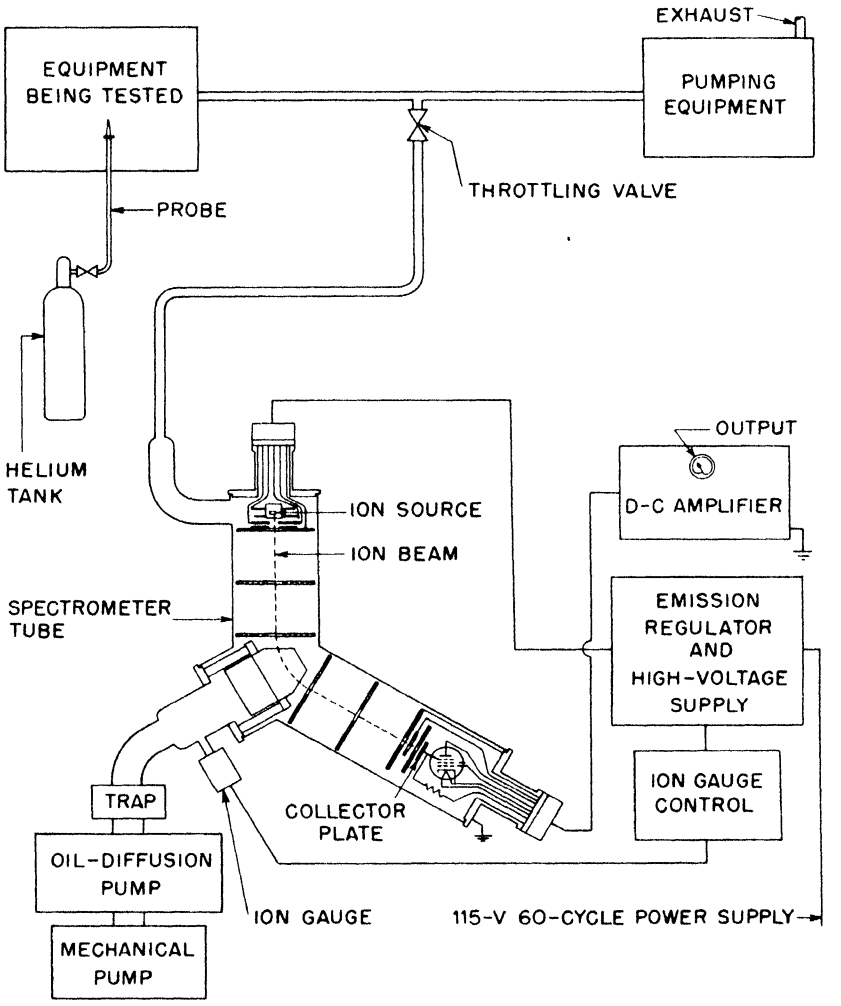

Fig. 4.1—Schematic diagram of typical leak-testing setup, showing interconnections of mass-spectrometer components.

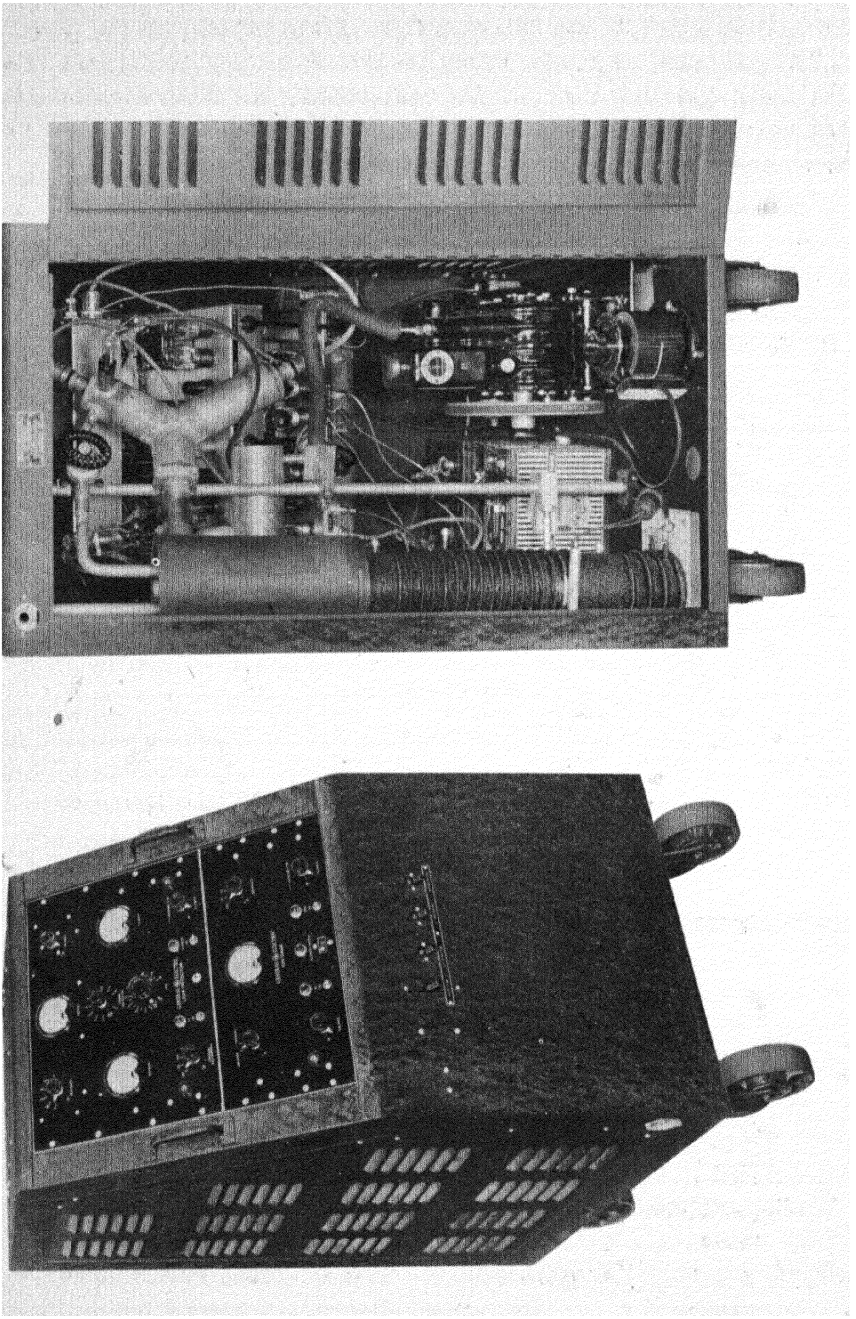

Fig. 4.2 — Leak-detecting mass spectrometer as manufactured by the General Electric Company. Left, front view; right, rear view.

A magnetic field is produced between the iron pole pieces by a permanent magnet. Since the magnetic field is wedge-shaped, it has a refocusing property for divergent ion beams as well as a resolving property.[3-6] The magnetic strength is such that an ion-accelerating voltage of about 300 volts is required for collecting helium ions.

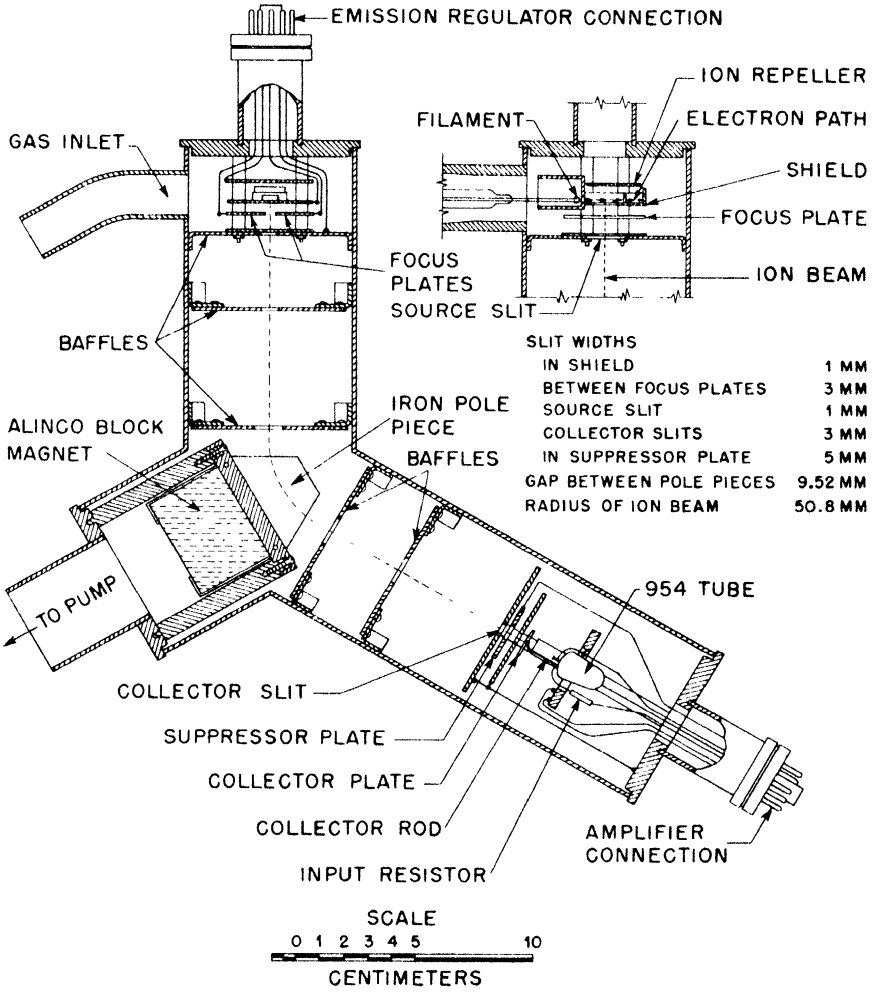

Fig. 4.3 — All-metal spectrometer tube for leak-detecting mass spectrometer of the Nier-Kellex-General Electric type.

After leaving the magnetic field, the selected ion beam passes through two baffle plates and a suppressor plate before striking the collector plate. The intensity of the selected ion beam is measured by a conventional battery-powered negative-feedback amplifier with a milliammeter as an output meter. As shown in Fig. 4.3, the first stage of the amplifier, which consists of a 954 tube and a 10^{11}-ohm input resistor, is mounted inside the spectrometer tube.

The pressure in the spectrometer tube is measured by an ion gauge whose electron emission is held constant by electronic regulating circuits. The ion gauge is provided with a special filament-cutoff circuit consisting of an amplifier tube and a relay. This circuit protects the ion-gauge and spectrometer-tube filaments from burning out by automatically cutting off their currents when the pressure exceeds a predetermined value.

The tube is evacuated by a high-speed oil-diffusion pump. A liquid-nitrogen trap between the pump and the spectrometer tube is used to achieve a residual pressure of 2×10^{-6} mm Hg in the tube. The pumping speed measured at the ionization gauge is about 30 liters/sec. This ensures a rapid response of the instrument to the changes in tracer-gas concentration at the throttling valve. In probing, an indication is obtained on the output meter within a few seconds after the probe passes a leak.

Performance of the Leak-detecting Mass Spectrometer. Although the instrument can be used to detect any one of several different gases by the adjustment of the ion-accelerating voltage, it is normally tuned to indicate only He^+ ions. The selectivity of the instrument is shown by the mass spectrum of air containing a small amount of helium; the spectrum is plotted in Fig. 4.4. The amplifier output current is plotted for the different values of the ion-accelerating voltage. The heights of the current peaks are proportional to the relative concentrations of the ionized gases in the sample. High sensitivity is made possible by two special features of the tube, which will be explained below.

If the pressure in the tube is increased, the peaks increase in height since more ions are produced. Unfortunately, increased pressure also greatly increases the width of the peaks at the base, especially on the high-voltage side of the peak. This produces an increase in background that more than offsets the advantage gained because of the increased height of the peaks. The background is increased because at the higher pressure more nitrogen and oxygen ions lose

energy by collision in passing through the region between the source and the magnet and are collected at the same time as the ions of lower mass.

The insertion of a baffle between the ionization chamber and the rest of the tube ensures a high pressure in the ion source without a correspondingly high pressure in the rest of the tube. Thus this baffle materially increases the effective sensitivity of the tube.

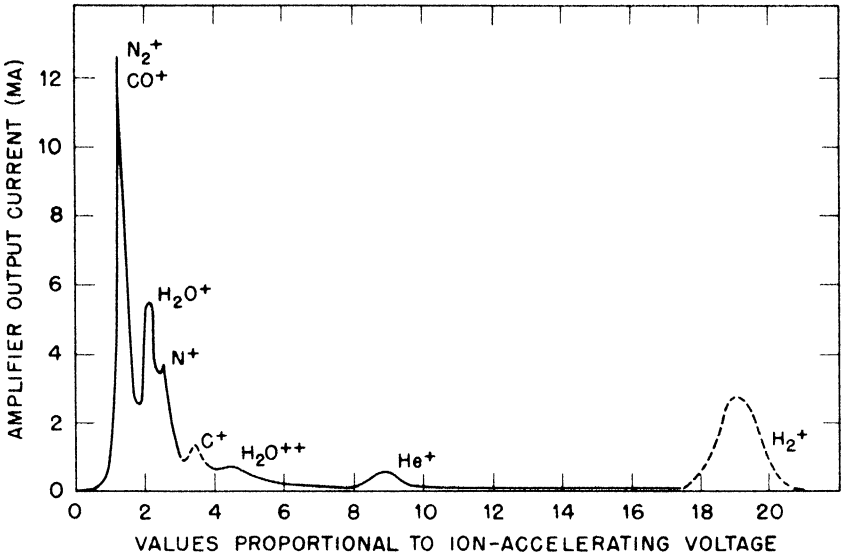

Fig. 4.4 — A typical mass spectrum of air and helium taken on a leak-detecting mass spectrometer.

A further increase in sensitivity has been obtained by the use of a suppressor plate, which is placed just ahead of the collector plate. This plate is operated at a potential near that of the ionizing region, so that those ions which have lost energy by collision cannot pass through the slit in the suppressor plate and are not collected on the collector plate. Thus the oxygen and nitrogen ions, which have lost energy and would otherwise be collected along with He^+ ions, are repelled, and the background is again decreased to materially increase the sensitivity to helium as shown in Fig. 4.5. Moreover, the He^+ ions in passing through the suppressor plate lose almost all their energy, so that they produce only a negligible number of undesirable secondary electrons.

Under normal conditions the throttling valve connecting the spectrometer was opened until the ion gauge indicated a pressure of 10^{-5} mm Hg in the spectrometer-pump lead. This corresponded to an ion-source pressure of 2×10^{-4} mm Hg. With an electron emission of 5 ma and a helium-air mixture of 1:10,000, a He^+ ion current of 6×10^{-12} amp was obtained. This corresponded to a full-scale deflection of the output meter. Since it was possible to detect conveniently He^+ peaks as small as 5 per cent of full-scale reading of the output meter, the sensitivity of the instrument was said to be 1 in 200,000.

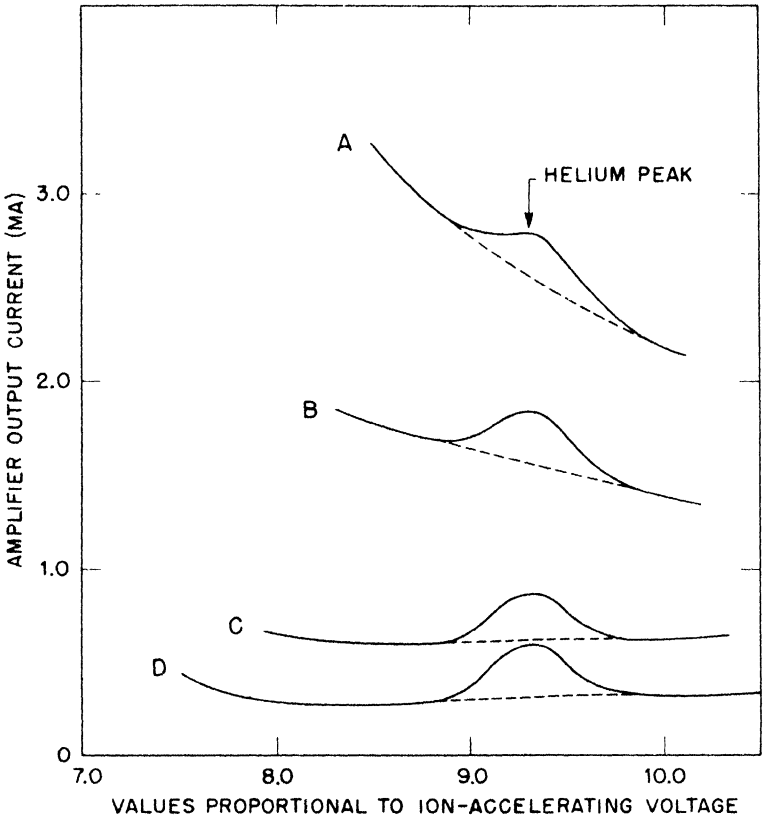

Fig. 4.5—Effect of suppressor field on mass-spectrometer background current in the region of the He^+ peak, for a sample having 1 part He to 50,000 parts of air. Pressure in spectrometer-tube body = 1.1×10^{-5} mm Hg. Pressure at ion source = 20×10^{-5} mm Hg. Suppressor voltage: curve A, 0 volts; curve B, +175 volts; curve C, +250 volts; curve D, +400 volts.

In order to reduce the sensitivity of the apparatus, it was possible to reduce the electron emission or add resistance to the output-meter circuit. A sensitivity reduction of a factor of 1,000 could be obtained.

3. MASS SPECTROMETER OF NEW DESIGN — S.A.M. MODEL

The leak detector described in Sec. 2 was found to decrease in sensitivity over periods of continued use because of an insulating, carbonaceous deposit formed on the source electrodes by electron bombardment. This required the tedious procedure of dismantling, cleaning, and reassembling the instruments at intervals ranging from one to four weeks.

Further disadvantages of this machine were: (1) occasional instability of the output of the d-c amplifier because of the high gain required in measuring currents as small as 10^{-14} amp; (2) bulkiness due to an excessive amount of electronic equipment and batteries; (3) unsatisfactory suppression of low-energy ions; and (4) inconvenient method of assembly of the envelope and source of the mass spectrometer.

In order to overcome these difficulties, the spectrometer about to be described was developed in the S.A.M. Laboratories by Stein and Binns. Magnetic focusing by means of a solenoid in the source and curved pole pieces in the analyzer is utilized.

3.1 The Magnet. The pole pieces were designed to bring to a line focus all the ions formed in a broad region and traveling in the axial direction. This arrangement leads to several advantages: (1) Higher sensitivity is achieved because ions from a large volume are collected. (2) New types of source design, containing electrodes not readily contaminated, may be used. (3) The magnet is located externally, reducing the size of the tube and leading to general convenience.

The design was adapted from that used in 1934 by Smythe, Rumbaugh, and West for collecting small quantities of isotopes.[7] A brief account of the method of construction follows.

Assume the edge effect of the magnetic field to be effectively equal to the gap width W between the pole pieces, and choose an appropriate value R for the radius of curvature which must be imposed on the ions to be collected. Considering the first quadrant of a rectangular coordinate system, construct arcs of radii $(R + W)$ and $(R\sqrt{2} - W)$ with their respective centers at the points (0,0) and (R,0). The latter arc represents the incident side of the analyzer. Then every ion path that can be represented in the construction by a line $x = k$, where x is measured along the abscissa and $0 \leq k \leq (R + R\sqrt{2})$, will be curved in the magnetic field and pass through the origin, or focal point.

The gap width W was made ½ in., and only values of k between 1.2R and 1.5R were used. The values for R and for the magnetic-field intensity were chosen with the object of increasing the voltage required to accelerate helium ions, in order to increase resolving power. Table 4.1 compares these and other pertinent data with the corresponding values for the early models of leak detectors. The magnet assembly is shown in Fig. 4.6. Soft iron was used for the pole pieces and yokes, and the magnet was cast of Alnico V.

Table 4.1—Comparison between Mass Spectrometers

	Early models, average	New model
Radius of curvature, cm	5.08	7.00
Field intensity, oersteds	910	1,050
Accelerating potential for He^+, volts	250	640
Collector current, for standard helium sample, amp	5×10^{-12}	100×10^{-12}
Amplifier sensitivity, arbitrary units	10	1
Over-all instrument sensitivity, scale divisions	150	350
Decrease in sensitivity after 3 weeks of continuous operation, %	60–95	0

3.2 The Collector Assembly. Three circular metal plates, having successively larger rectangular apertures at their centers and spaced at 3-mm intervals, are mounted on a flange at the exit end of the mass spectrometer along with the first amplifier tube (954) and its grid resistor of 10^{10} ohms. The first of these electrodes, located at the center of curvature of the concave sides of the pole pieces, serves as the collector slit. This is followed by the suppressor plate and a grounded shield plate, behind which a rectangular metal plate serves as the ion collector.

The need for the suppressor may be attributed to pressure scattering, which is much in evidence at the operating pressure (about 10^{-4} mm Hg). This causes the simultaneous collection of ions of various e/m ratios, with the result that even if no helium is in the system an output reading may appear when the voltage is such that only helium ions should be collected.

This background reading, which limits the sensitivity of the instrument, is minimized in practice by setting the suppressor and the first accelerating grid at the same potential. Thus ions which are formed at a further point or which have lost energy by collision will not have sufficient energy to penetrate the suppressor retarding field. Several

fine wires spot-welded across the slit act to increase the efficiency of the suppressor. Some background may appear owing to scattered high-energy hydrogen ions, but the effect is small because of the wide voltage separation between the hydrogen and the helium peaks.

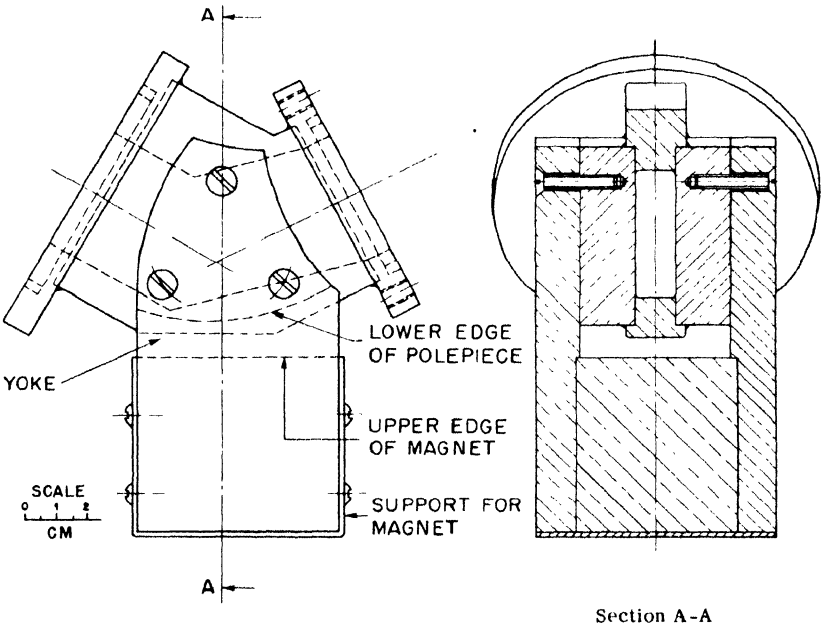

Fig. 4.6 — Left, magnet assembly of the S.A.M. spectrometer; right, cross section A-A of S.A.M. spectrometer.

3.3 The Envelope. The tube design permits ready dismantling and reassembling when necessary. Onto the brass section which supports the magnet assembly (see Fig. 4.6a and b) are soldered two grooved flanges. Into the larger of these fits a 5-in. length of brass pipe, which contains a side arm used as the pumping channel for the tube and as a support. On the opposite end of this pipe rests the flange on which the source is mounted (Fig. 4.7). Annular rubber gaskets in the grooves allow compression seals to be effected, with the aid of three long studs that span the pair of flanges. The flange supporting the collector assembly is similarly mounted; in this case the studs are also needed to ensure proper alignment of the collector slit.

3.4 The Ion Source. The construction of the source is indicated in Fig. 4.7. Three studs support the electrodes, and two Kovar-glass seals are used in making electrical connections. The grids consist of fine-mesh screen. One grid fits tightly into the anode, and the other

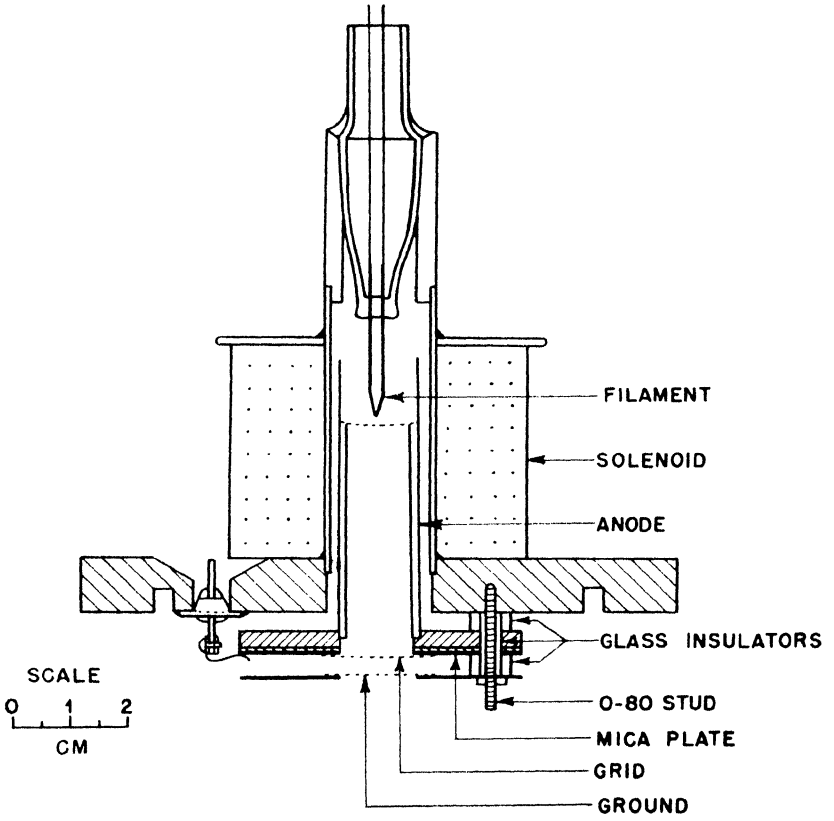

Fig. 4.7—Cross section of S.A.M. spectrometer source mounted on flange.

two grids are spot-welded to nichrome plates. The center grid is insulated from the anode by a thin sheet of mica, so that a potential difference may be applied between the two electrodes. The external solenoid, supplied by the A battery required in the d-c amplifier circuit, provides the electron-focusing magnetic field.

In operation the magnetic field has an optimum value at the center of the anode of 700 oersteds. This imposes on the 140-volt filament

electrons a radius of curvature of approximately 2 mm. A 15-volt field between the center grid and the anode serves to draw out the positive ions formed therein. The ions then receive a further acceleration of 640 volts between the two closely spaced grids when the mass spectrometer is adjusted for helium.

Among the advantages arising from the use of a magnetron source of this kind are the following:

1. Because of close spiraling of the electrons, their path lengths are greatly increased, thereby increasing the probability of ionization, and, in addition, they are prevented from reaching the anode and contaminating it. They are prevented from hitting the lower part of the anode by using magnetic material for the annulus at the base of the anode and thereby straightening out the magnetic field.

2. All electrons leaving the filament are impelled to move in the desired direction, because the field from the grid below the filament attracts the electrons while the ground field, which penetrates from above, repels them strongly.

3. The filament grid resists contamination, since it is kept hot by radiation and electron bombardment from the filament. It can be replaced very simply, if necessary.

4. The source can easily be disassembled and reassembled. Cylindrical symmetry ensures ready centering and alignment of the electrodes.

5. The power supply is relatively simple (see Fig. 4.8). Only three electrodes and the filament need be supplied. The latter requires no emission-regulator circuit, since space charge regulates emission perfectly.

6. The ion current to the collector has been increased over that in the sector-type mass spectrometer by a factor of 20. A less sensitive, and therefore more stable, amplifier may thus be used while retaining a sufficiently high sensitivity (see Table 4.1). At present a conventional four-stage d-c amplifier is used. If further increases in collector current can be attained, the time constant of the circuit may be reduced sufficiently so that an a-c amplifier may be used. Simplification in electronic equipment, including the elimination of batteries, would result.

3.5 Conclusion. The mass spectrometer described above has been found to resist contamination and for this reason retains its high sensitivity for extended periods of time. It is thought capable of operating for several months without having to be cleaned. It is sufficiently sensitive so that 1 part of helium in 150,000 parts of air can be readily detected. Simplicity of design and ease of maintenance are outstanding features. Further development of the instrument is warranted.

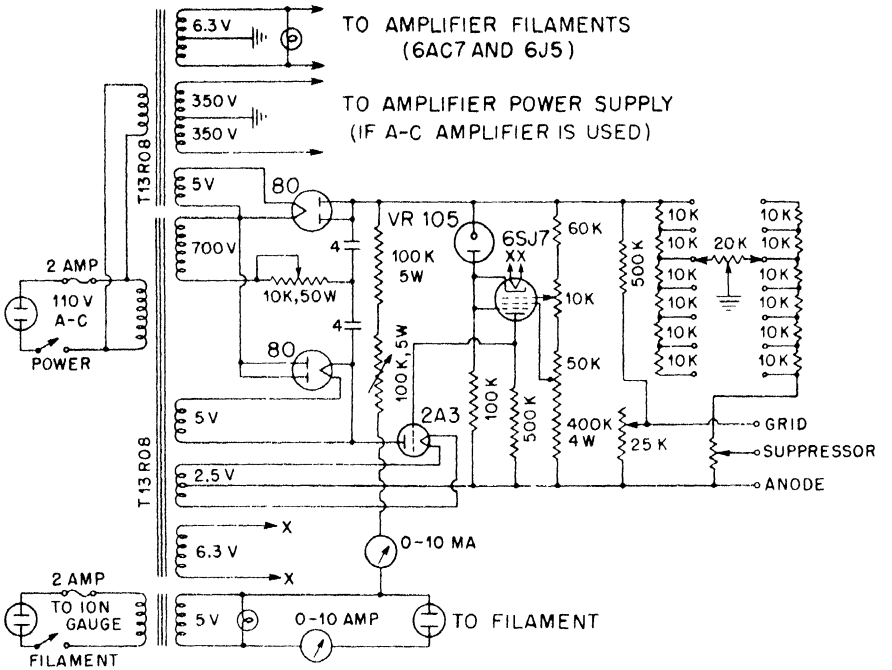

Fig. 4.8 — Power supply for the S.A.M. spectrometer.

REFERENCES

1. J. Strong, "Procedures in Experimental Physics," pp. 134–137, Prentice-Hall, Inc., New York, 1942.
2. E. J. Lawton, More about Vacuum Leak Testing, Rev. Sci. Instruments, 11: 134 (1940).
3. A. O. Nier, A Mass Spectrometer for Routine Isotope Abundance Measurement, Rev. Sci. Instruments, 11: 212 (1940).
4. W. E. Stephens and A. L. Hughes, Refocussing of Electron Paths by Means of a Magnetic Field (Abstract of paper read at the Proceedings of the American Physical Society), Phys. Rev., 45: 123 (1934).
5. W. E. Stephens, Magnetic Refocusing of Electron Paths, Phys. Rev., 45: 513 (1934).
6. N. F. Barber, Shape of an Electron Beam Bent in a Magnetic Field, Proc. Leeds Phil. Lit. Soc., 2: 427 (1933).
7. W. R. Smythe, L. H. Rumbaugh, and S. S. West, A High Intensity Mass-Spectrometer, Phys. Rev., 45: 724 (1934).

Chapter 5

NEW DEVELOPMENTS IN VACUUM ENGINEERING

By Robert B. Jacobs and Herbert F. Zuhr

1. INTRODUCTION

1.1 Degree of Vacuum Tightness Required. The development of leak-detection techniques for the gaseous diffusion plant for the separation of U^{235} was one of the major engineering problems connected with the project. A greater degree of tightness was required than had hitherto been achieved in any commercial plant, but the construction schedule did not permit the use of the time-consuming methods of testing for tightness that were generally employed. It was recognized that vastly improved techniques were necessary to greatly increase the sensitivity and speed of testing, otherwise a prolonged period of testing would intervene between the completion of construction and the initiation of operations. After all known methods and several new ones had been considered, the mass spectrometer was selected as the basic testing instrument. This chapter describes the techniques for leak detection developed with the mass spectrometer and indicates the general utilization of those techniques.

(a) Process Specifications. Process design required that the inleakage of ambient air into the process stream be no greater than one one-hundredth of a standard cubic foot per hour per thousand cubic feet of plant volume. This is equivalent to a pressure build-up at high vacuum of 8μ (0.00015 psi) per hour. Ambient air must be kept from the process stream, principally because of its water-vapor content. Water causes destruction of the uranium hexafluoride, the products of the reaction plugging the minute pores of the barrier. To assure continued, efficient operation of the plant by reducing the effects of inleakage to a minimum, a large portion of the plant equipment was surrounded by air with a dew point of $-40°F$. Elaborate precautions still were necessary to make sure that the tightness of the plant was maintained.

A corresponding tightness was required in the heat-exchange equipment, which might otherwise leak coolant into the process system.

(b) Precedents. Industrial precedent for vacuum tightness of the required degree had been limited to compact equipment of relatively small volumes, such as radio tubes and some of the smaller mercury rectifiers. Indeed, the general trend in industry had been toward accepting leakage in vacuum systems and evacuating continuously with large, high-speed diffusion pumps in order to maintain sufficiently low pressures. The continuously pumped mercury-arc rectifier, with a volume of about 70 cu ft, composed of some fifteen separate parts, had constituted the largest piece of high-vacuum equipment generally used on a commercial scale. A few mercury-turbine installations had been made with inleakage approximately ten times that permitted the gaseous diffusion plant. Perhaps the modern vacuum still for petroleum oil most closely approximated the complexity and size of the proposed plant. These units had been considered tight when the inleakage was approximately 500 times that permitted by process specifications for the gaseous diffusion plant.

1.2 Schedule vs. Effort Required. Early experience in the laboratories and pilot plants working in the diffusion process, both here and in England, indicated that the existent testing methods, if applied to a full-scale plant, would require at least as many man-hours as the manufacture and assembly of such a plant. Indeed, in many laboratories it was common practice—after numerous unsuccessful attempts to make experimental setups tight—to coat vessels with organic "vacuum" waxes. But the requirement that the process stream be free from organic contaminants precluded the use of such subterfuge in the gaseous diffusion plant. Further, the exigencies of the project would not permit such an uncertain method of excluding air from the process stream.

Through application of the leak-detection techniques developed, with the use of the mass spectrometer as the basic testing instrument, it was possible to make a fourfold improvement on the process specifications. A pressure build-up of 2μ (0.00004 psi) per hour in the assembled plant was achieved at an effort measuring approximately 1 per cent of the total effort required to manufacture and assemble the process plant.

1.3 Pressure Units. Pressure units employed in high-vacuum work differ from those most commonly encountered in engineering practice. The unit most frequently used is the micron, written μ, which is 0.001 mm Hg absolute or 1/760,000 of standard atmospheric pressure (14.7 psia). Therefore, 1μ corresponds to a pressure of

1.94×10^{-5} psia. The so-called "high-vacuum range" usually refers to pressures lower than 1μ.

1.4 Leakage Units. Leakage units of measure are usually microns per hour, when referring to a particular vessel; for vessels in general, the unit is micron cubic feet per hour (μcfh). Multiplying the rate of rise of pressure in microns per hour due to inleakage by the volume of the vessel in cubic feet gives the value of the inleakage in micron cubic feet per hour. The latter unit completely defines the leak, since it is independent of the volume of the vessel, and from it the mass rate of inleakage may be computed directly. Hence, a leak of 1 μcfh means a leak at a rate that will cause a pressure rise of 1 μ/hr in a volume of 1 cu ft.

2. KNOWN TESTING TECHNOLOGY AT THE BEGINNING OF THE PROGRAM

2.1 Pressure Methods. It was general practice to test process equipment operating under vacuum, using an internal test medium under pressure in conjunction with an external indicator for location of the leaks. After all possible leaks had been discovered and repaired in this procedure, the system was evacuated and the rate of pressure rise observed as a measure of the inleakage. If the pressure rise exceeded specifications, the system was repressured, and the entire cycle was repeated. These pressure-testing techniques are discussed in more detail in Sec. 7.2. Where applicable to process service lines, these techniques were used in the construction of the gaseous diffusion plant. Design of the process equipment would not permit the application of more than 5 psig to most of the plant, which further decreased the applicability of pressure-testing techniques. However, a several-hundredfold improvement was necessary for use in the testing program for the plant proper.

2.2 Vacuum Methods. Small pieces of vacuum equipment were usually tested by the use of vacuum techniques. Such methods consisted in observing the change in apparent pressure in the system, as measured with either a hot-wire or an ionization gauge when the nature of the residual gas in the system was changed by the substitution of a probe gas (or vapor) for the air normally entering through the leak. Most commonly used was the technique of observing a hot-wire gauge, while the exterior of the vessel was sprayed with acetone. A more detailed account of these methods is given in Sec. 7.3. Results obtained with these methods indicated that some improvement over pressure-testing techniques could reasonably be expected. However, an increase in the caliber of the personnel using these methods was also indicated, and the increase in the speed of testing was uncertain.

3. DEVELOPMENT OF DYNAMIC VACUUM-TESTING TECHNIQUES

Study of the evidence on hand indicated that further advances in pressure testing methods would, at best, advance their useful sensitivity to equivalence with the then existing vacuum techniques, at the expense of an increase in testing time. It was evident that improvement of the existing vacuum techniques could have been effected, but again only at the expense of additional testing time. The increased time factor made both proposals most unattractive. However, new vacuum techniques were visualized which would permit a tenfold improvement in sensitivity and a simultaneous improvement in the speed of testing. These new techniques included:

1. Use of selective instruments, that is, instruments which give a nearly null reading for air and residual gases and respond only to a probe gas.

2. Use of these instruments dynamically, that is, as adjuncts to a high-speed evacuating system permitting their use under optimum conditions.

3. Use of the selectivity of the indicating instruments to permit estimation of the amount of leakage even in the presence of outgassing and unrepaired leaks.

It was therefore decided to investigate and develop, if practicable, a selective, continuously sampling leak detector, and to determine the optimum conditions for its use.

3.1 Leak Detectors Developed and Investigated. The Kellex vacuum engineering group developed the differential Pirani gauge as a new continuous sampling unit and investigated the use of the optical spectrometer as a continuous sampling unit. The University of Minnesota group had developed a compact specialized mass spectrometer (see Chap. 4). The use of this instrument as a continuous sampling (or dynamic) instrument was developed by the Kellex group. All three of these instruments were selective. Comparison of the differential Pirani gauge and the mass spectrometer with instruments used in older methods is made in Table 5.1.

(a) Optical Spectrometer. The optical spectrometer, offhand, would appear to be a suitable instrument for leak-detection work. It is simple, its response is instantaneous, and its sensitivity for certain probe gases is very high. However, under actual working conditions it is found to be unreliable owing to the uncertain cleanup of the discharge tube used as a source after exposure to different gases.

(b) Differential Pirani Gauge. The differential Pirani gauge consists of two Pirani gauges connected electrically in opposite arms of

a Wheatstone bridge. The two gauges are connected to the vacuum line of the system under test by a short T connection. A cold trap is placed on one of the arms of the T leading to the gauges, but not on the other.

Table 5.1 — Analysis of Basic Leak-detection Instruments

	Mass spectrometer	Differential Pirani gauge	Single Pirani gauge	Pressure testing
Inherent instrument sensitivity (ratio of probe gas to air detectable)	$\frac{1}{100,000}$	$\frac{1}{3,000}$	$\frac{1}{300}$	Bubble growth at 10 cu mm/hr
Operating pressure	<0.1 μ	<25 μ	<50 μ	45 psig
Speed of probing	5 ft/min	As fast as area can be wet with spray gun	As fast as area can be wet with spray gun	Observation of smooth soap film for at least 5 min
Smallest leak detectable (μcfh) on vessels having a pressure build-up at 200 μ/hr and a volume of:				
<1 cu ft	<0.01	0.10	1.0	5
1 – 10 cu ft	0.01 – 0.02	0.10 – 1.0	1.0 – 10.0	5
10 – 100 cu ft	0.02 – 0.2	1.0 – 10.0	10.0 – 50.0	5
100 – 1,000 cu ft	0.2 – 2.0	10.0 – 50.0	50.0 – 500	5

When air is the only gas present, the pressures in the two gauges are equal, and the galvanometer reads zero. However, when a leak is probed with a liquid such as methanol, the latter reaches one gauge only, owing to the presence of the trap in front of the other gauge, and the Wheatstone bridge is thrown off balance. The instrument thus acts as a detector for condensible probe gases, being little affected by the presence of other gases.

(c) Mass Spectrometer. The mass spectrometer has been used by physicists for many years, principally to determine the isotopic constitution of different substances. In its usual form it is a large and rather complex instrument requiring a highly skilled operator.

A simplified instrument specifically designed for vacuum testing was developed at the University of Minnesota. A considerable reduction in size and weight was made, making a portable instrument possible. Several electronic controls were incorporated, reducing the number of manual adjustments required. However, carefully trained operating and maintenance crews are required to use these instruments successfully for leak detection on a large scale.

In popular literature, the mass spectrometer is referred to as an "atom-sifter," because of the ability of the instrument to "sift out" and measure the concentration of atoms of any kind.

This characteristic of the mass spectrometer was the basis in choosing a probe medium. This medium should have the following properties:

1. It should be unique in the mass spectrum of residual gas in the system under test and practically nonexistent in the normal atmosphere surrounding the equipment under test.
2. It should be readily removable from the system by pumping and should not contaminate the system.
3. It should be of low molecular weight and low viscosity and should be readily available.

Helium fulfills all these requirements and was chosen as the probe gas for use in the testing program.

The instrument (see Fig. 4.1) works in the following manner: The gaseous mixture to be analyzed is pumped into that part of the spectrometer which includes the source. When used as a leak detector, the spectrometer is fed by means of a throttle valve connected to the main vacuum lines. The pressure in the spectrometer is kept less than 10^{-4} mm Hg by continuous pumping. In the source of the spectrometer, molecules of the different elements present are ionized by an electron beam. The number of ions of any particular element so produced is a function of the concentration of that element in the gaseous mixture fed into the spectrometer.

The ions thus formed are collimated and given a certain momentum toward the analyzer by suitable electrical potentials. While passing through the wedge-shaped magnetic field, the ions are deflected through certain angles which depend upon their respective masses.

In Fig. 4.1, the electrical fields are adjusted so that He^+ ions enter the collector, where they are measured. Ions of greater or smaller mass fall on either side of the collector slit and are not measured. Ions of any given mass may be brought into the collector by properly adjusting the electrical fields. For leak-detecting purposes, the instrument is adjusted for He^+ ions, since helium is a most satisfactory probe gas. Theoretically, the instrument, when thus adjusted, will show a zero reading, unless helium is present in the gas stream under analysis. Actually, however, owing to unavoidable physical imperfections in the apparatus, there is a continuous background reading. The presence of helium then is indicated by an increase over the normal background reading.

Chapter 4 gives detailed information on the construction and operation of the instrument developed at the University of Minnesota. We

are concerned here, principally, with the performance of the instrument as a leak detector.

The first mass spectrometers used for leak-testing purposes were all-glass instruments using mercury-diffusion pumps. The fragility of these machines for plant use was recognized, but the magnitude of the trouble caused thereby was discovered only after attempting to institute the production-testing program. The entire spectrometer was redesigned by the Kellex special instrument group. In addition to greater durability due to the practically all-metal construction (only the filament stem and the ion gauges remained of glass), the new tube possessed a higher inherent sensitivity because of its design, and a greater sampling capacity because of substitution of an oil-diffusion pump for the mercury model.

3.2 Dyanamic Requirements for Rapid, High-sensitivity Vacuum Testing. Use of a high-sensitivity, dynamic leak detector such as the mass spectrometer is of little avail if the system under test does not possess the required characteristics. It is shown mathematically, in Sec. 7.4, that the ratio of S/V (pumping speed of the system with respect to the volume pumped) is of greatest importance, with respect to both dynamic sensitivity and speed of leak hunting. In Fig. 5.1, the response (at the leak detector) after exposing the leak to probe gas for 1 sec is plotted for different pumping speeds.

The sharpness of the response to probing will, in a large measure, determine the ability of any leak detector to function efficiently. Figure 5.1 illustrates the impossibility of attaining a sharp response without a sufficiently high S/V ratio, i.e., about 6 or more reciprocal minutes.

When a large leak is probed, the system becomes temporarily "flooded" with a probe gas, and it is impossible to continue leak hunting until this gas is removed. In Fig. 5.1, probing is discontinued at the end of 1 sec. Those parts of the curves for time greater than 1 sec represent the cleanup period. The length of time required for cleanup is a function of the ratio S/V. Thus, for example, if a large leak is probed until a probe response of 25 per cent of maximum is obtained, and pumping is then continued until all but 0.5 per cent of the probe gas is removed, the cleanup times indicated in Table 5.2 are obtained. These calculations have been confirmed experimentally.

Loss of time by slow cleanup can prolong the leak-hunting period considerably, perhaps much more than is indicated in Table 5.2. The reason for this is the following: When one is hunting for leaks with too small a pump (low S/V), the dynamic sensitivity is low, and as a result leaks must be carefully and repeatedly probed to establish

their exact location. Consequently, by the time this is done, a considerable quantity of probe material will be introduced into the system. Since this must be removed before probing can continue, the leak-detecting crew finds it necessary to remove a large quantity of probe gas at a slow rate, which is doubly time-consuming.

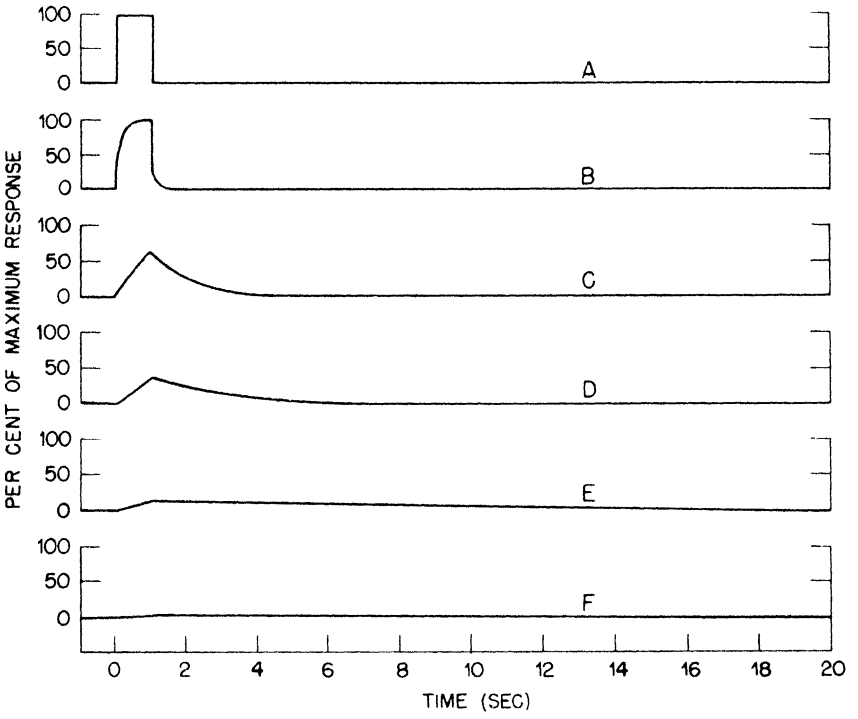

Fig. 5.1—Response at the leak detector after the leak has been exposed to probe gas for 1 sec for different pumping speeds. A, shape of probe pulse at leak. B, effective pumping speed for 40 cu ft = 24,000 cu ft/min; S/V = 600 min^{-1}. C, effective pumping speed for 40 cu ft = 2,400 cu ft/min; S/V = 60 min^{-1}. D, effective pumping speed for 40 cu ft = 1,200 cu ft/min; S/V = 30 min^{-1}. E, effective pumping speed for 40 cu ft = 240 cu ft/min; S/V = 6 min^{-1}. F, effective pumping speed for 40 cu ft = 48 cu ft/min; S/V = 1.2 min^{-1}.

A simple experiment was made which confirmed the above predicted results. This experiment is described in Sec. 7.4. The calculations have since been confirmed many times in practice, under both mass production and field conditions.

It must be recognized that the S/V ratio refers to the speed of the entire vacuum system, including the process equipment under test. Thus the use of the largest high-speed vacuum pump will be of little avail if the rest of the system throttles the flow to the pump. Rather, the use of a pump oversize for the system speed will further penalize the sensitivity by making it impossible to obtain an adequate sample

Table 5.2 — Evaluation of Cleanup Time as Function of S/V

S/V, min^{-1}	300	60	30	6	3
Cleanup time, sec	1.7	5.8	11.1	139	546

from the gas evacuation line through the leak detector. It is necessary that the lines of the system under test be sized to permit maximum speed of pumping. This can be done by sizing them for molecular flow according to the formula, Speed = 14 D^3/L, where the speed is expressed in cubic feet per minute, D is the internal pipe diameter in inches, and L is the length in feet. One of the more important functions of the vacuum engineering division was to check all design to make sure that the maximum speed was always attained at the test connections. A review of mechanical design is of paramount importance if vacuum tightness is to be achieved quickly and efficiently.

The need for high-speed pumps is apparent from the preceding discussion. These pumps have other special requirements:

1. The pumps and all associated vacuum equipment, i.e., valves, gauges, and piping, must be tight, and engineered to maintain this tightness.

2. Provision to reduce the back diffusion of diffusion-pump oil, without seriously impeding the speed characteristics of the pump, is necessary to prevent the contamination of the process equipment under test.

3. The complete pump unit, including mechanical and diffusion pumps and all necessary controls, must be self-contained and portable, and should require only connections to the system under test and to the water, power, and drain lines to permit operation.

A typical vacuum pump unit is shown in Fig. 5.2. For initial evacuation, provision is made to by-pass the diffusion pumps through a roughing line. Pump units of suitable design were developed by Westinghouse Electric & Manufacturing Company, National Research Company, and Distillation Products, Inc., in conjunction with the Kellex vacuum engineering division.

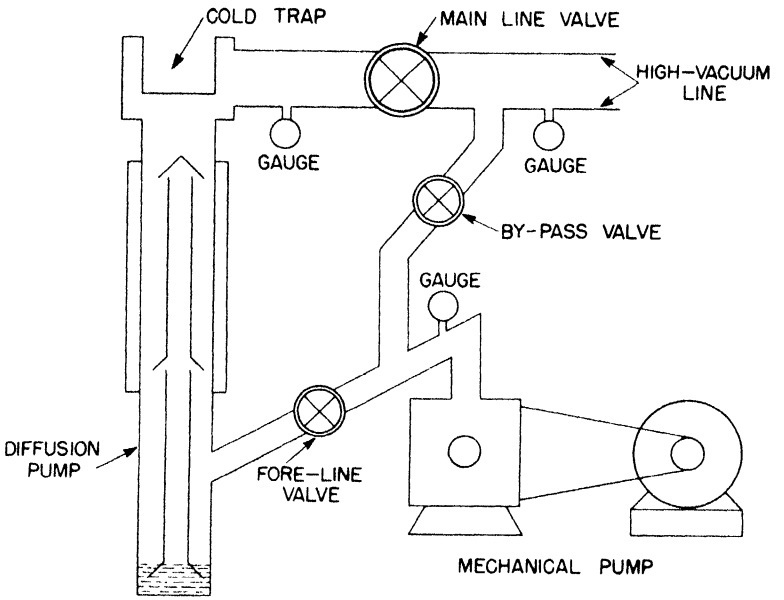

Fig. 5.2 — Typical pumping unit.

4. MEASUREMENT OF TIGHTNESS

The general plan of attack to secure over-all plant tightness was to apportion the total allowable leakage among the different plant components, and to check each such component individually for tightness one or more times prior to its installation.

This measurement of tightness, involving about 1,000,000 individual tests, threatened to be a serious holdup in the fabrication schedule. The only known method for measuring tightness consisted in evacuating the equipment a sufficiently long time to outgas it thoroughly and then measuring the pressure rise. This method usually required an average of 12 hr of continuous evacuation for each piece of equipment tested. Approximately 1,000 leak-rate stations, each working more than 8,000 hr, would be required to prove the tightness of equipment. This estimate does not include the time spent leak hunting, setting up the equipment for test, and retesting of rejects.

Evaluation of the mass spectrometer as the basic leak-detection instrument indicated that its quantitative aspects could be adapted to

measurement of the inleakage into the vacuum system. Accordingly, the so-called "hood method" for tightness testing was devised. Using this method in conjunction with the rapidly responding dynamic system for leak detection, the testing load for production testing was reduced to approximately 100 stations, each working 2,450 hr.

The hood method consisted in surrounding the equipment under test with a gastight hood in which a fixed concentration of probe gas was maintained, and comparing the amount of the probe gas entering the system through the leaks in the equipment with the amount of probe gas entering through a standard calibrated leak. This comparison was made by direct reading of the output of the mass spectrometer. The results thus obtained have been quantitatively checked against results obtained by measuring the inleakage of thoroughly outgassed vessels by the usual pressure build-up method.

A typical hood setup is shown in Fig. 5.3. For small objects several manifolds are attached to one leak-detector and pump combination, allowing the objects to be set up or taken down on one manifold while the units on the other are under test. For larger equipment, individual leak-detector and pump combinations are required. The test is made in the following manner:

With the valve leading to the calibrated leak in an open position, helium is forced into the hood until its concentration there is sufficient to give a predetermined reading on the leak detector. This reading (reading 1) is proportional to the total inleakage consisting of (a) unknown vessel leakage and (b) known leakage from the calibrated leak.

The valve leading to the calibrated leak is then closed, and a second reading is taken (reading 2). This reading is, of course, proportional to the unknown leakage alone. From these two readings the following equation may be derived:

$$\text{Unknown leakage} = \frac{\text{Rdg 2}}{\text{Rdg 1} - \text{Rdg 2}} \times \text{calibrated leak}$$

This equation gives the unknown leakage in terms of the two readings referred to above and the value of the calibrated leak. Knowledge of the helium concentration in the hood is not necessary. The only requirement is that this concentration shall remain substantially constant during the time the readings are taken. Normally, this requires from 5 to 10 min. Well-constructed hoods show practically no decrease in helium concentration for considerably longer periods.

A modification of the hood technique that has proved extremely useful for testing hidden leaks involves the use of pure helium on both the standard leak and the unit under test. This method is best achieved by evacuation of the reentrant interior volume, from which it is suspected that the leak into the vacuum space proper occurs.

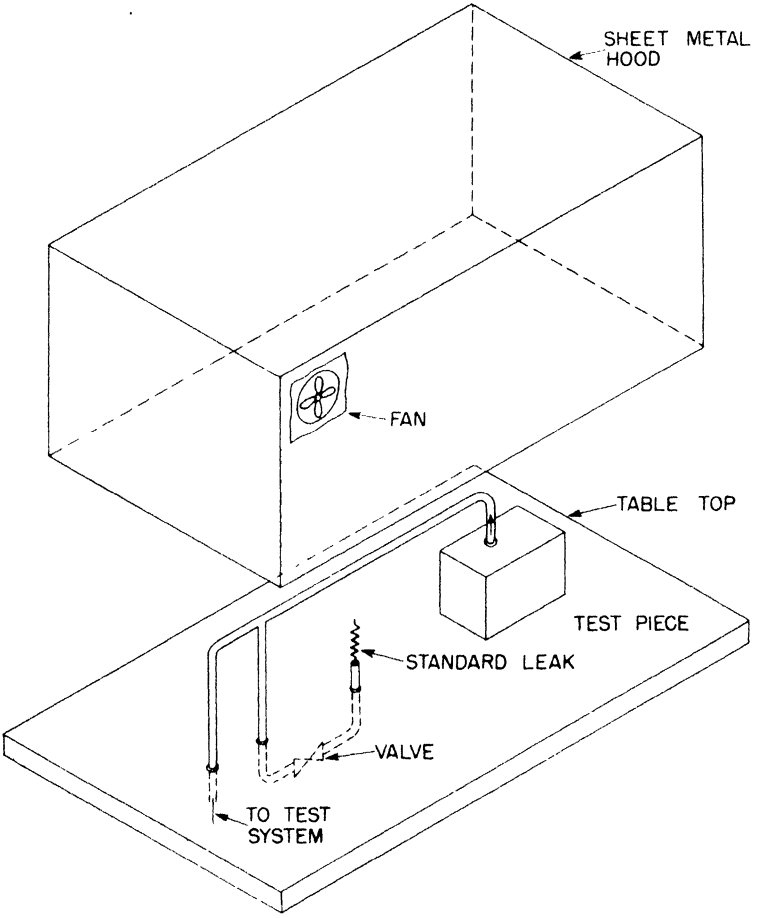

Fig. 5.3 — Typical hood-test setup.

When pure helium is admitted, the reading of the mass spectrometer output is compared with that obtained when a standard leak is surrounded by pure helium.

5. PRODUCTION TESTING

Experimental evidence indicated that the process specifications could probably be reduced from 8 μ/hr to 2 μ/hr through the use of the methods just described. It was evident that most careful preassembly testing would be necessary to hold the number of leaks in the assembled plant to an absolute minimum. That is, it was essential to be able to certify that various complex pieces of process equipment would not have to be disassembled for repair in the field, and that the vacuum-testing crews in the field could have confidence in the tightness of the component pieces of equipment. The decision to pretest every piece of process equipment and piping subassembly required the preparation of many varied procedures and specifications, and the education of personnel to use these new techniques in the different places of manufacture. Specifications for each unit were made on the basis of mechanical complexity and the number of such units occurring in each assembled cell of the plant. Table 5.3 lists the major components of each cell, the contribution of their volume per

Table 5.3—Contribution of Various Process Components to Inleakage
(Based on manufacturer's specifications)

Component	Volume contribution per 100 cu ft	Inleakage specification pressure build-up, μ/hr	Inleakage contribution, μcfh
Diffusers	68.6	0.25	17.1
Pumps	2.2	0.50	1.1
Process drums	3.8	0.1 – 1.0	0.4
Process piping and valves	25.4	1.00	25.4
Instruments	<0.1	<1.00	<0.1
Total	100.0	0.44*	44.0

*This figure is a weighted average for the component parts, not a numerical sum.

100 cu ft of cell volume, the specified inleakage rate, and the inleakage contribution. It should be noted that, if no damage occurred during transport and erection, and if all field welds were tight, the assembled plant would have an inleakage rate considerably below 2 μ pressure rise per hour. Thus a margin was available for depreciation and safety.

Each manufacturer was asked to send several engineers to Kellex for training in the techniques of leak hunting, using the high-sensitivity dynamic method and the hood test for the tightness testing. At

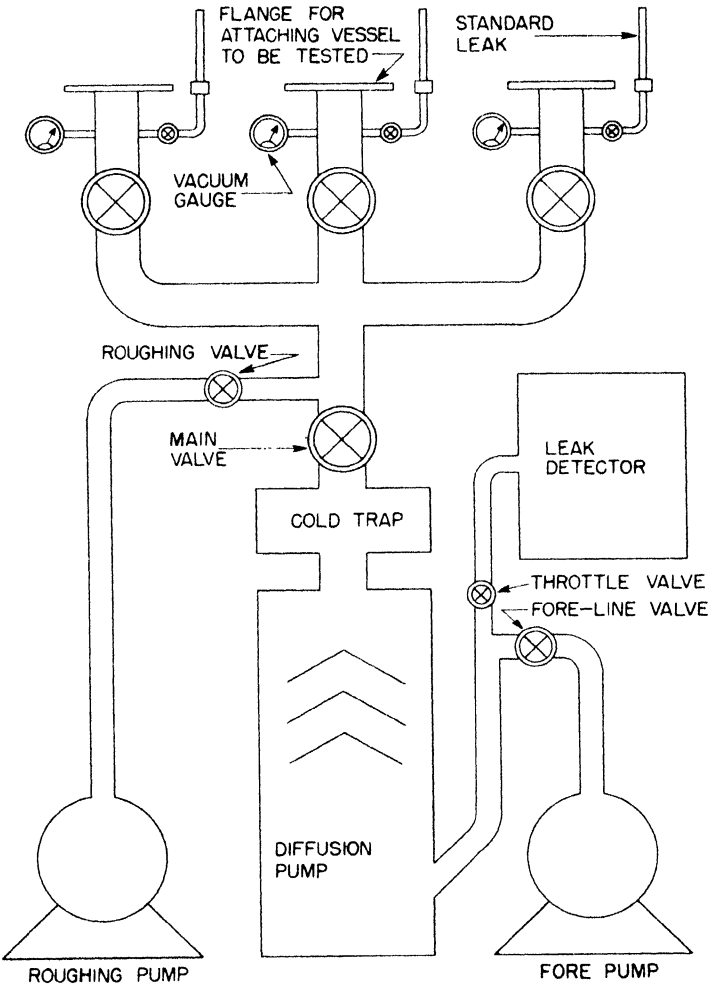

Fig. 5.4 — Manifold for medium-volume medium-production vacuum testing.

the conclusion of the training program these engineers were asked to prepare detailed procedures applicable to their particular process unit. These procedures were reviewed by the Kellex vacuum engineering division before they were put into practice. In all cases high

S/V ratios were maintained for production testing in keeping with the accelerated production schedules. Many jigs and fixtures were designed and built for this purpose. Since the undependability of rubber

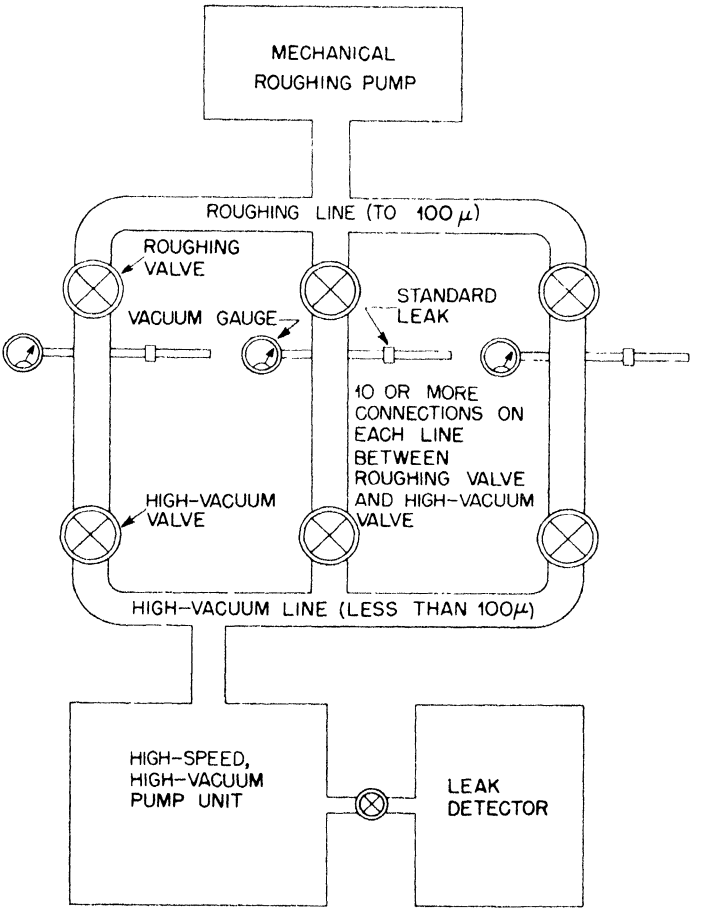

Fig. 5.5— Manifold for small-volume high-production vacuum testing.

hose and similar makeshift connections was recognized, large-sized equipment had flanged connections for testing, while for small equipment the Dresser-type coupling proved successful. Best vacuum practice was followed in the construction of testing rigs; packless valves were used, and all possible joints were welded, brazed, or hard-soldered. In several instances, rigs were equipped with packed

valves and sliding jigs; however, these units always proved to have lower sensitivity than those of all-metal construction. Figures 5.4 and 5.5 show schematically some of the manifolds used for production testing.

6. TESTING THE ASSEMBLED PLANT

Delivering sound, vacuum-tight equipment to the plant site was one job. Perhaps a bigger one was to see that this equipment was assembled without injury and that the assemblies were made tight. This program required the following groups: (1) vacuum engineering; (2) construction coordination; (3) vacuum testing; (4) acceptance control and records.

The vacuum engineering group for the assembled plant was concerned with four major problems:

1. Definition of the parts of the plant to be tested as units.
2. Location of test connections in the process system to ensure sufficiently high S/V ratios for efficient testing.
3. The magnified effect of sorption of the probe gas, when a large number of diffusers were tested simultaneously.
4. Excessive extraneous leakage through the shaft seals of the pumps.

Provision of sufficient test connections on the test cells allowed a careful study of all these problems to be made.

The process design of the plant largely determined the basic sections for testing, since the addition of valves to facilitate testing might interfere with orderly process operation. Thus each cell, the building and cell by-pass lines, and the cold traps were individually tested so that the limits and state of completion of each were accurately defined.

Each proposed layout of test connections was analyzed by means of electrical analogy. The resistance of the piping to gas flow may be considered equivalent to electrical resistance. Consequently, an analysis of resistance network was used to demonstrate the optimum location for the test connections. These analyses were made mathematically or were measured on resistance networks. The results were quantitatively confirmed by later field measurements.

The construction coordination group reviewed the progress of construction and established standards for completion of defined subsections. Briefly, these subsections were defined so that (1) no interference between construction and testing could exist (i.e., all subsections were ended past a limiting valve, so that opening of the valve to permit welding was unnecessary); (2) operations could follow vacuum testing so as to put the process in operation in a practical orderly

manner. Before transfer of buildings or sections to the vacuum testing groups, the construction coordination group reviewed the unfinished construction items that might interfere with vacuum testing, and checked the results of preliminary pressure testing. Once a section of the plant was turned over to the vacuum testing group, further construction, made necessary by redesign or for some other reason, was subject to the approval of the construction coordination group.

Actual vacuum testing was performed by three-man crews assigned to each leak-detector pump-unit combination. The crews were headed by a person of at least high-school education and were all given a two-weeks special training course in the mechanics of the leak-testing operation. Because of the complicated nature of the leak detectors and pump units, the test crews were not permitted to make any adjustments or repairs to the equipment. Highly trained personnel was used for the maintenance of all leak-detection equipment.

The acceptance control and records groups kept records of all leaks found, the status of testing, and repairs. The results of studies made by these groups suggested several changes in design, erection procedures, and testing sequence, which considerably reduced both the probability of leaks and the time required for testing. Their major function was to review the test data for conformance to specifications.

The efforts of the vacuum testing program, involving well over 1,100 men, were climaxed when the plant was brought below a leak rate of 2 μ/hr. This was accomplished in the face of a constantly accelerated construction schedule and within a very narrow margin of time allotted for vacuum testing after the completion of construction.

7. DISCUSSION*

7.1 Fundamentals of Vacuum Engineering. Industrial uses of high vacuum have increased very rapidly in the past few years. Among such applications may be listed the manufacture of radio and X-ray tubes, lamp bulbs, rectifiers, etc., and the reduction of various metal-bearing ores.

To satisfy the growing needs of industry in these fields, much time and energy have been spent in the design and development of rugged, high-capacity pumping equipment, by means of which the pressure in vessels of several hundred cubic feet of volume may be reduced to exceedingly low values with great rapidity.

*By J. R. Downing.

(a) Tightness and Cleanliness. Tightness and cleanliness are absolutely essential in all vessels used in high-vacuum systems. This becomes obvious when it is considered that 1 cu in. of standard air will occupy a volume of approximately 760,000 cu in. at 1 μ pressure, and that 1 cu in. of water when vaporized will occupy 945,000,000 cu in. at 1 μ pressure. Unless systems are clean and free from leaks, it is, therefore, extremely difficult to reduce the pressure in them to the high-vacuum range.

(b) Vacuum Pumping System. A vacuum pumping system consists of three essential units—the diffusion pump, the fore pump, and the vapor trap (see Fig. 5.2).

Diffusion Pump. The diffusion pump provides a means of obtaining large volumetric pumping capacities in the high-vacuum range of pressures. The pumping action originates in the streaming of either oil or mercury vapor from a suitably designed jet. The gases to be pumped diffuse into this vapor stream and are carried along with it away from the system being evacuated. Pumps of this type usually attain their full volumetric capacity at about 1 μ pressure, and they maintain this same value to very low pressures. The capacity of a well-designed pump is approximately 50 cfm/sq in. of opening at the jet, and is therefore nearly one-third of the molecular flow through a hole equal in diameter to the pump housing when absolute vacuum is maintained on one side.

The diffusion pump will not exhaust directly against atmospheric pressure. There is a critical forepressure, or threshold pressure, above which it will not pump at all. This required forepressure (about 50 μ) is maintained by a mechanical pump, by an ejector, or by a combination of the two.

Fore Pump. The fore pump is a mechanical pump or ejector. It must have sufficient capacity to handle the gases compressed by the diffusion pump and maintain the forepressure against which the diffusion pump operates at a value lower than the critical threshold pressure. Mechanical pumps will not in themselves produce pressures lower than about 1 μ. For lower pressures the diffusion pump must be added.

Vapor Trap. The vapor trap is necessary to prevent the migration of oil vapor from the diffusion pump to the system being evacuated. In most cases a suitably designed water-cooled baffle will suffice. However, a refrigerated cold trap is required to obtain pressures lower than 0.01 μ, or when it is desirable to prevent small traces of oil from entering the system which is being exhausted. Pressures lower than 0.01 μ may be obtained without the use of cold traps, but only with great difficulty and an excessively long "conditioning" time.

(c) Flow of Gases. The flow of gases in the high-vacuum range obeys laws quite different from those familiar to the hydraulic engineer. This fact cannot be stressed too highly, since it is overlooked all too frequently by the uninitiated.

Extremely large and short pipes must be used to handle the large capacities of a diffusion pump, although the resultant mass transfer is very small. For piping systems longer than a few feet, the pipe size used must be of larger diameter than the pump opening. It is customary to calculate pumping-system capacities in terms of the capacity of the pump and the flow capacity of the pipe. The expression for over-all pumping capacity is:

$$\frac{1}{S_{system}} = \frac{1}{S_{pump}} + \frac{1}{S_{pipe}}$$

where the various pumping capacities are expressed in cubic feet per minute. If the length of the pipe is more than ten times the diameter, the capacity of the pipe for air is given by

$$S_{pipe} = \frac{0.51\ D^4P}{L} + \frac{14\ D^3}{L}\,\frac{1 + 0.62\ DP}{1 + 0.76\ DP}$$

where D is the pipe diameter in inches, L is the length in feet, and P is the average line pressure in microns. A second, semiempirical, expression for the capacity of short lengths of pipe at pressures less than 0.1 μ is given by

$$S_{pipe} = \frac{14\ D^3}{L + (D/9)}$$

where L, D, and S have the same units as in the previous formula. It is evident from these expressions that the pipe size may be the limiting factor in the capacity of a pumping system, regardless of the capacity of the pump. Table 5.4 gives the reduction in capacity caused by various lengths of pipe connecting a 2,600 cfm diffusion pump to the vessel being evacuated.

(d) Precautions and Techniques. Precautions and techniques necessary to the attainment and maintenance of high vacuum are so many and varied that the subject will be dealt with here only in the most general way. This is summed up by saying that vacuum systems must be capable of attaining high vacuums without use of waxes, greases, lacquers, soft solders, and the like.

Sound engineering, cleanliness, ruggedness, and good materials are all of prime importance.

The equivalent in weight and strength of standard 150-lb flanges and fittings is recommended. These may seem excessively heavy, but in view of their reliability and record of trouble-free operations they are well worth the additional cost.

Table 5.4 — Capacity Loss through Pipe Connections to a Diffusion Pump
(Capacity 2,600 cfm below 0.1 μ)

Length of pipe, ft	Per cent capacity reduction		
	4-in. ID	8-in. ID	12-in. ID
2	88	52	27
6	95	73	45
20	98	89	71

(e) Evacuation Time. The time required for evacuation may be calculated fairly well for the range of pressures from atmospheric down to a few hundred microns. The expression is

$$T = \frac{V}{S} \ln \frac{P_1 - P_0}{P_2 - P_0}$$

where T is time in minutes, V is volume of vessel in cubic feet, S is the pump capacity in cubic feet per minute, P_1 is the initial pressure, P_0 is the limiting pressure attained by the pump, excluding the volumes being measured for evacuation time, and P_2 is the final pressure. Since P_0 is small compared to P_1 and P_2, the expression may be simplified to:

$$T = \frac{V}{S} \ln \frac{P_1}{P_2}$$

With P_1 atmospheric pressure and P_2 a few hundred microns, the term involving the logarithm becomes about 8, so that the time required for "roughing" a vessel becomes

$$T = 8(V/S)$$

The latter expression holds very well, provided the system is free from inleakage and the volumetric capacity S of the pump stays reasonably constant. For most mechanical vacuum pumps the latter condition is true down to pressures of a few hundred microns.

In the range of pressures lower than 100 μ the above expression is quite useless for three reasons:

1. The capacity of the diffusion pump is by no means independent of pressure.

2. Degassing and vaporization of substances on the inner walls of a vessel contribute so greatly to the volume of gases which must be handled by the pump that the residual volume of air becomes negligible by comparison.

3. Impedance of connecting pipes becomes an important factor.

If the amount of degassing per unit surface area is known as a function of time and pressure, then the pump-down time may be estimated by a graphic integration method. However, such data are usually not known very accurately, so that choice of pump size is dictated largely by experience. The modern trend is to use diffusion pumps of very large capacity, so that a high vacuum may be produced quickly and in spite of degassing, small leaks, etc.

(f) Special Gauges. Special gauges have been developed for the measurement of pressures lower than 1 mm Hg. The forces involved are so small that a direct measure of the pressure by observing the deflection of a diaphragm, or the equivalent, does not prove practicable. Some other property of the gas — one that varies with pressure and is capable of easy application — must be chosen.

The McLeod gauge has long been the standard for the accurate measurement of pressures less than 1 mm Hg. A sample of the gas in the system is entrapped and compressed by a known ratio. A measure of the resulting pressure then permits calculation of the initial pressure. Compression ratios as high as a million may be used, enabling the measurement of pressures as low as 0.001 μ. Because of the high compression ratio, the gauge may only be used for the measurement of pressures due to permanent gases.

The thermocouple and Pirani gauges depend upon variation of heat conductivity with pressure of the gas. These gauges are therefore not absolute and must be calibrated by comparison with the McLeod gauge. They are sensitive in the range of pressures between 1 mm Hg and 1 μ.

The ionization gauge is capable of measuring pressures from 1 μ to the lowest attainable, which, at present, is about one-millionth of a micron. The gauge is essentially a three-element vacuum tube operating with its grid at a positive potential and its plate negative with respect to the filament. Electrons from the filament gain energy in their passage to the grid and so will cause ionization of those gas molecules with which they may collide. The resulting positive ions are collected at the plate and constitute the plate current. Since the

probability for ionization is proportional to the molecular concentration of the gas, the plate current represents a measure of the pressure.

Like the thermocouple and Pirani gauges, ionization gauges are not absolute, but must be calibrated by comparison with a McLeod gauge.

A number of other gauges have been developed for measuring low pressure, but few if any of them have ever proved practicable in industrial applications. There is considerable room for improvement in apparatus for measuring low pressures, since none of the gauges now in use are wholly satisfactory.

7.2 Pressure-testing Techniques. Pressure testing for tightness has been applied to vessels in both vacuum and pressure service for many years. Therefore this section will merely indicate the various methods briefly and discuss their applicability to testing process equipment for high-vacuum service. Table 5.5 indicates the various

Table 5.5 — Pressure Testing Techniques

Test medium	Probe	Response	Leak size at 45 psig, μcfh	Special requirements
Air-nitrogen	Flame	Wavering	5,000	Draft-free room
	Sound	Hissing	5,000	Low noise level
	Soap film	Bubbles	5	Each area to be observed under good light for at least 5 min and soap film maintained
	Immersion	Bubbles	20	5 to 15 min observation; occluded air on surface must be avoided
Organic halide	Halide torch	Flame color change	5	
Acidic gas (CO_2 or SO_2)	Ammonia	Fumes	5	
Ammonia	CO_2; HCl	Fumes	5	
Liquid under high pressure		Wet exterior surface	500	

methods in general use and the smallest leak that may be detected practically. Extremely careful application of each method will perhaps yield a twofold to fivefold decrease in the figures given for the leak sizes.

These techniques are used only to locate leaks and do not permit any measure of the amount of leakage to be made. Application of

pressure-drop measurements is not, in general, suitable for checking the tightness of systems for vacuum service, the permissible drop being beyond the limits of accuracy of the best commercial gauges generally available. This drop for diffusion-plant standards would be less than 0.001 psi per hour and corresponds to a temperature change of about 0.005°F. The uncertainty of the temperature correction further invalidates this method for measurement of the vacuum tightness of process vacuum equipment.

After all leaks are thought to have been found, the equipment under test must be evacuated and the rate of pressure rise observed. Consideration of the gas laws reveals that the temperature correction in the absolute-pressure range of 1 to 100 μ is negligible. Vacuum gauges can readily measure the pressure changes required for tightness. However, a serious drawback is the effect of outgassing on the observed leak rate. The subject is more completely discussed in Sec. 7.3.

Other practical drawbacks to the use of pressure-testing techniques are (1) the requirement that the system be depressured before repairs are attempted, and (2) inability to check hidden leaks (leaks that are not visible on the exterior of the system) such as those at valve seats and heat-exchanger tubes.

7.3 Vacuum-testing Techniques Prior to 1943. Many devices used in vacuum practice will not stand internal overpressures high enough to make pressure testing practical. Therefore the use of vacuum testing techniques became necessary in the laboratories and specialty shops dealing with high-vacuum equipment. These methods were considered usable only by specialists and were not considered applicable to commercial process equipment before the inception of the testing program described in this chapter. The earliest form of vacuum testing was on all-glass systems. After evacuation of the system was begun, the discharge of a Tesla coil was played over the glass surface. A leak would show up as a bright spot, or "pip." Experienced operators could also detect leaks on metal systems by observing the color change of the discharge when the leaks were sprayed with water or acetone. However, considerable uncertainty was attached to this technique, and the final resort in such cases was to paint the system with a vacuum wax or a lacquer, on a wiped layer of solder or lead.

Perhaps the first large-scale vacuum testing of metal systems was done by research groups working with cyclotrons and similar equipment used in nuclear research. In general, those methods depended upon the effect on a hot-wire gauge of the change of composition of the gas in the system when the probe fluid displaced the air flowing through the leak. Precautions were taken to ensure electrical stability

and sensitivity of the measuring circuits and mechanical stability of the gauges used. Probe fluids were carefully chosen to ensure maximum effect on the gauge. Thus the ideal probe fluid had low viscosity and either high or low thermal conductance compared to air.

When tightness requirements became more severe, the hot-wire gauge was replaced with an ion gauge, since the tightness was sufficient to permit the evacuating pumps to reduce the pressure below the operating maximum of this gauge ($<0.5\ \mu$). Hydrogen gas or a gaseous hydrocarbon was most generally used for the probe fluid, although good results were also reported for other fluids. Ease of ionization of the probe molecules is a determining factor in the choice of the probe fluid, since the ionization produced by electron bombardment is proportional both to the concentration of the gas in the gauge and to the character of the gas.

To obtain the ultimate sensitivity of these methods, the dynamic method was discarded and one of the following was adopted: (1) the "backing space" technique, or (2) the technique of analysis of apparent change in rate of pressure build-up when probe gas displaces air flowing through the leak. Both methods achieve improved sensitivity at the expense of an increase in testing time.

"Backing space" is the name given to the process of multiplying the effect of the probe gas by permitting the diffusion pump to compress the gas into a dead volume. This is achieved by shutting the valve in the foreline leading to the mechanical pump. The method requires judgment in the analysis of the signal indicated on the gauge controls. The caliber of the personnel required to assure foolproof operation is high. Groups that have reported this method have consisted wholly of college graduates.

Analysis of the apparent change in pressure build-up caused by the introduction of probe gas is very time-consuming. A careful schedule for probing must be adhered to, and a subsequent analysis of the time-pressure graph in conjunction with this schedule must be made. A further drawback of the technique is the entirely nonproductive testing time spent reducing the outgassing of the system under test. This period varies from 8 to 48 hr per unit, depending on the volume and area of outgassing surface involved.

After all possible leaks have been found, a measure of tightness is taken in the following manner: The equipment under test is valved off from the evacuating pump, and the pressure rise of the system is observed. Evacuation of the equipment during the leak-hunting period in general has reduced the outgassing sufficiently so that the pressure rise is an approximately true measure of the inleakage. Outgassing may be detected on the pressure-time graph of the leak rate by a pronounced change of slope. The measurement of the true leak is

generally taken after this change of slope has been noted. The rate thus measured does not differ appreciably from the rate of the same system after it has been completely outgassed.

Outgassing is a complex and unpredictable effect, as the gas contributing to the effect may be adsorbed, absorbed in solid or liquid solution, or evaporated from a liquid, or it may be the product of chemical decomposition.

A summary of vacuum testing methods prior to 1943 is presented in Table 5.6.

Table 5.6 — Vacuum Testing Methods in Use Prior to 1943

Leak detector	Operating range, μ	Size of leak discernible, μcfh	Commonly used probes	Remarks
Tesla coil	50 – 1,000		Tesla coil	Can be used only on glass systems
Discharge tube	100 – 1,000		Acetone; methanol; CO_2; H_2	Residual gases confusing
Hot-wire gauge	Less than 100	10 – 1,000	Acetone; methanol, H_2	Affected by pressure changes and residual vapors
Ionization gauge	Less than 0.5	1 – 100	Gaseous hydrocarbons; H_2; O_2	Affected by pressure changes and residual vapors
Hot wire with backing space	Less than 100	50 – 100	Gaseous hydrocarbons; CO_2; H_2	Time-consuming since method is discontinuous
Ionization gauge with backing space	Less than 0.5	1 – 100	Gaseous hydrocarbons; CO_2; H_2	Time-consuming since method is discontinuous
Hot wire with pressure build-up	Less than 50	1 – 100	Gaseous hydrocarbons; H_2; CO_2; masking with vacuum putty	Extensive outgassing required
Ionization gauge with pressure build-up	Less than 0.5	1 – 100	Gaseous hydrocarbons; H_2; CO_2; masking with vacuum putty	Extensive outgassing required

7.4 Relation between the Volume Pumped, Pumping Speed, and the Response to the Probe. Assume that L standard cubic feet per minute are leaking into a volume of V cubic feet which is being pumped at a rate of S cubic feet per minute at the total pressure existing in V.

Then, if, at time t = 0, probing of the leak is initiated, the volume V will

(1) gain: L dt (standard cubic feet of probe gas per differential of time, dt)

(2) lose: pS dt (standard cubic feet of probe gas per differential of time, dt), where p is the partial pressure of probe gas, expressed in atmospheres, in volume V.

The net gain of probe gas in volume V is

$$d(pV) = (L - pS)\, dt$$

or

$$V \frac{dp}{dt} = (L - pS)$$

Integration of this differential equation gives the partial pressure of the probe gas in the volume and accordingly the partial pressure p_t of the probe gas in the stream passing the leak detector at any time t after probing of the leak has begun

$$p_t = \frac{L}{S} \left(1 - \exp \frac{-St}{V}\right)$$

If, at time T, the probing is discontinued, a similar analysis will show that the partial pressure of the probe gas remaining in the system will be given by the equation:

$$p_T = \frac{L}{S} \left(1 - \exp \frac{-ST}{V}\right) \exp \left[\frac{-S(t - T)}{V}\right]$$

In Fig. 5.1 the response to a probe applied to a leak into a volume of 40 cu ft for a period of 1 sec is shown. The response is expressed in terms of per cent of the equilibrium response, which is given by the equation

$$p_\infty = \frac{L}{S}$$

Part 3

DEVELOPMENT OF HEAT-TRANSFER EQUIPMENT

Chapter 6

THEORY OF HEAT AND MASS TRANSFER IN BATCH CONDENSATION OF SOLIDS

By W. I. Thompson

1. INTRODUCTION

One of the auxiliaries of the gaseous diffusion plant for separation of uranium isotopes is a refrigerated cold trap for condensing uranium hexafluoride to a solid from its gaseous mixtures with nitrogen. Because of the lack of time for extensive testing of these traps a special effort was made to develop a design procedure that would require only simple heat-transfer tests for confirmation. It is felt that the rather compact method that was developed might be of general interest in the design of equipment for condensing gases to solids.

The collecting efficiency of a trap is a function of the outlet temperature and pressure, assuming that the exit gas is saturated, and this temperature may be calculated by the use of methods already available[1] for the cooling of a mixture of a condensible gas with an inert gas. The solid capacity of a trap is determined by the manner in which solid is deposited and on the disposition of cooling surface. In order to design a trap for a given service it is necessary to know approximately the rate of solid deposit at each point.

2. STATEMENT OF PROBLEM

The rate of solid deposit on the heat-transfer surface of a trap may be expressed in terms of the gas flow and average composition by making a material balance on a unit area. For the purpose of this balance it will be assumed that all condensate settles out at the point of formation. The rate of deposit of condensate per unit area per mole is given by

$$-V\frac{dY}{dA} = \frac{\rho_S}{M_1}\frac{db}{d\theta}$$

By rearranging the equation it may be written in the following form:

$$\frac{db}{d\theta} = -\frac{M_1}{\rho_s} V \frac{dY}{dA} = \frac{hM_1}{\rho_s} \left(-\frac{V}{h}\frac{dY}{dA}\right) \quad (1)$$

where A = trap heat-transfer area, sq ft
b = thickness of deposit, ft
h = convective heat-transfer coefficient, Btu/(hr)(sq ft)(°F)
M_1 = molecular weight of condensible gas
V = flow rate of inert gas, lb-moles/hr
Y = moles of condensible gas per mole of inert gas
θ = time, hr
ρ_s = density of solid deposit, lb/cu ft

The main purpose of this chapter is the evaluation of the quantity $-(V/h)(dY/dA)$ appearing in Eq. 1. If this quantity is known for each point in the trap as a function of time and if the heat-transfer coefficient can be estimated, the total deposit thickness at any point may be determined by integration.

3. GENERAL PRINCIPLES

The principles of heat and mass transfer which are used in this study have been extensively developed. Colburn[2] presented a theoretical relationship between mass transfer and friction drop based on the Reynolds analogy, which was substantiated by data for fluids inside tubes. He continued this work,[3] introducing j-factor plots to correlate heat-transfer and friction data for various types of surfaces. Finally Chilton and Colburn[4] pointed out that the Reynolds analogy as applied to heat and mass transfer should be valid for most types of surfaces, since the mechanisms are so closely similar.

These relationships between heat and mass transfer have been used to design equipment in which both processes occur simultaneously. The design of condensers from the point of view of heat-transfer surface required is described by Colburn and Hougen.[1] The phenomenon of mist formation from a saturated mixture is treated by Colburn and Edison,[5] and essentially the same approach will be used in the present study.

Chilton and Colburn[4] presented the following relationship between heat and mass transfer rates based on the Reynolds analogy. The dimensionless factor, j, is found in the case of turbulent flow to be a

function of the Reynolds number with mass velocity and diameter suitably defined for each type of surface.

$$j = \frac{Kp_{gf}}{G/M_m}\left(\frac{\mu}{\rho D_v}\right)^{\frac{2}{3}} = \frac{h}{c_m G}\left(\frac{c_m \mu}{k}\right)^{\frac{2}{3}} \tag{2}$$

where c_m = heat capacity at constant pressure for gas mixture, Btu/(lb)(°F)
G = mass velocity of gas mixture at minimum cross section, lb/(hr)(sq ft)
h = heat-transfer coefficient, Btu/(hr)(sq ft)(°F)
K = mass-transfer coefficient, lb-moles/(hr)(sq ft)(atm)
M_m = mean molecular weight of gas mixture
p_{gf} = logarithmic mean film partial pressure of inert gas, atm

$\frac{c_m \mu}{k}$ = Prandtl number (N_{Pr}) of gas mixture

$\frac{\mu}{\rho D_v}$ = Schmidt number (N_{Sc}) of gas mixture

Equation 2 will be assumed to define the relationship between K and h.

4. DERIVATION OF DESIGN EQUATIONS

The principles of heat and mass transfer described in Sec. 3 will now be used to develop relationships which can be used in the design of condensation equipment. The subject divides naturally into two parts: (1) superheated gas mixtures in which condensation takes place only at the cold surface and (2) saturated gas mixtures in which condensation takes place both at the cold surface and in the main body of the gas.

4.1 Superheated Gas Mixture. The rate of condensation from a superheated gas mixture is given by

$$-V\frac{dY}{dA} = K(p - p_w) = Kp(1 - \beta) \tag{3}$$

where p = partial pressure of condensible gas, atm
p_w = vapor pressure of condensed solid on wall, atm
β = ratio p_w/p

In most cases the vapor pressure of the condensed solid may be neglected so that the ratio β approaches zero. However, where the temperature difference between gas and wall is small, the ratio β will not approach zero.

Equation 3 may be written in terms of a convective heat-transfer coefficient by the use of Eq. 2. Eliminating K between these two equations, the result may be written

$$h \frac{dA}{V} = - \frac{M_m c_m p_{gf}}{p(1 - \beta) \left(\frac{c_m \rho D_v}{k}\right)^{\frac{2}{3}}} \, dY$$

or, substituting for p_{gf}/p its equivalent $\left[\frac{1}{\ln (1 + Y)}\right]^*$, in terms of mole ratios:

$$h \frac{dA}{V} = - \frac{M_m c_m}{(1 - \beta) \left(\frac{c_m \rho D_v}{k}\right)^{\frac{2}{3}}} \frac{dY}{\ln (1 + Y)} \tag{4}$$

Equation 4 may be integrated to give a relationship between composition and trap area, since the right-hand side is practically independent of temperature. At any point where the composition has been determined, the quantity required by Eq. 1 may be obtained by rearranging Eq. 4. Thus

$$- \frac{V}{h} \frac{dY}{dA} = \frac{\left(\frac{c_m \rho D_v}{k}\right)^{\frac{2}{3}} (1 - \beta) \ln (1 + Y)}{M_m c_m} \tag{5}$$

This relation holds only for a superheated gas mixture. In order to predict the point where the mixture becomes saturated, the method described by Colburn and Edison[5] will be used.

The temperature gradient is determined by equating the loss in sensible heat of the gas to the heat carried to the wall by convection. If T is the temperature of the gas mixture,

$$-V(1 + Y)M_m c_m \, dT = h(T - T_w) \, dA \tag{6}$$

* This is strictly accurate only if the partial pressure of condensed solid is negligible. It is a good approximation in any case if the mole ratio Y is small compared with unity.

Since the relationship between A and Y may be obtained from Eq. 4 (by graphical integration, for example), Eq. 6 may be integrated in the form

$$-\frac{dT}{h(T - T_w)} = \frac{dA}{V(1 + Y)\, M_m c_m} \tag{7}$$

By combining Eqs. 4 and 7, a direct relationship may be obtained between Y and T as follows:

$$\frac{dY}{dT} = \frac{(1 - \beta)(1 + Y) \ln (1 + Y)}{T - T_w} \left(\frac{c_m \rho D_v}{k}\right)^{\frac{2}{3}} \tag{8}$$

This expression may be integrated and the point of saturation determined by comparing this relationship with the saturation curve of Y vs. T.

The relationship given by Colburn and Edison[5] is identical with Eq. 8 except for a factor

$$\frac{e^x - 1}{x}$$

where

$$x = \left(\frac{c_m \rho D_v}{k}\right)^{\frac{2}{3}} \ln (1 + Y)$$

which is close to unity at the relatively low concentrations that are considered here. Incidentally, Colburn and Edison point out that, in the absence of auxiliary heating surface to keep the gas temperature up, any mixture will tend to approach saturation.

4.2 Saturated Gas Mixture. The method of calculation for a saturated gas is somewhat more involved, since condensation takes place both at the cold surface and in the main body of the mixture.

If the gas mixture is saturated, it is first necessary to establish whether or not it will remain saturated. This is done by computing the fraction of the condensate which comes out as mist. If this fraction is positive, the gas mixture will tend to remain saturated.

The fraction of condensate appearing as mist is given by

$$\alpha = 1 - \frac{L_1}{L} \tag{9}$$

where α = fraction of condensate as mist

L_1 = rate of diffusion of condensable gas across film per unit area

L = total rate of condensation per unit area

The quantities on the right-hand side of Eq. 9 can be evaluated in terms of gas composition and temperature.

The rate of diffusion is given by the following expression, making use of Eq. 2 to express the result in terms of a convective heat-transfer coefficient:

$$L_1 = K(p - p_w) = \frac{h}{M_m c_m} \left(\frac{c_m \rho D_v}{k}\right)^{\frac{2}{3}} \frac{p(1-\beta)}{p_{gf}} = L(1-\alpha)$$

or

$$L(1-\alpha) = \frac{h}{M_m c_m} \left(\frac{c_m \rho D_v}{k}\right)^{\frac{2}{3}} (1-\beta) \ln (1+Y) \tag{10}$$

The total rate of condensation is obtained from a material balance on the flowing stream over a unit area. Obviously,

$$L = -V \frac{dY}{dA} = -V \frac{dY}{dT} \frac{dT}{dA} \tag{11}$$

The second form of Eq. 11 is included because dY/dT and dT/dA can be evaluated separately.

Assuming that the gas remains saturated and that the condensible gas obeys the perfect gas law, the quantity dY/dT may be evaluated by the use of the modified Clapeyron equation as follows:

$$\frac{dY}{dT} = Y(1+Y) \frac{\lambda}{RT^2} \tag{12}$$

where λ = heat of condensation per lb-mole

R = gas constant

The temperature gradient, dT/dA, is evalued by equating the loss in sensible heat of the gas, plus the heat of condensation of the material condensing as mist, to the heat transferred to the wall by convection. The balance is taken over a unit area,

$$h(T - T_w) = \lambda L \alpha - V(1+Y) M_m c_m \frac{dT}{dA} \tag{13}$$

The next step is to eliminate L, dY/dT, and dT/dA from Eqs. 10, 11, 12, and 13 and solve for α, the fraction of condensate appearing as mist. The result is

$$\alpha = 1 - \frac{a_1 + a_2}{T - T_w + a_1} \tag{14}$$

where $a_1 = \frac{\lambda}{M_m c_m} \left(\frac{c_m \rho D_v}{k}\right)^{\frac{2}{3}} (1 - \beta) \ln (1 + Y)$

$$a_2 = \frac{RT^2}{\lambda Y} \left(\frac{c_m \rho D_v}{k}\right)^{\frac{2}{3}} (1 - \beta) \ln (1 + Y)$$

where a_1 and a_2 are positive functions of the composition and temperature of the gas mixture. The equation is written in this form to show specifically the effect of wall temperature, T_w, on the fraction condensing as mist. The maximum value of α is unity, negative values indicating a tendency of the gas to become superheated, and positive values of α indicating that the gas will remain saturated. It is assumed in the following that α is positive. Incidentally, a_1 approaches zero as the mole ratio of condensible gas approaches zero.

Returning again to Eqs. 10, 11, 12, and 13, eliminating α, L, and dY/dT and solving for dT/dA, the result is

$$-\frac{dT}{dA} = \frac{h(T - T_w) + \frac{h\lambda}{M_m c_m} \left(\frac{c_m \rho D_v}{k}\right)^{\frac{2}{3}} (1 - \beta) \ln (1 + Y)}{\frac{\lambda^2}{RT^2} VY(1 + Y) + V(1 + Y) M_m c_m}$$

$$= \frac{h(T - T_w + a_1)}{V(1 + Y) M_m c_m \left(1 + \frac{a_1}{a_2}\right)} \tag{15}$$

or, rearranging,

$$-h \frac{dA}{V} = \frac{(1 + Y) M_m c_m \left(1 + \frac{a_1}{a_2}\right)}{T \quad T_w + a_1} dT \tag{16}$$

Equation 16 may be integrated directly, since all quantities on the right-hand side are functions of the temperature.

The rate of solid deposit may now be evaluated as follows. The parenthetical quantity called for in Eq. 1 is

$$-\frac{V}{h}\frac{dY}{dA} = -\frac{V}{h}\frac{dY}{dT}\frac{dT}{dA} \tag{17}$$

Substituting for dY/dT from Eq. 12 and for dT/dA from Eq. 15, the result is

$$-\frac{V}{h}\frac{dY}{dA} = \frac{\lambda Y(T - T_w + a_1)}{RT^2 M_m c_m \left(1 + \frac{a_1}{a_2}\right)} \tag{18}$$

This completes the analysis of condensation from the point of view of heat and mass transfer and provides the basis for a rational design procedure for a trap.

4.3 Summary. The following outline indicates the procedure necessary in treating superheated or saturated gas mixtures:

1. Superheated gas mixture
   (a) Temperature vs. area is obtained from Eq. 7.
   (b) Composition vs. area is obtained from Eq. 4.
   (c) Saturation point is obtained by comparing temperature vs. composition with saturation curve.
   (d) Rate of solid build-up is obtained from Eqs. 1 and 5.
2. Saturated gas mixture
   (a) Tendency toward staying saturated is obtained from Eq. 14.
   (b) Temperature vs. area is obtained from Eq. 16.
   (c) Composition is obtained from temperature, since mixture is saturated.
   (d) Rate of solid build-up is obtained from Eqs. 1 and 18.

5. DISCUSSION

With the use of the relationships derived above it is now possible to make a detailed study of rate of condensation that may be applied to any trap for which an estimate of convective heat-transfer coefficient may be made. Data on the convective heat-transfer coefficients are available for a variety of types of surfaces. Conversely, the performance of any particular trap may be predicted from heat-transfer coefficient measurements, which are relatively easy to obtain.

In proceeding to detailed trap designs, there are a number of further considerations, which will be discussed briefly. These considerations have to do with simplifying assumptions which were made in the derivations. It has been assumed that the condensable gas will diffuse across the boundary film under the influence of a partial-pressure gradient and that this film is the same as that for convective heat transfer. Since the temperature within the film will vary between the main gas temperature and the wall temperature, there will probably be a point where gas will tend to condense as mist. This will have the net effect of somewhat increasing the partial-pressure gradient and thereby increasing the fraction which is condensed close to the wall. No attempt has been made to allow for this effect.

The temperature of the condensed solid on the wall is assumed equal to the wall temperature. Actually this temperature will be higher than the wall temperature, since all the heat load must be transferred across the solid film. If the thermal conductivity of the condensed film can be determined, the surface temperature may be computed from the heat density. Neglecting the sensible heat of the solid condensate between the gas temperature and the wall temperature, the heat load at any point is given by

$$Q = h(T - T_w) + K(p - p_w)\lambda$$

in which the first term represents heat transferred across the film by convection and the second term represents heat liberated by gas that diffuses directly to the wall and condenses there. Substituting for K its equivalent from Eq. 2, the heat load is

$$Q = h(T - T_w + a_1) \tag{19}$$

for either a saturated gas mixture or a superheated gas mixture. This load may be used to calculate the temperature drop across the solid film.

The phenomenon of mist formation has not been discussed except to calculate the fraction that would be expected to appear as mist. The separation of such mist might constitute a serious problem if high recovery is required.

Finally, the hydrodynamics of flow through the trap should be considered. If the two gases in the mixture are of considerably different molecular weight, the change in density of the mixture as the condensable gas is removed may give rise to by-passing or "stack effect" if the flow path is too short or the flow resistance too small. For

example, in cooling a mixture of nitrogen and UF_6, the density will first decrease sharply as the UF_6 is condensed out and will then increase as the residual gas, mainly nitrogen, is further cooled. These considerations affect the choice of the type and orientation of heat-transfer surface.

REFERENCES

1. A. P. Colburn and D. A. Hougen, Ind. Eng. Chem., 26: 1178 (1934).
2. A. P. Colburn, Ind. Eng. Chem., 22: 967 (1930).
3. A. P. Colburn, Trans. Am. Inst. Chem. Engrs., 29: 174 (1933).
4. T. H. Chilton and A. P. Colburn, Ind. Eng. Chem., 26: 1183 (1934).
5. A. P. Colburn and A. G. Edison, Ind. Eng. Chem., 33: 457 (1941).

Part 4

ABSORPTION OF UF_6 AND FLUORINE

Chapter 7

ABSORPTION IN A HIGH-MOLECULAR-WEIGHT NONAQUEOUS SYSTEM — URANIUM HEXAFLUORIDE IN HEAVY OIL

By Ralph Landau, C. E. Birchenall, George G. Joris, and Joseph C. Elgin*

1. INTRODUCTION

Very little information is available to the industrial designer of absorption and stripping equipment regarding the extrapolation of existing data to radically new systems or conditions. In connection with the industrial design of a system for the absorption from inert gases of uranium hexafluoride (molecular weight 352) by a special heavy oil (molecular weight 750), an attempt was made to check the validity of established techniques of calculation (modified to some extent) by a limited experimental program. Making use of the generally accepted theory and extrapolating the data available for the common absorption systems, the performance to be expected in the present system was first predicted. The experimental study in a small-scale packed tower followed. Since the molecular weights and associated properties for this nonaqueous system differed very widely from published data for other systems (mostly aqueous), and since the temperature of operation (200°F) was also beyond the range of most available data, it was felt that the results of this study would provide a severe critique of existing design methods and lend some confidence to their use in similar cases in the future. This chapter presents a summary of the results obtained.

A corollary aim of this work was to check whether, by suitable scaling up, the results of limited small-tower experiments would

* The collaboration of V. I. Montenyohl, L. C. Bostian, W. C. Carter, and J. L. Kulp is gratefully acknowledged; stimulating discussions were provided by Dr. H. Eyring and Dr. R. Rosen.

suffice for the design of the large-scale industrial equipment. Insufficient time was available to permit a thoroughly scientific study. Furthermore, the analytical and other problems associated with such

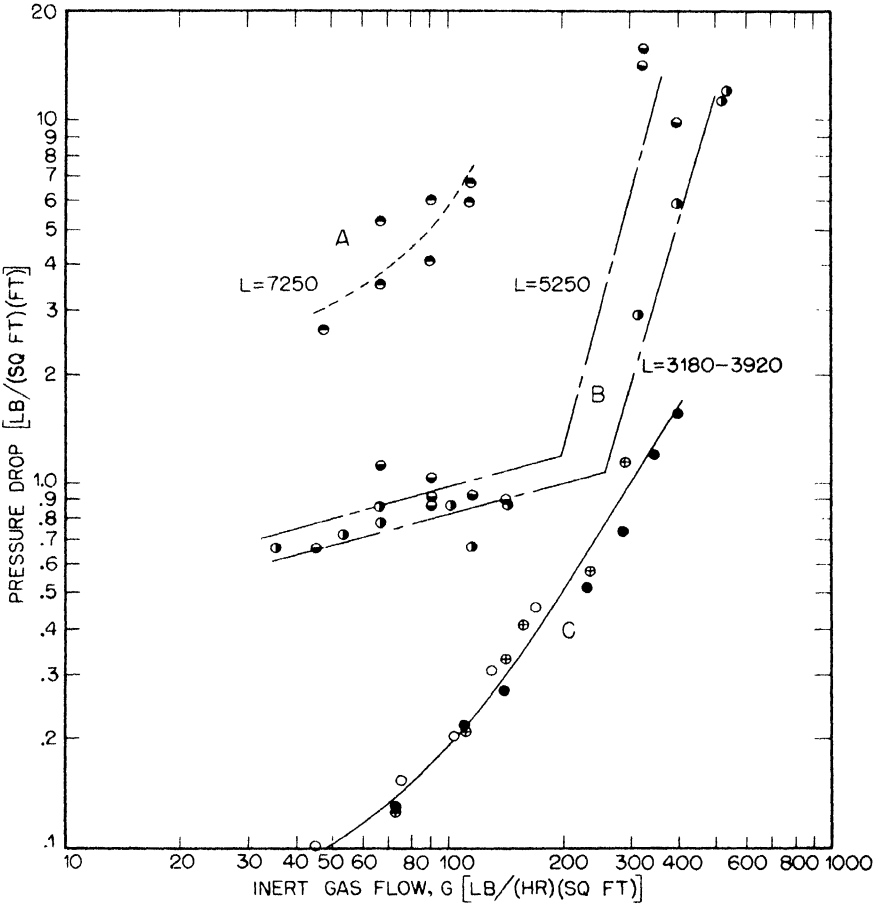

Fig. 7.1 — Pressure drops. Curve A: nitrogen, heavy-oil packing; curve B: nitrogen, water packing; curve C: nitrogen, dry packing. ○ represents gas-film coefficient with initial packing; ● represents coefficient after absorption runs; ⊗ represents coefficient after repacking.

a novel system were of more than ordinary difficulty. Consequently the results obtained were less precise than would normally be desirable in a study of this kind. Nevertheless the interpretation of the data has been carried as far as possible, since data of this sort are still useful for many industrial design problems.

2. THEORETICAL DISCUSSION

In the countercurrent absorption of gases by liquids and in the reverse operation of stripping, it is generally assumed that the controlling mechanism (in the absence of chemical reactions) involves diffusion across two stagnant-fluid films at the phase interfaces, these films being gas and liquid. The quantitative application of the two-film theory of absorption has been described in the literature.[1,2,3] In the case of a system following Henry's law, it may be shown that

$$\frac{1}{K_G a} = \frac{1}{k_G a} + \frac{1}{H k_L a} \tag{1}$$

where $K_G a$ = over-all absorption coefficient, lb-moles/(hr)(cu ft)(atm)
$k_G a$ = gas-film absorption coefficient, lb-moles/(hr)(cu ft)(atm)
$k_L a$ = liquid-film absorption coefficient, lb-moles/(hr)(cu ft) (lb-moles/cu ft)
H = Henry's law constant, lb-moles/(cu ft)(atm)

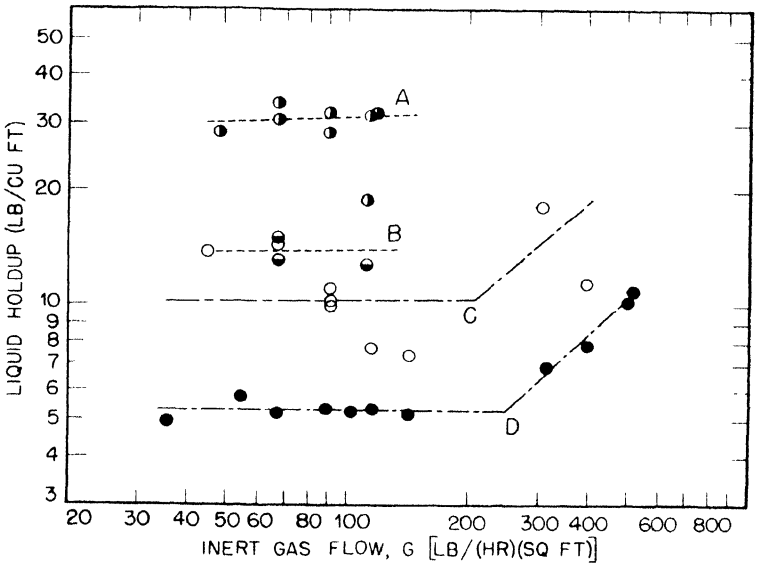

Fig. 7.2—Liquid holdups. Curve A: nitrogen, heavy-oil packing, L = 7,250 lb/(hr)(sq ft); curve B: nitrogen, heavy-oil packing, L = 1,450 to 1,813 lb/(hr)(sq ft); curve C: nitrogen, water packing, L = 5,250 lb/(sq ft)(hr); curve D: nitrogen, water packing, L = 3,180 to 3,920 lb/(sq ft)(hr).

If information is available to permit calculations of the individual film resistances, then the over-all coefficients may be calculated for various conditions and the apparatus can be properly designed. If Henry's law does not hold, then this equation can be used only differentially at points in the apparatus.

A somewhat different approach, developed by Colburn,[4] is also useful, but in the present case it was considered more difficult to interpret and hence is not employed in this study.

The authors' application of existing methods and their introduction of some new devices for estimating the individual film coefficients are described in the following section.

2.1 Gas Film. Unpublished studies by Fellinger[5] provide data on over-all coefficients for the system ammonia and water in different-size packings at varying gas and liquid flow rates. Correction of these data for the liquid-film coefficients permitted preparation of the curves for gas-film coefficients shown in Fig. 7.3 for packings of ¼ to 2 in. Data for Berl saddles were also obtained by Fellinger but were not used in the present study. Additional data on the same system have been obtained by Dwyer and Dodge[6] and by Molstad, McKinney, and Abbey.[7] Corrected to comparable conditions, these are also shown in Fig. 7.3.

Despite some uncertainty regarding effect of packing size, all the data agree rather well.

Extension of these data to other solute gases may be made by multiplying the gas-film coefficients for ammonia-air by the 0.56 power of the ratio of the diffusivity of the desired system to that of ammonia-air. The proper value of the exponent is somewhat uncertain, and more experimentation is needed to determine it more definitely. Calculation of the diffusivity is made using Gilliland's correlation[8] and employing a molecular volume calculated from experimental data on the density at the normal boiling point. Correction for the effect of temperature on the gas-film coefficient is much less certain. The quoted data[6,7] and the earlier recommendation of Haslam, Hershey, and Kean[9] indicate a decrease in gas-film coefficient with increasing temperature. The data of Molstad *et al.*,[7] when fitted by an equation involving a power of the absolute temperature, indicate that the coefficient varies as $T^{2.2}$. The data of Dwyer and Dodge[6] suggest $T^{3.1}$. On the other hand, Kowalke, Hougen, and Watson[10] indicate a much smaller variation. In this chapter the data of Molstad *et al.*[7] were employed.

2.2 Liquid Film. The correlation of Sherwood and Holloway,[3] which provides for the effect of temperature and diffusivity, is employed.

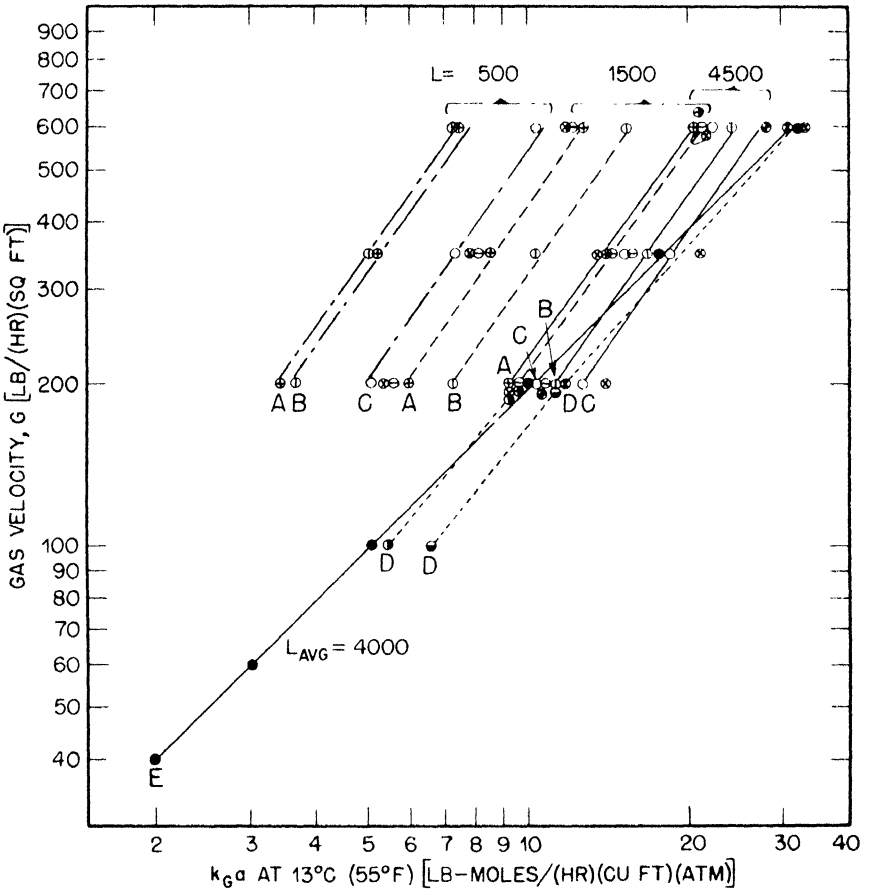

Fig. 7.3—Gas-film coefficients. Absorption of ammonia in water, tower packed with Raschig rings; temperature 13°C (55°F). Curve A: 2-in. packing; curve B: 1½-in. packing; curve C: 1- to ½-in. packing; curve D: 1-in. packing; curve E: ¼-in. packing.

Data of Fellinger (adjusted): ⊖ represents ⅜-in. packing; ○ represents ½-in. packing; ⊗ represents 1-in. packing; ⊕ represents 1½-in. packing; ⊕ represents 2-in. packing.

Data of Molstad (adjusted): ◑ represents 1-in. packing, L = 4,500 lb/(sq ft)(hr); ◔ represents 1-in. packing, L = 1,500 lb/(sq ft)(hr); ◑ represents 1-in. packing, L = 500 lb/(sq ft)(hr).

Data of Dwyer and Dodge (adjusted): ◒ represents 1-in. packing, L = 4,500 lb/(sq ft)(hr); ◑ represents 1-in. packing, L = 1,500 lb/(sq ft)(hr).

Data of this study (adjusted): ● represents ¼-in. packing, L = 4,000 lb/(sq ft)(hr).

Where the liquid-phase diffusivity is unknown, as in the present case, a semiempirical prediction has been postulated, based on the theory of absolute reaction rates,[11]

$$\frac{D_x}{D_s} = \left(\frac{T_x}{T_s}\right)\left(\frac{\eta_s}{\eta_x}\right)\left(\frac{V_s}{V_x}\right) \tag{2}$$

where D = diffusivity, sq cm/sec or sq ft/hr
T = absolute temperature, °K
η = viscosity of liquid film, centipoises
V = molecular volume of diffusing substance, ml

Subscripts x and s stand for an unknown and a known system, respectively. In this equation, V is calculated, as above, from the volume at the normal boiling point or from the Gilliland atomic volumes.[8] This equation was derived from Eq. 108 of Glasstone, Laidler, and Eyring[11] and checked by a brief survey of some data on diffusion coefficients in organic systems of relatively high molecular weight. Table 7.1 presents the results of calculations made with a few systems for which at least approximate data were available. It is not

Table 7.1a — Diffusion Coefficients for Known Systems

System	Solute			Solvent		Temp., °C	D, (sq cm/sec) × 10^5
	Formula	η	V	Formula	η		
1	C_6H_5Br	1.45	108	$(C_2H_5)_2O$	0.28	7.5	3.5
2	I_2	2.8	56	CS_2	1.6	20	3.12
3	CCl_4	1.2	100	C_6H_6	0.8	7.5	1.51
4	CCl_4	1.2	100	C_6H_6	0.8	7.5	1.51
5	C_6H_5Br	1.45	108	$(C_2H_5)_2O$	0.28	7.5	3.5
6	CCl_4	1.2	100	C_6H_6	0.8	7.5	1.51

Table 7.1b — Comparison of Calculated and Measured Diffusion Coefficients for "Unknown" Systems

System	Solute			Solvent		Temp., °C	D, (sq cm/sec) × 10^5			
							Calculated, using			Observed*
	Formula	η	V	Formula	η		Avg. visc.	Solvent visc.	Avg.	
1	$CHBr_3$	2.3	97	$C_5H_{11}OH$	6.5	7.5	0.66	0.16	0.41	0.52
2	$CHBr_3$	2.3	97	$C_5H_{11}OH$	6.5	7.5	0.9	0.15	0.53	0.52
3	$C_{10}H_8$	5.5	136	C_6H_6	0.8	7.5	0.43	1.37	0.90	1.19
4	$C_2Br_4H_2$		120	$C_2Cl_4H_2$	2	15		0.58		0.50
5	$C_2Br_4H_2$		120	$C_2Cl_4H_2$	2	15		0.49		0.50
6	UF_6	0.75	96	Oil	17	93	0.225	0.094	0.16	

*This column gives actual data reported in the literature[11] for the systems cited. In order to check the assumed extrapolation method, these systems were considered to be "unknown," and the diffusion coefficients thus calculated were compared with the literature values.

possible to conclude finally from these meager data that correction by the molecular-volume ratio factor as used is correct or helpful, since its effect is small. It may be that an average of this function for solute and solvent would be best. However, the greatest uncertainty lies in the choice of a proper average viscosity of the film (η). Calculations were therefore made, (1) using the arithmetic average of solute and solvent viscosities and (2) using only the solvent viscosities. An average of the diffusion coefficients obtained in this way gave a rather close approximation to diffusion coefficients reported in the literature, and the method was used to calculate a coefficient for the present system. This device is an approximate method for calculating the true average film viscosity. Since the concentration gradient of solute in the film is rather steep and logarithmic, the average concentration of solute is less than the arithmetic average, and the average viscosity should take this into account. There was insufficient time available to permit further examination. A more extensive study of published data may reveal a better correlation. Since diffusivity appears in the Sherwood-Holloway equation to the 0.5 power, the errors in extrapolation are reduced when $k_L a$ is calculated.

At specified gas rates, the foregoing techniques may be expressed in terms of the measured coefficients for ammonia in water as follows:

$$(k_G a)_x = (k_G a)_{NH_3} \left[\left(\frac{\frac{1}{M_x} + \frac{1}{M_i}}{\frac{1}{17} + \frac{1}{29}} \right)^{\frac{1}{2}} \left(\frac{1}{\frac{V_x^{\frac{1}{3}} + V_i^{\frac{1}{3}}}{(25)^{\frac{1}{3}} + (27.8)^{\frac{1}{3}}}} \right)^2 \right]^{0.56} \left(\frac{286}{T_x} \right)^{2.2} \qquad (3)$$

where $(k_G a)_{NH_3}$ is obtained from Fig. 7.3, and M_i and V_i are the molecular weight and volume of the inert carrier gas.

At specified liquid rates, the techniques may be expressed as follows:

$$(k_L a)_x = \alpha \left[D_3 \left(\frac{T_x}{T_s} \right) \left(\frac{\eta_s}{\eta_x} \right) \left(\frac{V_s}{V_x} \right)^{\frac{1}{3}} \right]^{0.5} \left(\frac{L_s}{\mu_x} \right)^{1-n} \left(\frac{\mu_x}{\rho_x} \right)^{0.5} \qquad (4)$$

where α and n are constants which depend on the packing; L is the liquid rate, lb/(hr)(sq ft); μ is the liquid viscosity, lb/(hr)(ft); ρ is the liquid density, lb/cu ft; and η is the average liquid film viscosity, which differs from μ since the film contains solute to a much greater extent than the main body, as explained above. The subscript s refers to the reference system chosen, and x to the unknown system.

In this work, the respective constants for ammonia (in air) and water are:

V_{NH_3} = 25 (calculated from the actual volume at the boiling point; the atomic-volume rule of Gilliland gives 26.7)

V_{air} = 27.8 (from Gilliland's atomic-volume rule)

$D_{NH_3\text{-}H_2O}$ = 7.6×10^{-5} sq ft/hr at 20°C (68°F)

$\eta_{NH_3\text{-}H_2O}$ = 1 centipoise at 20°C (68°F) = 2.4 lb/(hr)(ft)

H = 4.44 lb-moles/(cu ft)(atm) at 20°C (calculated from log $\frac{p}{c} = 4.699 - \frac{1{,}922}{T}$, where p = partial pressure of NH_3 in atmospheres, c = moles/liter of NH_3 in solution, and T = °K)

The constants for UF_6 in the oil used are:

M_{UF_6} = 352

M_{N_2} = 28

V_{UF_6} = 96

μ_{oil} = 17 centipoises = 41 lb/(ft)(hr)

μ_{UF_6} = 0.75 centipoise = 1.8 lb/(ft)(hr)

η_{film} = 8.9 centipoises (average of above) = 21.5 lb/(ft)(hr)

ρ_{oil} = 113 lb/cu ft

$H_{UF_6\text{-}oil}$ = 0.0446 (see Fig. 7.11)

3. SAMPLE CALCULATIONS

The foregoing methods were employed in predicting an over-all design coefficient for the absorption of UF_6 from nitrogen in a heavy oil at 93°C (200°F). Both gas and liquid were dilute with respect to UF_6.

The adjustment of the gas-film coefficient for ammonia to the gas-film coefficients of this system is summarized in Figs. 7.4 and 7.7; the coefficient for ½-in. rings was employed. These figures therefore summarize the predicted values for absorption coefficients in this system. The liquid-film coefficients were calculated for 2- to ⅜-in. rings and extrapolated to ¼-in. rings. The over-all coefficients (expressed in gas-film units) were calculated from Eq. 1.

1. Gas-film coefficient (L = 4,500; G = 100)

From Fig. 7.3, $(k_G a)_{NH_3} = 7.9$

From Eq. 3,

$$k_G a = 8.0 \left[\left(\frac{\frac{1}{352} + \frac{1}{28}}{\frac{1}{17} + \frac{1}{29}} \right)^{\frac{1}{2}} \left(\frac{1}{(96)^{\frac{1}{3}} + (31.2)^{\frac{1}{3}}} \Big/ \frac{1}{(25)^{\frac{1}{3}} + (27.8)^{\frac{1}{3}}} \right)^2 \right]^{0.56} \times \left(\frac{286}{366} \right)^{2.2}$$

$$= 2.3 \text{ lb-moles/(hr)(cu ft)(atm)}$$

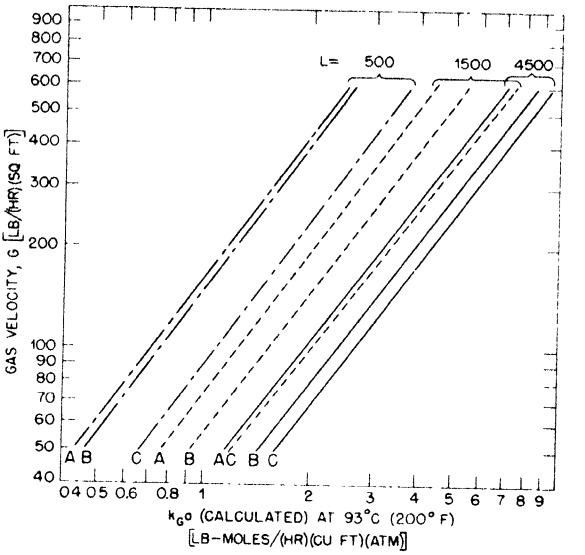

Fig. 7.4 — Calculated gas-film coefficient, $k_G a$. Absorption of UF_6 in heavy oil, towers packed with Raschig rings; temperature 93°C (200°F). Curve A: 2-in. packing; curve B: 1½-in. packing; curve C: 1- to ½-in. packing.

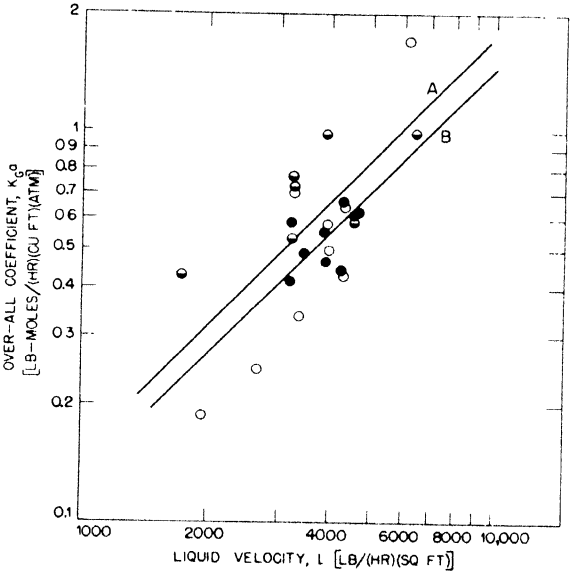

Fig. 7.5 — Dependence of measured over-all coefficient, $K_G a$, on liquid velocity; absorption of UF_6 in heavy oil at 93°C (200°F). Curve A: G = 100 lb/(sq ft)(hr); curve B: G = 50 lb/(sq ft)(hr). ○ represents absorption where G = approximately 100 lb/(sq ft)(hr); ● represents absorption where G = approximately 50 lb/(sq ft)(hr); ◒ represents stripping where G = approximately 50 lb/(sq ft)(hr).

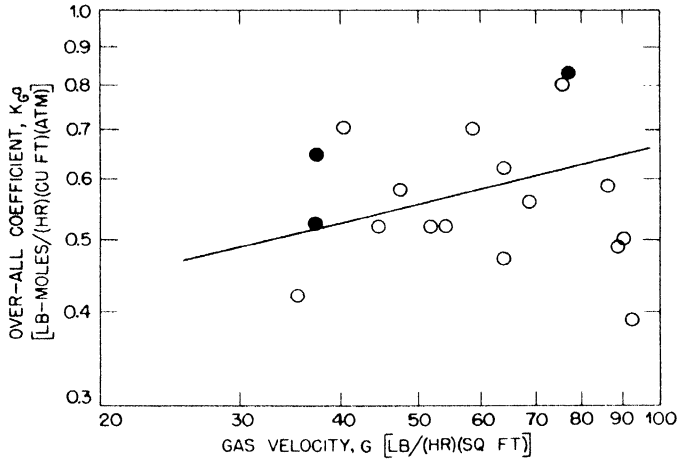

Fig. 7.6 — Dependence of measured over-all coefficient, K_Ga, on gas velocity; absorption of UF_6 in heavy oil at 93°C (200°F). ○ represents absorption where L = 4,000 lb/(sq ft)(hr); ● represents stripping where L = 4,000 lb/(sq ft)(hr).

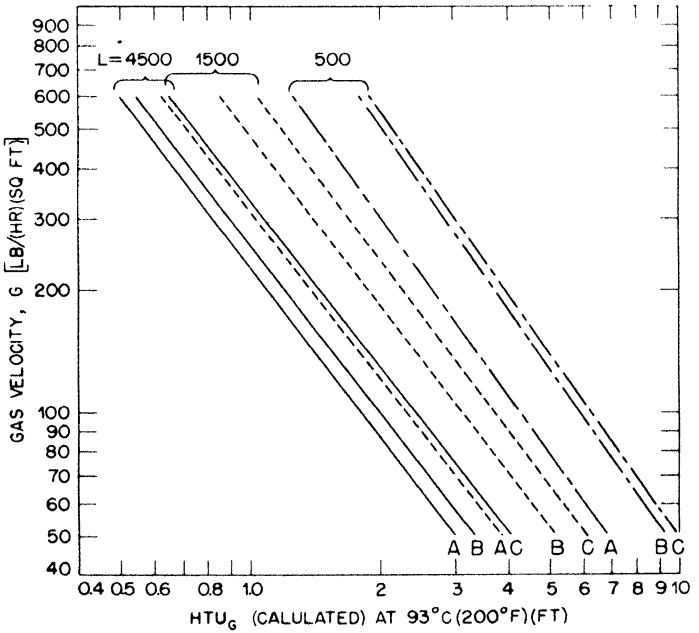

Fig. 7.7 — Calculated gas-film height of a transfer unit. Absorption of UF_6 in heavy oil, towers packed with Raschig rings; temperature, 93°C (200°F). Curve A: ½- to 1-in. packing; curve B: 1½-in. packing; curve C: 2-in. packing.

2. Liquid-film coefficient (L = 4,500)
For 2-in. rings, $k_L a = 80 \times 0.62 \times 10^{-5} \left(\frac{4,500}{41}\right)^{0.78} \left(\frac{41}{141}\right)^{0.5}$

$= 4.5$ lb-moles/(hr)(cu ft)(lb-moles/cu ft)

Similar calculations were made for other rings and extrapolated to ¼ in., giving a $k_L a = 13.1$.

Then, from Eq. 1,

$$\frac{1}{K_G a} = \frac{1}{2.3} + \frac{1}{13.1 \times 0.0446}$$

or

$$K_G a = 0.47 \text{ lb-moles/(hr)(cu ft)(atm)}$$

4. EXPERIMENTAL PROCEDURE

Obviously the foregoing procedure involved so many extrapolations that the design of a plant could not safely be undertaken without experimental corroboration. Since the time was limited, only a small tower could be set up, but it was hoped that by using the design procedure described above the extrapolation to larger packing and towers might be made with some confidence, provided a suitable check on the predicted coefficient for ¼-in. rings could be obtained.

As an additional check on this theory, it was decided to run the absorption of ammonia in water in the same tower, to see whether the general operating technique gave results consistent with previous data obtained on larger towers. Finally, by measuring the effect of gas rate on the over-all coefficient and extrapolating to infinite liquor rate, a measure of the actual gas-film absorption coefficient could be obtained, and comparison could be made with that predicted by the proposed design method.

Accordingly, a 3-in. ID stainless steel tower packed to a height of 4 ft with ¼-in. monel Raschig rings was built. These rings averaged 0.259 in. OD, 0.180 in. ID, 0.04 in. wall thickness, and 0.375 in. height. Most rings had a small gap, which was responsible for the deviation from the nominal size of 0.25 in. They were not perfect circles. The packing operation was done under carbon tetrachloride. Later the column was repacked under acetone to test for reproducibility.

The heavy oil was stored in 25-gal stainless-steel tanks, each containing a 2- and 3-kw immersion heater for maintaining the oil at 200°F (93°C). The tanks were connected in such a way that they could be used interchangeably as inlet and outlet reservoirs. Nitrogen pressure was used to raise the liquid to the tower head.

The uranium hexafluoride was supplied from a large tank by heating to 100°C (212°F). This gave sufficient pressure for the flows employed.

Stainless steel, brass, and copper were used almost exclusively as construction materials. A nickel mixing can with copper baffles was inserted in the gas inlet line, and a nickel spray trap removed liquid from the gas exit line. The tower head was fitted with a stainless-steel shower head distributor to provide even flow over the packing. A perforated copper tube served as the gas inlet in the tower foot.

The whole system was wound with chromel heating coils to control the temperature and covered with asbestos lagging. Thermometers were inserted in the fluid streams at several points to observe the temperature during the runs.

Dry nitrogen, of a dew point less than −70°F, was used as an inert carrier gas for UF_6. Water-pumped nitrogen was employed in the same role during the ammonia and water experiments. The system was dried before use by evacuating and heating.

The oil flow was measured with a rotameter containing a nickel float calibrated under operating conditions. The nitrogen flow was measured with a rotameter calibrated against a wet-test meter. The UF_6 rate was kept constant throughout a run by keeping a constant pressure drop across an orifice. From the analytical data, the absolute rate based on the nitrogen flow could be calculated. A similar procedure was used for metering ammonia, but in this case a rotameter was employed for high flows and a mercury manometer for low flows.

When used for ammonia absorption, much of the metal in the auxiliary parts of the system (i.e., all but the tower, head and foot) was replaced with glass, tygon, and rubber, so that the liquid flow could be observed and the level at the tower base could be regulated. This change was possible since elevated temperatures were not required. Water was stored in 13-gal glass carboys, and the flow was regulated with nitrogen pressure. Distilled water was used for all absorption runs.

The pressure drop and liquid holdups for various flow rates were first determined. Holdup was calculated from drainage data, and pressure drops were determined by a differential manometer connected across the tower.

The UF_6 absorption runs lasted 30 to 60 min after all the flows became stabilized. Liquid samples were taken from the inlet tank and from the outlet line through a valve at the bottom of the U tube leading from the tower foot. Gas samples were taken in evacuated bulbs

from the gas entry and exit lines by opening valves into the gas stream. Three sets of samples were taken at intervals of 5 to 10 min for each run. Stripping runs differed from absorption runs only in the omission of gas entry samples, since pure nitrogen was used.

In the ammonia absorption runs, a steady state was attained almost immediately, and sampling was begun shortly thereafter, three sets of liquid samples being taken in rapid succession.

5. RESULTS

The experimental data are presented in Tables 7.2 to 7.7 inclusive. They have been summarized and correlated in Figs. 7.1 to 7.6 inclusive. The liquid-vapor equilibria, which closely approximate Raoult's law, are presented in Figs. 7.9, 7.10, and 7.11. They are based on data obtained by F. E. McKenna and T. P. Wilson.

Table 7.2—Pressure Drop through Dry Packing

Nitrogen flow		Δ P/N,
Ft/sec	Lb/(sq ft)(hr)	lb/(sq ft)(ft)
0.1785	45.0	0.102
0.301	76.0	0.153
0.415	105	0.204
0.517	130	0.307
0.670	170	0.461
After absorption experiments		
0.927	234	0.516
1.152	290	0.748
1.38	348	1.212
1.59	400	1.573
0.143	36.0	0.0516
0.292	73.7	0.129
0.442	112	0.217
0.560	142	0.273
Tower repacked		
0.143	36.0	0.077
0.292	73.7	0.129
0.442	112	0.206
0.560	142	0.335
0.625	158	0.413
0.934	236	0.588
1.160	292	1.160

Table 7.3—Holdup and Pressure Drop: Oil-Nitrogen

Liquid velocity, lb/(sq ft)(hr)	Gas velocity, lb/(sq ft)(hr)	Δ P/N, lb/(sq ft)(ft)	Holdup, lb/cu ft
1,813	67.2	1.91	14.9
3,625	67.2	2.27	21.8
5,438	67.2	3.26	24.0
7,250	67.2	5.27	34.0
9,063	67.2	13.3	40.0
7,250	90.0	6.00	28.4
7,250	113.6	5.95	18.8
1,450	113.6	1.24	12.6
2,900	113.6	2.17	18.8
4,350	113.6	3.26	23.2
5,800	113.6	4.65	27.2
7,250	113.6	6.62	31.6
7,250	67.2	3.52	30.4
...	90.0	4.03	31.6
...	113.6	6.62	31.6
7,250	47.8	2.69	28.6
1,813	67.2	1.04	13.2

5.1 Pressure Drops. The data on dry packing (see Fig. 7.1 and Table 7.2) are reproducible even after repacking. They are somewhat lower than when calculated by conventional methods. However, the pressure drops were small (between 0.1 and 1 in. H_2O) and the precision was not great. The slight curvature at about G = 100 is due to a shift from turbulent to streamline flow, as calculated from the modified Reynolds numbers.

The pressure-drop data in wetted systems (Fig. 7.1 and Tables 7.3 and 7.4) show the flooding points. These data appear to be in fairly good agreement with published data.[12] The values for nitrogen-water are consistent with those obtained by Elgin and Weiss[13] on 0.625-in. clay Raschig rings.

5.2 Liquid Holdup. The holdup shows a flooding point approximately at the same value indicated by the wet pressure drops. Up to the flooding point, holdup (unlike pressure drop) showed virtually no dependence on gas rate, but was only a function of liquid rate.

5.3 Absorption and Stripping of UF_6 in Heavy Oil. The data obtained in runs showing material balances within 20 per cent are given in Tables 7.5a, 7.5b, and 7.6, and plotted in Figs. 7.5 and 7.6. Since Raoult's law applied and the system was dilute, the use of the arithmetic-mean driving force was justified. The correlations shown in these figures are only approximate, owing to the scatter caused by

Table 7.4 — Holdup and Pressure Drop: H_2O-Nitrogen

Liquid velocity, lb/(sq ft)(hr)	Gas velocity, lb/(sq ft)(hr)	Δ P/N, lb/(sq ft)(ft)	Holdup, lb/cu ft
1,690	399	4.03	4.17
	523	6.45	4.79
1,890	116	0.670	3.76
2,510	116	0.722	3.98
2,730	315	2.63	4.31
	399	4.65	5.97
	523	8.93	6.26
3,180	35.8	0.670	5.11
	53.5	0.721	5.77
	67.6	0.783	5.20
	87.9	0.670	5.36
	102	0.875	5.25
	116	0.670	5.34
	141	0.875	5.14
3,360	523	12.90	10.72
3,920	315	2.99	6.83
	399	5.94	7.90
	523	11.87	10.60
4,600	315	3.82	7.04
	399	8.53	9.80
4,690	116	0.929	7.38
		0.825	6.40
5,250	45.1	0.670	14.33
	67.6	1.133	14.97
		3.720	18.74
	91.5	1.030	10.38
		0.928	11.15
		0.876	10.15
	116	0.929	7.68
	143	0.902	7.33
	315	16.25	18.52
		14.5	Flooded
	399	9.80	11.50

analytical difficulties and the accumulation of a limited amount of corrosion products on the packing. The dependence on gas velocity shown in Fig. 7.6 was derived by choosing data from runs with liquor velocities between 3,250 and 4,650 lb/(hr)(sq ft), and correcting to 4,000 lb/(hr)(sq ft) by the use of the curves in Fig. 7.5. In turn, the latter were presented as functions of the gas rate, using the correlation of Fig. 7.6.

Table 7.5a — Absorption of Uranium Hexafluoride in Oil

Series	N_2 velocity, cfm	Oil velocity		Pressure at tower foot, psi	UF_6 (gas), %		UF_6 (liquid), g/liter	
		Gph	Lb/(sq ft)(hr)		In	Out	In	Out
1-5	0.99	6.5	2,015	2.5	10.6	8.6	0	19.4
2-2	1.03	11.2	3,445	2.5	6.40	4.40	0.2	11.5
3	1.035	11.0		2.5	5.90	4.47	0.2	11.7
3-1	1.04	20.0	6,215	3.25	6.60	3.25	1.1	16.5
2	1.07	20.2		3.25	5.90	2.42	1.1	16.2
4-1	0.996	14.7		0.75	6.44	4.73	0.27	12.2
2	1.00	14.4	4,460	0.75	6.72	3.60	0.24	12.7
3	1.005	14.4		0.75	5.10	4.10	0.21	5.82
5-1	1.02	8.8	2,730	1.7	6.20	4.70	1.10	10.5
2	1.02	8.8		1.7	6.10	5.10	0.91	12.8
6-1	0.996	13.0	4,030	1.25	5.08	3.58	0.72	11.28
3	1.00	13.0		1.25	5.17	3.67	0.56	10.86
8-1	0.49	15.0		0.5	10.3	4.50	0.11	17.0
2	0.49	15.0	4,650	0.55	9.12	4.46	0.11	17.3
3	0.49	15.0		0.55	9.62	4.46	0.11	16.2
9-1	0.82	10.5		0.9	7.74	5.23	1.22	18.3
2	0.83	10.5		1.05	7.78	5.00	1.22	19.3
3	0.84	10.5		1.22	7.26	5.90	1 22	16.4
10-1	0.591	10.5		1.0	8.16	5 87	1.61	15.4
2	0.595	10.5		1.0	8.16	5.40	1.61	16 5
11-1	0.440	10.5	3,250	0.55	10.1	4.52	1.29	19.4
2	0.445	10.5		0.60	9.85	4.48	1.29	18.5
3	0.445	10.5		0.60	10.7	4.48	1.29	18.9
12-1	0.641	10.5		0.95	9.03	4.94	1.29	19.6
2	0.646	10.5		1.00	8.46	4.98	1.29	17.9
3	0.646	10.5		1.00	8.55	5.09	1.29	18.1
13-1	0.71	14.0		1.35	6.30	3.50	0.08	12.7
2	0.72	14.0		1.35	6.31	3.30	0.04	12.6
3	0.71	14.0	4,340	1.35	6.54	2.89	0.06	12.5
14-1	0.39	14.0		1.00	8.95	3.40	0.03	12.3
2	0.39	14.0		1.00	9.14	3.64	0.03	12.8
3	0.39	14.0		1.00	8.88	3.57	0.03	11.5
15-1	0.572	15.0		0.75	5.91	2.49	0.53	9.76
2	0.57	15.0	4,650	0.75	5.94	2.80	0.60	10.10
3	0.58	15.0		0.75	5.84	2.61	0.67	10.40
16-1	0.782	11.2		1.25	4.36	2.84	0.45	9.18
2	0.782	11.2	3,445	1.25	4.53	2.96	0.39	8.88
3	0.782	11.2		1.25	4.76	2.88	0.32	9.13
17-1	0.53	12.8		0.60	5.04	2.32	0.92	8.55
2	0.53	12.8		0.60	5.04	2.20	0.85	8.33
3	0.58	12.8		0.65	4.90	2.20	0.79	8.33
18-1	0.954	12.8		1.2	4.30	2.82	0.79	8.64
2	0.954	12.8	3,960	1.2	4.65	2.81	0.79	8.90
3	0.964	12.8		1.2	4.54	2.90	0.79	8.61
19-1	0.71	12.8		0.93	5.54	3.06	0.79	8.95
2	0.71	12.8		0.93	5.40	3.12	0.79	8.29
3	0.71	12.8		0.93	5.25	3.03	0.79	8.48

Table 7.5b--Absorption of Uranium Hexafluoride in Oil

Series	UF_6, (lb-moles/hr) × 10^{-3}, absorbed from		$K_G a$, lb-moles/(hr)(cu ft)(atm)		Gas flow	
	Gas	Liquid	Observed	Average	Observed, cfm	Average, lb/(sq ft)(hr)
1-5	3.74	2.80	0.189		1.083	92.8
2-2	3.52	2.83	0.351	0.336	1.082	92.9
3	2.64	2.75	0.320		1.087	
3-1	6.10	6.85	1.29	1.67	1.092	94.6
2	6.70	6.75	2.04		1.118	
4-1	2.98	3.88	0.426		1.052	90.0
2	5.38	3.88	0.653		1.052	
3	1.70	1.79	0.248		1.054	
5-1	2.65	1.82	0.243	0.245	1.080	92.0
2	1.77	2.31	0.247		1.076	
6-1	2.53	3.00	0.494	0.496	1.042	89.3
3	2.58	2.96	0.498		1.044	
8-1	5.09	5.60	0.612		0.527	44.9
2	4.08	5.70		0.616	0.523	
3	4.53	5.30	0.620		0.524	
9-1	3.64	4.35	0.643		0.873	75.8
2	4.05	4.60	0.745	0.695	0.884	
3	2.02	3.90			0.897	
10-1	2.90	3.20	0.364	0.422	0.632	54.0
2	3.70	3.46	0.480		0.630	
11-1	4.41	4.20	0.600	0.590	0.471	40.5
2	4.31	4.00	0.580		0.475	
3					0.477	
12-1	4.84	4.26	0.665		0.687	58.9
2	4.01	3.86	0.559	0.596	0.690	
3	4.04	3.91	0.565		0.691	
13-1	3.40	3.91	0.635		0.745	64.0
2	3.74	3.89	0.685	0.664	0.757	
3	4.45	3.85	0.671		0.743	
14-1	3.74	3.80	0.448		0.415	35.5
2	3.78	3.95	0.442	0.435	0.416	
3	3.69	3.55	0.415		0 415	
15-1	3.23	3.06	0.649		0.598	51.8
2	3.07	3.16	0.565	0.614	0.608	
3	3.16	3.24	0.628		0.607	
16-1	2.00	2.16	0.527		0.809	69.3
2	2.03	2.10	0.460	0.497	0.810	
3	2.47	2.19	0.505		0 810	
17-1	2.40	2.16	0.566		0.558	47.6
2	2.51	2.12	0 576	0.575	0.558	
3	2.38	2.14	0.583		0.558	
18-1	2.37	2.22	0.560		1.00	85.6
2	2.95	2.30	0.608	0.574	1.00	
3	2.64	2.21	0.553		1.00	
19-1	2.97	2.31	0.493		0.75	64.1
2	2.74	2.12	0.493	0.468	0.75	
3	2.67	2.18	0.469		0.75	

Table 7.6—Stripping of Uranium Hexafluoride from Oil

Series	N_2 velocity		Oil velocity		Pressure at tower foot, psi	UF_6(gas), % out	UF_6 (liquid), g/liter		UF_6, (lb-moles/hr) × 10^{-3}, stripped from		$K_G a$, lb-moles/(hr)(cu ft)(atm)	
	Cfm	Lb/(sq ft)(hr)	Gph	Lb/(sq ft)(hr)			In	Out	Gas	Liquid	Observed	Average
10S-1	0.435		15.0		0.6	3.29	12.4	5.87	2.21	2.18	0 61	
2	0.435		15.0	4,650	0.6	3.28	12.4	6.66	2.21	1.91	0.54	0.58
3	0.435		15.0		0.6	3.25	12.4	6.04	2.19	2.14	0.58	
11S-1	0.435		10.5		0.6	2.89	12.4	4.49	1.95	1.84	0.54	
2	0.435	37.2	10.5	3,250	0.6	2.79	12.4	4.36	1.88	1.86	0.53	0.53
3	0.435		10.5		0.6	2.90	12.4	4.64	1.96	1.82	0.53	
12S-1	0.435		5.6		0.6	2.22	12.4	2.35	1.50	1.25	0.41	
2	0.435		5.6	1,735	0.6	2.16	12.4	1.86	1.46	1.30	0.43	0.44
3	0.435		5.6		0.6	2.39	12.4	1.72	1.61	1.32	0.50	
13S-1	0.90		10.5		1.00	1.11	7.45	0.97	1.54	1.50	0.75	
2	0.90	77.0	10.5		1.00	1.07	7.58	0.85	1.49	1.56	0.73	0.73
3	0.90		10.5		1.00	1.17	7.96	1.16	1.63	1.58	0.72	
14S-1	0.33		10.5		0.55	2.20	7.66	2.50	1.12	1.20	0.72	
2	0.33	28.2	10.5	3,250	0.55	2.43	7.66	2.66	1.24	1.16	0.83	0.78
3	0.33		10.5		0.55	2.30	7.66	2.45	1.17	1.21	0.80	
16S-1	0.44		10.5		0.50	1.90	6.44	1.63	1.32	1.12	1.05	
2	0.44	37.6	10.5		0.55	1.72	6.09	1.40	1.19	1.09	1.03	1.25
3	0.44		10.5		0.55	1.89	5.74	1.13	1.31	1.07	1.66	
18S-1	0.405		21.4		0.85	1.89	6.09	4.50	1.21			
2	0.405		21.4	6,630	0.85	1.92	6.09	2.89	1.23	1.52	0.947	0.992
3	0.405		21.4		0.85	2.14	6.09	3.16	1.38	1.38	1.038	
19S-1	0.405	34.6	12.8		0.55	1.63	6.02	1.89	1.04	1.17	0.80	
2	0.405		12.8	3,970	0.55	1.94	6.02	1.94	1.24	1.16	1.11	0.99
3	0.405		12.8		0.55	1.85	6.02	1.85	1.18	1.18	1.05	

Table 7.7 — Absorption of Ammonia in Water

H_2O velocity, lb/(sq ft)(hr)	N_2 velocity, lb/(sq ft)(hr)	NH_3, % in water	NH_3, (lb-moles/hr) × 100, absorbed from Gas	NH_3, (lb-moles/hr) × 100, absorbed from Liquid	K_Ga, lb-moles/(hr)(cu ft)(atm)
2,730	54.0	4.91	0.505	0.492	1.80
	68.0	9.67	1.24	1.28	1.81
	123.0	6.42	1.47	1.42	3.57
	198.3	4.06	1.65	1.93	12.5
	198.3	4.70	1.76	1.75	10.6
	208	3.70	1.46	1.82	14.8
	221	4.41	1.84	2.28	9.60
	235	3.72	1.65	2.26	11.3
	302	8.90	4.91	5.71	11.5
	302	8.90	5.36	5.89	12.2
	305	6.25	3.68	4.08	12.1
	305	8.17	5.36	5.89	12.2
	306.5	7.95	4.76	5.35	10.5
	308	8.78	5.37	5.75	12.6
	426	8.15	6.84	6.57	25.6
	401	8.17	6.81	6.45	18.3
	529	7.70	7.96	8.30	26.8
3,920	31.7	7.02	0.407	0.432	2.91
	54.0	4.35	0.443	0.457	1.32
	69.3	4.19	0.540	0.591	3.49
	93.8	2.44	0.425	0.424	2.35
	122.0	6.43	1.50	1.38	4.78
	146.3	3.21	0.88	0.82	9.50
	199.0	4.93	1.85	2.03	10.3
	202.0	4.90	1.86	1.87	9.30
	223.0	4.10	1.72	1.64	4.95
	300.0	9.90	5.96	5.71	12.4
	307.0	8.32	5.10	5.70	12.2
	401.0	8.29	6.53	6.46	19.6
	421	8.23	6.76	6.70	18.0
	430	7.99	6.74	7.00	21.1
	121*	7.97	1.90	1.86	6.57
	222	5.24	2.20	2.15	8.05
	426	8.66	7.21	6.96	15.9
4,530	408	9.02	7.30	7.05	21.9
5,250	46.0	5.61	0.495	0.515	2.77
	92.1	3.095	0.549	0.529	4.23
	120.0	5.33	1.21	1.24	4.91
	143.0	3.65	0.980	0.995	7.45
	236.2	3.44	1.53	1.56	12.6
	304.0	9.71	5.94	6.82	12.8
	306.5	6.56	3.91	4.57	12.6
5,300	72.1	11.35	1.66	1.55	3.07

*Repacked column.

Since, in general,

$$\frac{1}{K_G a} = \frac{1}{H k_L a} + \frac{1}{m G^n} \tag{5}$$

a graph of $1/K_G a$ vs. $1/G^n$, choosing a value of n to give the straightest line, will have a slope which is $1/m$. From this, the $k_G a$ for other conditions can be calculated. It was found that for n = 0.7 to 0.8 (the usually accepted value for n) the data from the correlation of Fig. 7.7 lay substantially on a straight line, with a slope m = 0.036 for n = 0.8. Hence,

$$k_G a = 0.036\ G^{0.8} \qquad [\text{for } L = 4{,}000 \text{ lb/(hr)(sq ft)}] \tag{6}$$

At G = 100, $k_G a = 1.45$; and at 200, $k_G a = 2.5$. From this, $k_L a$ values of 26.1 and 24.2, respectively, can be calculated by Eq. 1. Predicted values were half of these, based on the assumption for diffusivity as described below. Using the extrapolated data of Fellinger shown in Fig. 7.4, the predicted values would be (1-in., ½-in. rings), $k_G a = 2.4$ and 3.8, respectively. It should be noted, however, that Fellinger's data for ⅜-in. rings at L = 4,500 fell close to those for 1½-in. rings. If this were true also for ¼-in. rings, the predicted values of $k_G a$ would be 2.1 and 3.4, respectively. In view of the inaccuracies in both the calculated and experimental values, this agreement may be deemed rather satisfactory.

These considerations show that the liquid-film resistance is the major factor controlling the process, as was expected. No effect of the difference between absorption and stripping could be detected within the accuracy of the data.

The dependence of the over-all coefficient on liquid velocity is evidently much greater than is indicated by the Sherwood-Holloway equation.[3] It is indicated that for such viscous high-molecular-weight systems, a different correlation would be more appropriate. Since, in addition, no data on the diffusion coefficient of UF_6 in oil were available, it was not possible to deduce both the new correlation and the diffusion coefficient from the data obtained. If time had permitted, additional studies at varying flow rates would have made this possible.

Under the circumstances, the Sherwood-Holloway equation was assumed to be correct, and the diffusion coefficient could then be calculated. Actually, for convenience, several values of this coefficient were assumed, and the over-all coefficient $K_G a$ so obtained (using the design method previously described) was compared with

the measured coefficients. The results are shown in Fig. 7.8. It should be noted that a diffusion coefficient of 0.36×10^{-5} sq ft/hr corresponds to a calculation from Eq. 4 in which $\eta = \mu$ (this is probably a lower limit for D).

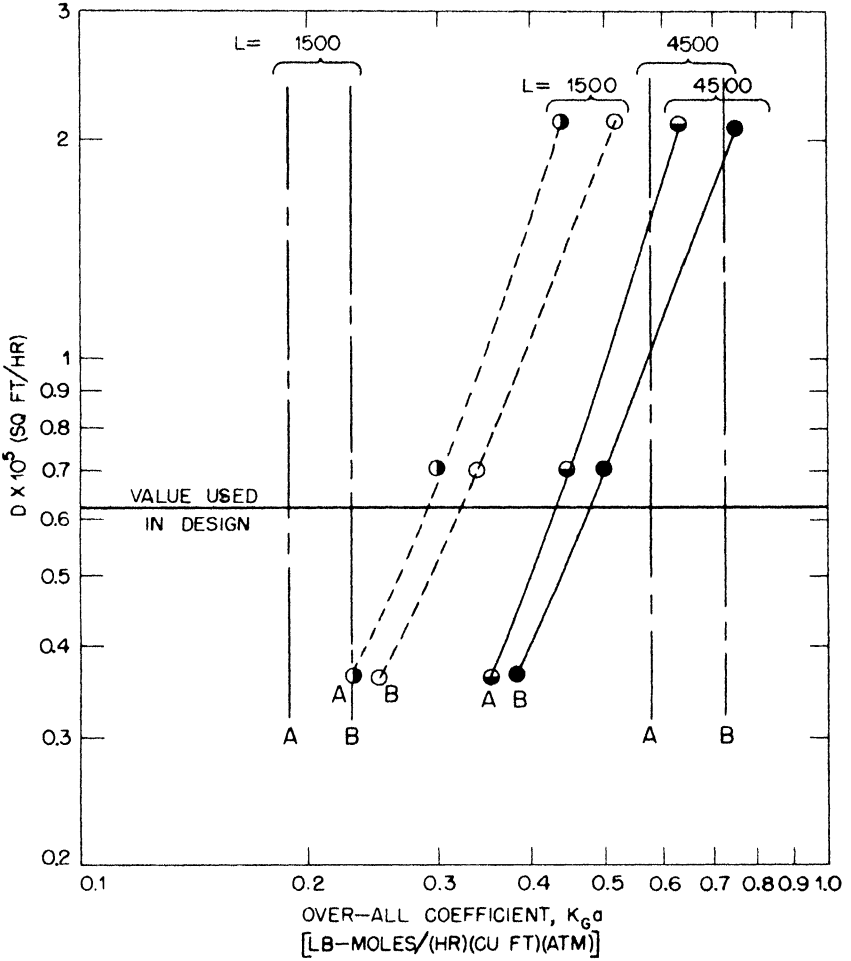

Fig. 7.8—Variation of predicted over-all absorption coefficient, $K_G a$, with assumed diffusivity and comparison with measured coefficients. Absorption of UF_6 in heavy oil at 93°C (200°F).—·—represents observed coefficients; - - - - represents calculated coefficients for L = 1,500 lb/(sq ft)(hr) at various diffusivities; —— represents calculated coefficients for L = 4,500 lb/(sq ft)(hr) at various diffusivities. Curve A: G = 50 lb/(sq ft)(hr); curve B: G = 100 lb/(sq ft)(hr).

The predicted coefficients, on the whole, agree surprisingly well with the observed values. This case is one of the few studies on non-aqueous systems available.[14] Comparable comparisons with theory

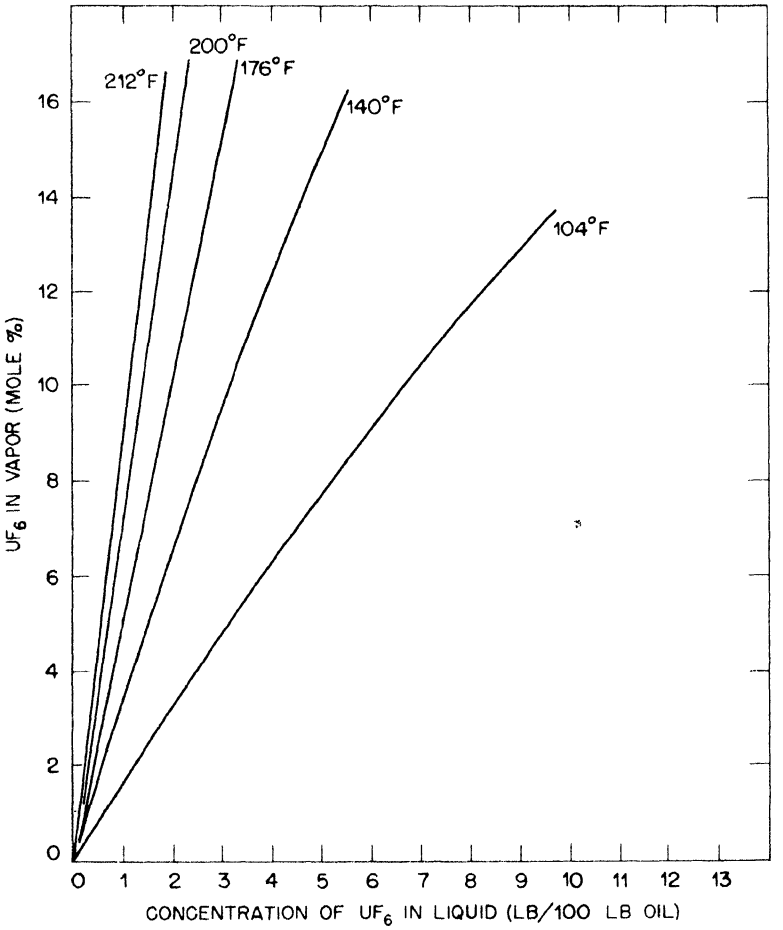

Fig. 7.9 — Change of vapor composition with UF_6 concentration in heavy oil at a total pressure of 1 atm and at various temperatures.

have not been made in these publications. Inasmuch as the Sherwood-Holloway equation does not reflect the large effect of liquid rate found, results calculated at L = 1,500 and L = 4,500 lie closer together than the observed values. For this system, the predicted values tend to be conservative at the higher liquid rates.

There seems to be considerable promise that further development of these design methods will permit design of large towers from data obtained in carefully planned small-scale tests.

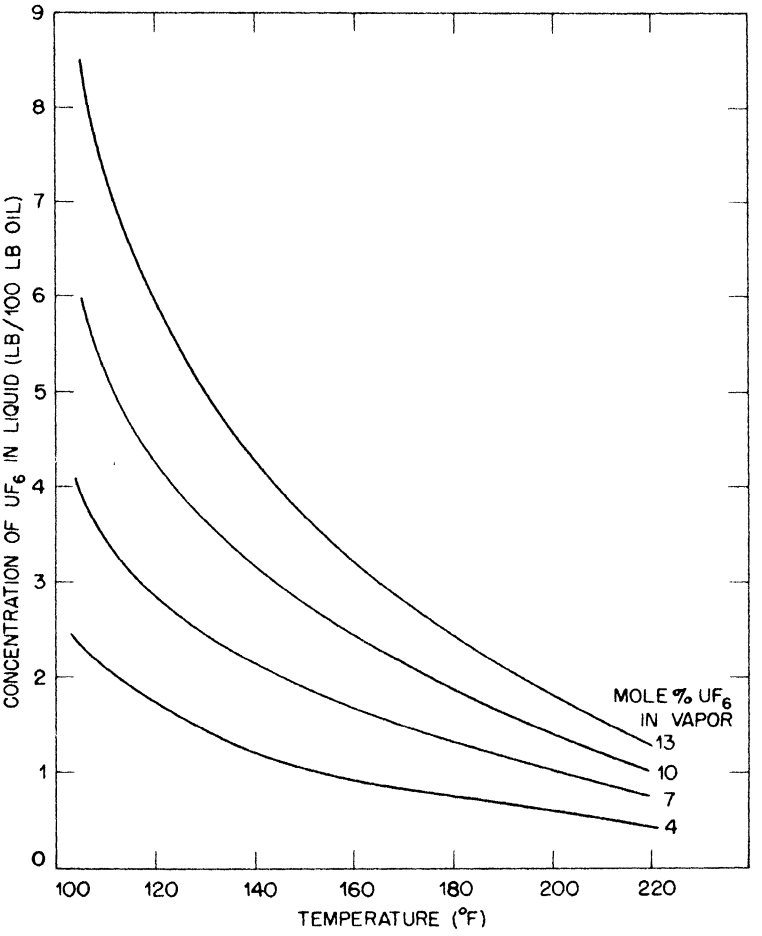

Fig. 7.10—Variation of UF_6 concentration in heavy oil with temperature at a total pressure of 1 atm.

5.4 Absorption of NH_3 in Water. The experimental data given in Table 7.7 were corrected for liquid-film coefficients as calculated by the Sherwood-Holloway equation, and the gas-film coefficients obtained were plotted in Fig. 7.3. The values at low gas rates (below

G = 200) were relatively inaccurate, because the exit gas concentration was so low. At the higher ranges the agreement with published data is good. This suggests that the experimental setup was adequate.

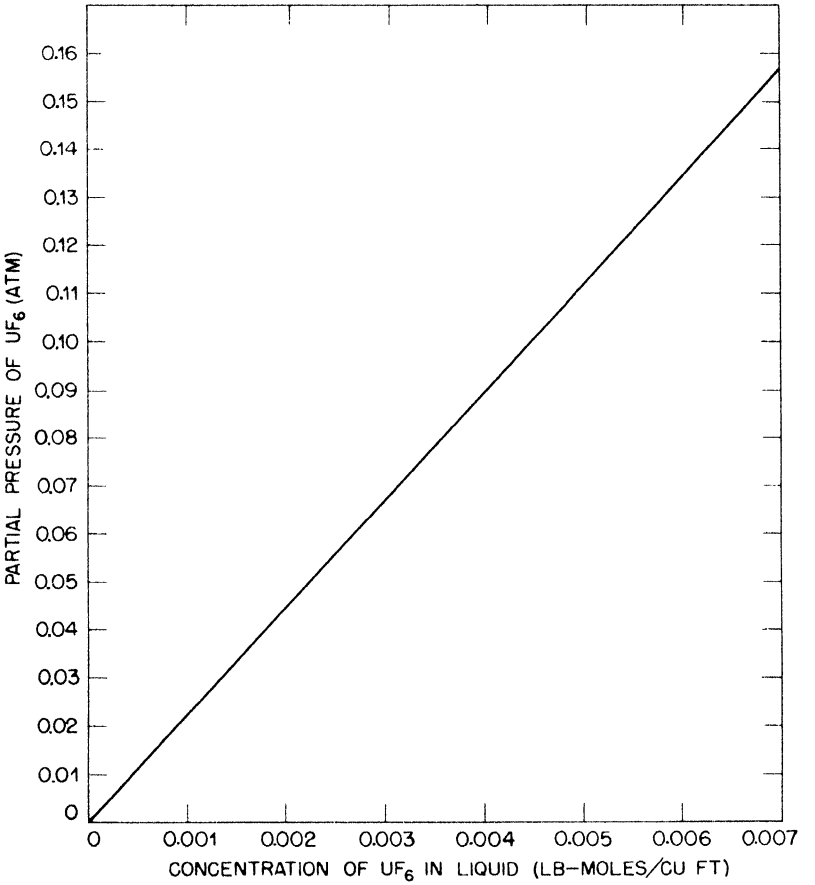

Fig. 7.11 — Partial pressure of UF_6 as a function of its concentration in heavy oil at 93°C (200°F).

6. APPLICATION TO DESIGN

For many industrial design problems it is not necessary to have data of great precision. Many absorption and stripping columns are designed with a safety factor of 2, and this permits the design of equipment for systems in which few data are known accurately. How-

ever, the system employed in the present work was so very far outside available data that this safety factor could not be relied on without experimental confirmation. The data have shown, however, that the design method proposed by the authors of this chapter does allow even this system to be designed safely within this safety factor, over a wide range of conditions. It appears probable, therefore, that many unknown systems, departing less markedly from available data than does the system considered here, can be treated by the proposed method within the same safety factor.

Nevertheless, the aim of all engineering designers is to reduce the safety factors required, since for large equipment the cost sacrifice is substantial. Furthermore, the trend is toward operation of towers near the flooding point and the use of an unnecessarily large safety factor in design will make operating costs higher. The need for certain types of additional data is therefore very great, and the following gaps, based on this study, are suggested:

1. Additional gas-film coefficients (from ammonia and water or similar aqueous and nonaqueous systems) showing the effect of packing type and size, and liquid and gas flow rates. Comparison of these, using the Gilliland correction for diffusivity, would be very desirable. In this connection, further information on the proper exponent used in the evaluation of the gas-film coefficient by correction for diffusivity is required. The development of a general empirical equation, comparable to that of Sherwood-Holloway for liquid films, would be welcome.

2. The effect of temperature on gas-film coefficients over a wide range for various systems.

3. Study of the Sherwood-Holloway correlation for viscous, high-molecular-weight systems, particularly nonaqueous media, to determine its applicability or to find a suitable modified form.

4. Correlations of liquid diffusion coefficients with molecular constants, along the lines suggested in this chapter or otherwise, particularly by obtaining direct diffusion measurements for a wide variety of systems so as to permit a correlation, such as that of Gilliland for gas-film coefficients, to be developed. Further study of the theory of absolute reaction rates in connection with such data is very desirable. Light might thereby be thrown on other phenomena of viscosity and diffusion, and engineering design methods might be extended by such correlations.

5. Comparisons between data taken in small towers using small packing (to preserve a ratio of diameter to packing of at least 10 to 1) and data obtained in larger systems using the same flow rates, etc., employing the correlations developed.

7. CONCLUSION

Sufficiently good agreement between theory and experiment has been obtained to suggest that the design technique employed in this study may be of considerable value in the absence of direct data, but that a substantial amount of coordinated work is still required to establish engineering design of absorption and stripping equipment on a sound and accurate basis. There is also encouraging evidence that small-scale experiments can be extrapolated to plant-scale operation if the underlying correlations can be strengthened along the lines suggested.

REFERENCES

1. J. H. Perry, ed., "Chemical Engineers' Handbook," Chap. X, McGraw-Hill Book Company, Inc., New York, 1941.
2. T. K. Sherwood, "Absorption and Extraction," McGraw-Hill Book Company, Inc., New York, 1937.
3. T. K. Sherwood and F. A. L. Holloway, Trans. Am. Inst. Chem. Engrs., 36: 21, 39 (1940).
4. A. P. Colburn, Trans. Am. Inst. Chem. Engrs., 35: 211 (1939).
5. L. L. Fellinger, Sc.D. Thesis, Dept. of Chem. Eng., Mass. Inst. Technol., Cambridge, 1941.
6. O. E. Dwyer and B. F. Dodge, Ind. Eng. Chem., 33: 485 (1941).
7. M. C. Molstad, J. F. McKinney, and R. C. Abbey, Trans. Am. Inst. Chem. Engrs., 39: 605 (1943).
8. E. R. Gilliland, Ind. Eng. Chem., 26: 516 (1934).
9. R. T. Haslam, R. L. Hershey, and R. H. Kean, Ind. Eng. Chem., 16: 1224 (1924).
10. O. L. Kowalke, O. A. Hougen, and K. M. Watson, Bull. Univ. Wis. Eng. Exp. Sta., 68 (June 1925).
11. S. Glasstone, K. J. Laidler, and H. Eyring, "The Theory of Rate Processes," McGraw-Hill Book Company, Inc., New York, 1941.
12. W. E. Lobo, L. Friend, F. Hashmall, and F. Zenz, Trans. Am. Inst. Chem. Engrs., 41: 693 (1945).
13. J. C. Elgin and F. B. Weiss, Ind. Eng. Chem., 31: 435 (1939).
14. W. F. Gross and Charles W. Simmons, Trans. Am. Inst. Chem. Engrs., 40: 121 (1944).

Chapter 8

CONTINUOUS FLUORINE-DISPOSAL PLANT

By Ralph Landau

1. INTRODUCTION

Waste fluorine can be disposed of by absorption in caustic soda solutions of strengths greater than about 2 per cent, but owing to the limited solubility of sodium fluoride in water or caustic solutions, erosion and plugging of equipment may result. Potassium fluoride is much more soluble than sodium fluoride, but caustic potash is more expensive than caustic soda. Consequently a plant was designed employing caustic soda. The plant was equipped for continuous chemical regeneration, so that the sodium fluoride concentration was always kept below the solubility limit. This chemical regeneration was accomplished by continuous treatment with lime slurry, which precipitated calcium fluoride and regenerated the caustic soda, as shown in the following equations:

$$F_2 + 2NaOH \rightarrow \tfrac{1}{2}O_2 + 2NaF + H_2O$$

$$2NaF + CaO + H_2O \rightarrow CaF_2 + 2NaOH$$

In this manner the caustic concentration was maintained constant, and the calcium fluoride could be removed continuously from the system by gravity settling. A brief description of the plant follows (see Fig. 8.1).

The fluorine-containing gases are introduced into a packed absorption tower 1 through a nozzle 2. The tower is fed with a countercurrent stream of 5 to 10 per cent sodium hydroxide solution, which is introduced at the top through 3. Inert gas is vented through the stack 3a. The effluent liquid from the tower, containing sodium fluoride in solution, is continuously withdrawn from the tower through the line 4 and passed into a regeneration tank 5, to which is supplied, through

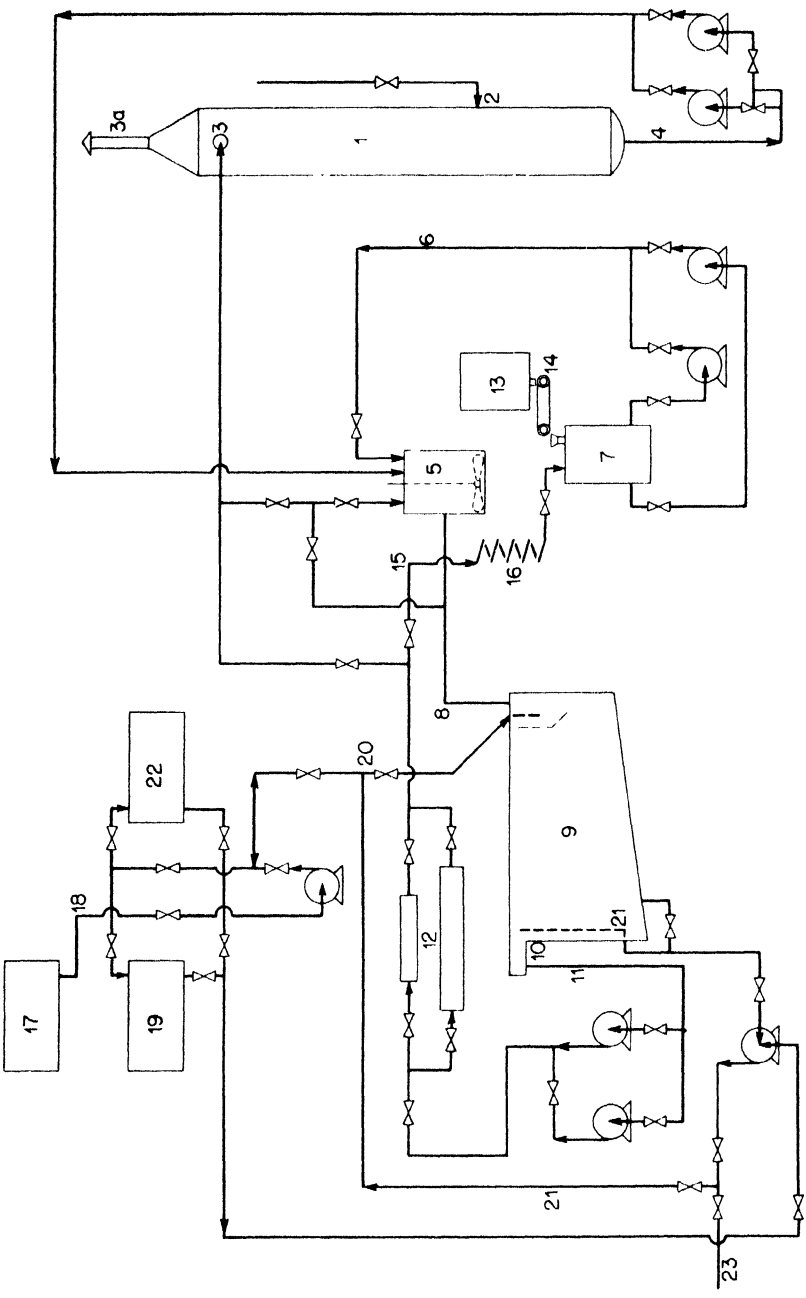

Fig. 8.1 — Process flow sheet of the continuous fluorine-disposal plant. See Sec. 1 for identification of the numbered components and description of the process.

line 6, a small stream of lime slurry, which enters from slaker 7. In the regeneration tank 5, the sodium fluoride formed is converted to calcium fluoride by reaction with lime under conditions of good agitation. The mixture flows through line 8 into the settling tank 9, wherein calcium fluoride and excess lime settle out. The clear, regenerated liquor overflows weir 10 and is discharged through line 11 back to the absorption tower 1.

In order to maintain temperature control on the tower, the discharge from settling tank 9 first passes through the heat-exchange system 12. This system is automatically regulated to maintain a constant temperature of 100 to 150°F on the tower feed.

The lime slurry is prepared by the introduction of lime (quick or hydrated) from bin 13 to the tank 7, using the belt feeder 14. The slaking, or slurrying, medium is a portion of fresh tower feed recycled to the tank 7 through line 15. This solution may be cooled by passage through the exchanger 16.

Incoming 50 per cent sodium hydroxide solution is pumped from the tank car 17 through line 18 to the storage tank 19, which is partially filled with water to make a 25 per cent solution. Make-up alkali can be withdrawn from 19 as needed and pumped through line 20 to the settling tank 9.

When sufficient solids have accumulated in the settling tank, the clear liquor is decanted through a swing pipe and pumped through line 21 to the decantation tank 22. After the settling tank has been cleaned, the clear liquor is returned thereto from the decantation tank 22.

Waste solids in the settling tank may be removed by adding sufficient water to make a slurry and pumping through line 23 to disposal.

2. OPERATION

A one-month test was made on the plant described in the preceding section. This section presents the results. Fluorine was fed to the system at a rate of about 60 lb/day, although there was some fluctuation (Fig. 8.2). The lime rate is shown in Fig. 8.3.

This test did not represent a detailed scientific study of the plant operation. Instead, it was intended to furnish engineering data for plant operation use. The results are of interest in demonstrating the basic operability of such a chemical regenerative process.

2.1 Reaction Tank. The soluble fluoride concentration in the tower feed is shown in Fig. 8.4. It will be noted that during the period of Oct. 13 to 22 the soluble fluoride concentration increased steadily from about 1,000 to 3,500 ppm. This was believed to be due to the lack of sufficient lime fed to the reaction tank. Accordingly the lime

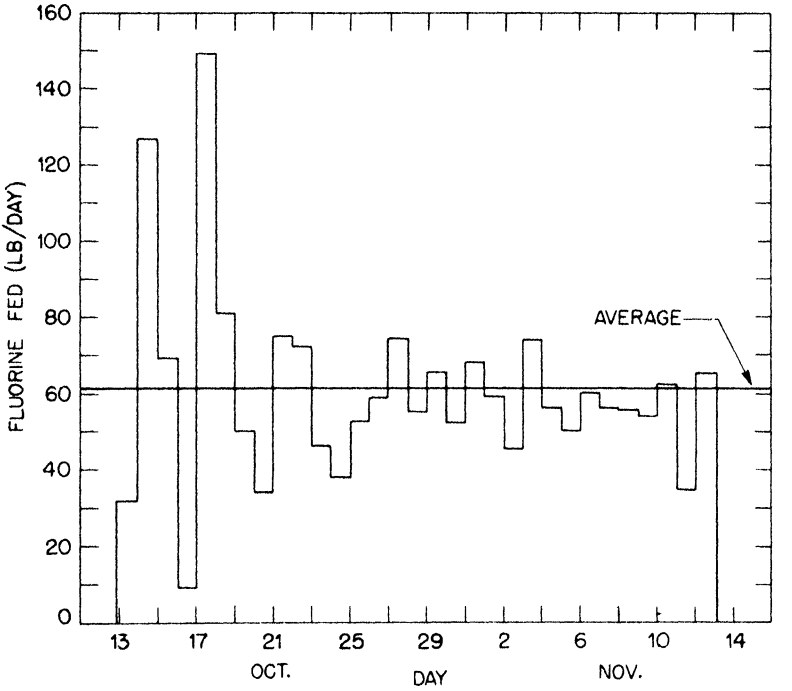

Fig. 8.2 —Daily fluctuations in the amount of fluorine received by the fluorine-disposal plant over a period of one month.

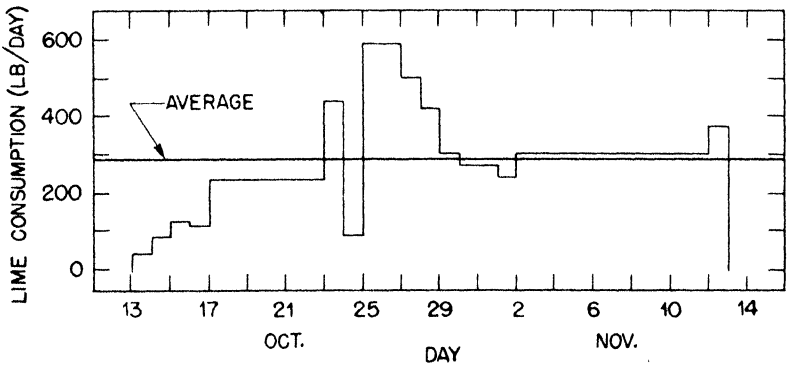

Fig. 8.3 —Daily and average lime consumption in the fluorine-disposal plant.

rate was increased on Oct. 23, and the fluoride concentration was then brought back to a level of about 1,000 ppm. It rose thereafter to about 1,500 ppm for a short while and subsequently dropped back to about 1,000 and remained at that figure. It is therefore clear that, over the month of operation, whatever fluoride was absorbed in the tower was

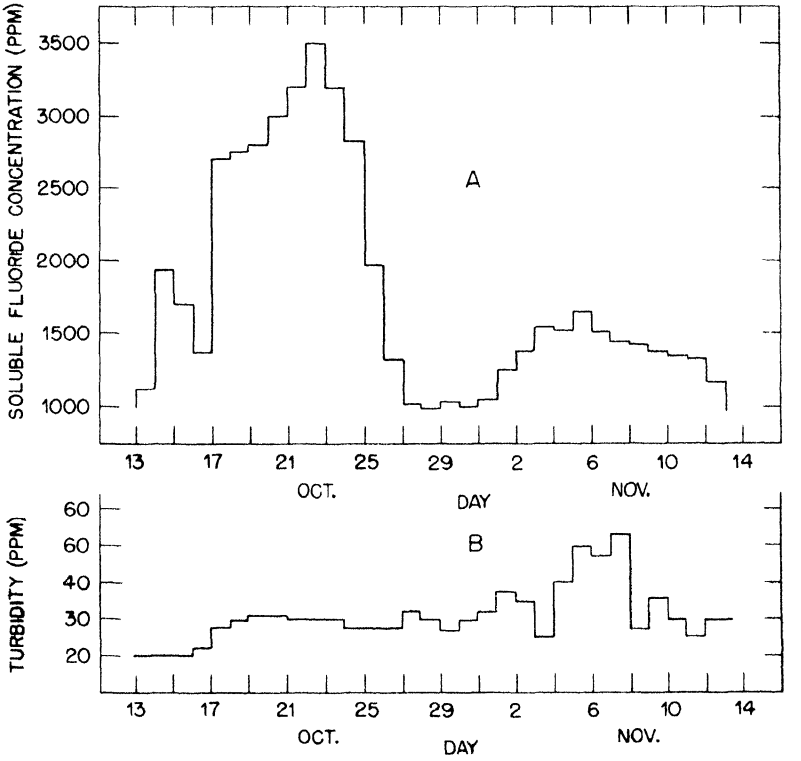

Fig. 8.4—Daily variations: A, in fluoride concentration in the settling-tank overflow and the tower effluent; B, in the turbidity of the settling-tank overflow.

precipitated out in the reaction tank. The value of 1,000 ppm, which could not be reduced appreciably by greater increase in the lime rate, evidently represents the limit of the equilibrium in the reaction of lime with soluble fluoride in the presence of caustic. If the lime treatment had not been used during the run, the total fluoride concentration in the caustic would have increased by 10,000 ppm, or to about 2.0 per cent sodium fluoride by weight. This probably would have resulted in precipitation of sodium fluoride in the tower (solubility of

sodium fluoride in caustic is about 1.5 per cent) and possible plugging. Along with regeneration of the caustic, it was this eventuality which the reaction with lime was designed to prevent.

Another confirmation of the effectiveness of the reaction tank is found in the data on the caustic strength from Nov. 1 to 11, during which time the caustic concentration remained at 7.4 per cent (see Fig. 8.5). Over this interval the tower absorbed 720 lb of fluorine,

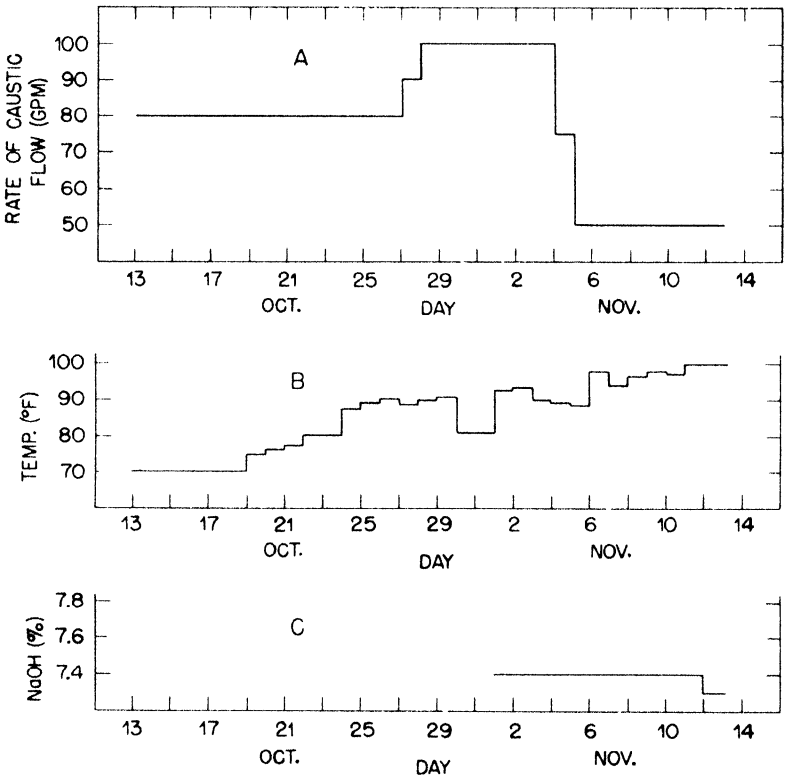

Fig. 8.5—Daily variations: A, in rate of caustic flow to tower; B, in caustic temperature; C, in concentration of caustic.

which would have caused a reduction of 0.8 per cent in the caustic concentration if no lime treatment had been in use. During the earlier part of the month's run (not shown in Fig. 8.5) the caustic concentration gradually dropped from about 8 to 7.4 per cent as water was added to the system for washing out the lime-slaking and other equipment.

During the month's operation the total fluorine fed was 1,882 lb, and the lime fed was 8,960 lb. The theoretical lime requirement to precipitate all the 1,882 lb of fluorine as calcium fluoride is 2,770 lb of lime. It is therefore evident that the lime consumed was more than three times the theoretical requirement. During the period of Oct. 13 to 22, the amount of fluorine absorbed was 697 lb and the amount of lime 1,780 lb. Since the theoretical requirement of lime for this weight of fluorine is 1,030 lb, the excess was only 70 per cent. However, as noted above, the fluoride content of the solution increased almost continuously during this period. In the ratio of actual to theoretical lime it therefore appears necessary, for completeness of reaction, to increase the actual lime to somewhere between two and three times the theoretical requirement. The data available are not adequate enough to permit calculation of the equilibrium constant of the reaction, and therefore the observed data cannot be checked. Calculations and analyses are complicated by the fact that the reaction occurs in very dilute solution (except for the caustic) and involves only small changes over short time intervals.

Calculations show that, at a flow rate of 60 lb of fluorine per day to the tower and a liquor rate of 100 gpm, the change in the fluoride content of the solution through the absorption tower would not exceed 50 ppm. This value is well within the experimental error of the determination, so that the chart presented in Fig. 8.4 is representative of the fluoride content at all points in the system at any given time. It is only over a period of some days that the trend becomes observable. It is therefore not necessary to obtain more than one sample at the tower feed for routine plant control.

During the period preceding the run, it was observed that the soluble fluoride content dropped between 100 and 900 ppm when the temperature was raised from about 70 to 90°F. This can probably be attributed to the increased solubility of lime, and perhaps to improved reaction rates. A similar effect would be found in the case of a reduction in caustic strength, although this has not yet been tried. It is felt that the optimum caustic strength for the whole plant is probably 5 to 8 per cent. Further reduction of this value would lower the tower efficiency and the efficiency of settling out the calcium fluoride.

The data demonstrate that it is possible to keep the soluble fluoride content of 5 to 10 per cent NaOH solution at a satisfactorily low level by feeding lime at a uniform daily rate, about two to three times the theoretical amount required to react with the fluorine consumed, without the necessity for close adjustment of lime rate to fluorine, since a deficiency or excess of lime feed one day can be remedied the next.

2.2 Settling Tank. The data presented in Table 8.1 were obtained during experiments designed to estimate the efficiency of the settling tank. It will be observed that, almost independently of the entering-solids content, the suspended solids in the effluent from the settling tank ranged from 93 to 154 mg/liter for samples taken at various times during the period Nov. 1 to 7. At the same time the range of entering solids in suspension was 202 to 900 mg/liter. The overflow from the settling tank was relatively clear, and the suspended parti-

Table 8.1 — Efficiency of Settling Tank

Date	Sample point	Suspended solids, mg/liter	CaF_2 in solids, %	CaF_2, mg/liter	Remarks
11/1	Settling tank	154	81.5	125	Control
11/1	Tower effluent	154	83.0	128	Sample
11/3	Reaction tank	211	70.4	148	Flow 100 gpm
11/3	Settling tank	140			Sample lost
11/4	Reaction tank	290	64.0	186	Flow 100 gpm
11/4	Settling tank	140	86.1	121	
11/6	Reaction tank	202	65.3	132	Flow 50 gpm
11/6	Settling tank	93	89.3	83	
11/7	Reaction tank	900	34.0	306	Flow 50 gpm
11/7	Settling tank	130	87.3	114	Increased lime feed

cles were very fine. Figure 8.4 presents data obtained with a turbidimeter. Although this instrument was calibrated for another suspension, and the data therefore have no absolute validity, it is clearly indicated that there was relatively little change in turbidity during the test, despite fluctuating lime and fluorine feed rates. There was some indication that at the lower liquor-circulating rates (50 gpm) the settling efficiency was improved somewhat, owing to the increased holding time in the settling tank, but the data are not accurate enough to establish a definite trend. To assure complete fluorine absorption, it is probable that 100 gpm is most satisfactory.

The data also show that the amount of calcium fluoride in the solution was substantially reduced by settling. Thus the outgoing calcium fluoride (in suspension) ranged from 83 to 121 mg/liter, whereas the incoming calcium fluoride ranged from 132 to 306 mg/liter. The amount of calcium fluoride that should settle out can be calculated readily from the amount of fluorine being absorbed by the tower. For the three days Nov. 4, 6, and 7, the amount of calcium fluoride settled out corresponded respectively to 3.5, 1.3, and 5.1 lb/hr. Since the

rate of fluorine absorbed during that period was about 60 lb/day, the hourly rate was about 2.5 lb, which is equivalent to 5 lb of calcium fluoride per hour. It is apparent that the amount of calcium fluoride settled out is in one case equivalent to that formed in the reaction tank, and in the other case of the same order of magnitude.

Because of the extreme difficulty of obtaining true representative samples, and because of short time variation in conditions, it is not believed that these results can be interpreted too quantitatively. They do indicate, however, that the amount of calcium fluoride that settled out is roughly equivalent to that entering the system. This can be confirmed in another way by noting that the calcium fluoride content of the caustic feed to the settling tank did not change much in the week during which the data were obtained (Table 8.1). During this week the amount of fluorine absorbed was approximately 420 lb, equivalent to about 860 lb of calcium fluoride. If this calcium fluoride had not settled out, the observed concentration would have increased by about 5,000 mg/liter. It is therefore clear that, within experimental accuracy, the settling tank performed its major function of keeping the solids content down to a low value and also allowed the calcium fluoride made in the reaction tank to settle.

It is possible that the minimum calcium fluoride retained in suspension (about 100 mg/liter) is the amount of colloidal suspension stable under the prevailing conditions, and that calcium fluoride over this minimum is coagulated sufficiently to permit settling in the holding time involved. Previous experiments have shown that the caustic helps coagulate calcium fluoride, and it appears likely that the suspended calcium fluoride circulating in the system would be much larger if water were used. On the basis of this consideration, the caustic concentration should not be reduced too much. In the absence of more data, it is suggested that 5 per cent be the minimum caustic concentration employed.

At the end of the run, inspection of the settling tank confirmed the findings of the efficiency determinations, namely, that most of the excess lime settled out near the entrance point, whereas the solids found near the weir overflow from the settling tank consisted of calcium fluoride. Solids were fairly uniformly distributed over the bottom of the tank in the transverse direction, indicating uniform flow from inlet to outlet across the tanks. There was considerably more deposit at the inlet point, corresponding to the fact that more excess lime than calcium fluoride had to be settled out, and the lime, being of larger particle size, settled first.

The solutions left at the bottom of the tank at the end of the run were slurried up with water and pumped to a holding pond.

Some measurements taken on Oct. 22 at sample points near the bottom of the settling tank (Table 8.2) indicated that, except for the very lowest sample point a few inches from the bottom of the tank, the caustic concentration and soluble fluoride content were identical

Table 8.2 — Concentration Study in Settling Tank

Sample location	Temp., °C	Soluble fluoride concentration, mg/liter	NaOH, %
Tower inlet	26.0	3,240	7.4
Tower outlet	26.0	3,250	7.4
Bottom of settling tank:			
Lowest point	27.3	900	10.4
Next lowest point	26.0	3,310	7.4
Next lowest point	26.0	3,320	7.4
Last point	26.0	3,380	7.4

with values obtained at the tower outlet and tower inlet. This indicated that there was sufficient mixing in the system to avoid stratification in the tank and that only at the lowest point, which probably represents solution occluded by settling solids, is there any deviation. Since this occluded solution was higher in caustic and lower in soluble fluoride, it probably represented fresh caustic from the beginning of the run.

2.3 Slaking Tank. Early tests run with a line feed rate of well over 1,500 lb/day showed that the slaking equipment could not handle such high feed rates, as evidenced by the fact that the lime settled out at the bottom of the slaker and various parts of the piping system, and the cloudiness of the settling tank overflow also increased sharply. However, after experience showed that the soluble fluoride content could be maintained at an approximately uniform flow by feeding a small but constant lime stream, the slaking problem was considerably simplified. It was found unnecessary to use a mechanical agitator for maintaining the lime in suspension, since air agitation was sufficient. A recycle rate of clear NaOH solution of about 10 gpm was employed, giving a lime slurry of several tenths of 1 per cent by weight of CaO. This slurry caused very little trouble in the lines and necessitated only occasional washdowns at the measuring orifice on the line, the point at which most of the plugging occurred. Toward the end of the run commercial hydrated lime was substituted for pebble quicklime, because of the unsatisfactory quality of the latter. This seemed to improve the slaking operation somewhat and did not visibly affect the

turbidity of the solution leaving the settling tank. (Experiments run with the pebble quicklime revealed the presence of a large part of silica and other inert material, and it was observed that at least 30 per cent of the lime added settled very rapidly and therefore probably did not materially contribute to the reaction.)

The lime feeders appeared to operate satisfactorily. As a result of the lower caustic temperatures employed during the run, there was substantially no steaming at the slaker and consequently no caking of lime on the belts, as was previously encountered with higher caustic temperatures.

As a result of the low lime feed rates, the heat of slaking became negligible, and it was not necessary to use the recycle caustic cooler.

Chapter 9

THE REACTION OF FLUORINE OXIDE WITH SODIUM HYDROXIDE

By Edward Simons, T. P. Wilson, and S. C. Schuman

1. INTRODUCTION

Preliminary pathological data indicated that of all the gases that might possibly be encountered in the operation of a UF_6 diffusion plant, fluorine oxide (F_2O) could be the most dangerous. Since the mechanism of production of this gas under various conditions was unknown, verification of the efficacy of dilute caustic to absorb F_2O was sought. Ishikawa, Murooka, and Hagisawa[1] had studied the reaction between F_2O and caustic. Confirmation of their work and additional information on the effect of temperature and agitation were sought.

The reaction of fluorine with gaseous or liquid water and with caustic is not completely understood. Oxygen, ozone, fluorine oxide, hydrogen peroxide, and hypofluorites have been postulated as reaction products. It is certain that the molecular mechanism of fluorine hydrolysis is not simple and that it is altered by phase, pH, temperature, reaction contact time, and specific reaction surface. It is difficult to evaluate the results given in the literature on this reaction, since either the fluorine was of dubious purity, or the method of handling the gaseous fluorine was crude, or the analysis of the oxygenated products was uncertain. Unfortunately, limitations of time prevented analysis of the reaction products in the work to be described.

2. EXPERIMENTAL WORK

The method used to prepare F_2O is that described by Yost.[2] Employing his procedure, a mixture containing approximately 40 vol. % F_2O in O_2 may be conveniently prepared and stored in cylinders.

Further purification was unnecessary for the intended purpose. However, the large increase in purity resulting from a single plate distillation of the reaction product indicates that essentially pure F_2O could be prepared in this way, using a low-temperature rectification column.

Table 9.1 — Reaction of F_2O with NaOH

Temp., °C	Pressure, mm Hg	NaOH, wt.%	Time, min	F_2O in gas, wt. %	F_2O left, wt. %	Remarks
21	760	1	0	33.2	100.0	
			6.5	25.1	75.7	
			12.0	19.6	59.0	
			25.0	10.4	31.3	
			31.0	6.4	19.4	
			40.0	4.0	12.0	
59	760	1	0	31.2	100.0	
			5.5	17.2	55.2	
			11.0	8.9	28.7	
			22.5	2.3	7.2	
			30.0	1.0	3.2	
29	761	10	0	36.0	100.0	
			2.0	17.7	49.2	
			5.0	6.9	19.1	
29	757	1	0	38.7	100.0	Reaction agitated
			2.0	8.4	21.8	
			5.0	2.5	6.3	
28	758	10	0	36.7	100.0	Reaction agitated
			2.0	5.9	16.1	
			4.0	0.9	2.3	
21	760	0.7	0	9.0	100.0	
			10.0	6.3	70.0	
			18.5	4.2	46.0	
			26.0	3.0	33.0	
			35.0	1.9	21.0	
			44.0	1.0	11.0	

Because of time limitations, experiments were simply effected by placing mixtures of gas and liquid in a glass bulb immersed in a constant-temperature bath, and removing samples at regular time intervals for analysis. In determining the effect of agitation, the bulb containing F_2O in contact with caustic was shaken by hand.

For the determination of F_2O, a conventional Orsat apparatus was employed, using KI as absorbent. To further substantiate this method of analysis, the I_2 formed on absorption was titrated with standard thiosulphate.

3. RESULTS

Results are given in Table 9.1. The weight per cent F_2O is the mean of results obtained gasometrically and by titration; the weight per cent F_2O left represents the per cent F_2O at time t divided by that at zero time. For each concentration of NaOH and temperature, results are expressible in accordance with the rate equation for a first-order reaction. The value of the specific rate constant, k, may be calculated to be:

with 10 % NaOH at 29°C, $k = 0.34 \ min^{-1}$
with 1 % NaOH at 59°C, $k = 0.10 \ min^{-1}$
with 1 % NaOH at 21°C, $k = 0.045 \ min^{-1}$

Table 9.1 indicates that the rate of reaction increased sharply upon agitation of the mixture of reactants. In general, the results obtained are in accord with those given by Ishikawa *et al.* However, no quantitative comparison is possible because of the sharp dependence of reaction velocity on specific reaction surface and on contact time.

REFERENCES

1. F. Ishikawa, T. Murooka, and H. Hagisawa, "Reactions of F_2O with Water and with Sodium Hydroxide," Bull. Inst. Phys. Chem. Research Tokyo, 12: 742 (1933).
2. H. S. Booth, ed., "Inorganic Syntheses," pp. 109-111, McGraw-Hill Book Company, Inc., New York, 1939.

SUBJECT INDEX

V

AUTHOR INDEX